



Advanced School on Direct and Inverse Problems of Seismology

27 September - 8 October, 2010

The Spectral-Element Method (SEM) and three-dimensional seismology

D. Komatitsch

*Universite de Pau et des Pays de'Adour
France*



The Spectral-Element Method (SEM) and three-dimensional seismology

Dimitri Komatitsch, University of Pau, France
ICTP, Trieste, October 1, 2010

*Note: the SPECFEM3D source code is freely available
for academic non-commercial research at
<http://www.geodynamics.org/cig/software>*

6 April 2009
M_w 6.2 L'Aquila (Italy)



260 dead
~1.000 hurt
~26.000 homeless



Istituto Nazionale di
Geofisica e Vulcanologia

Collaboration with
Emanuele Casarotti
(INGV, Roma, Italy)

M_w 6.2 L'Aquila



Part I

Theory and benchmarks

Brief history of numerical methods


Seismic wave equation : tremendous increase of computational power
⇒ development of numerical methods for accurate calculation of synthetic seismograms in complex 3D geological models has been a continuous effort in last 30 years.

Finite-difference methods : Yee 1966, Chorin 1968, Alterman and Karal 1968, Madariaga 1976, Virieux 1986, Moczo et al, Olsen et al..., difficult for boundary conditions, surface waves, topography, full Earth


Boundary-element or boundary-integral methods (Kawase 1988, Sanchez-Sesma et al. 1991) : homogeneous layers, expensive in 3D

Spectral and pseudo-spectral methods (Carcione 1990) : smooth media, difficult for boundary conditions, difficult on parallel computers

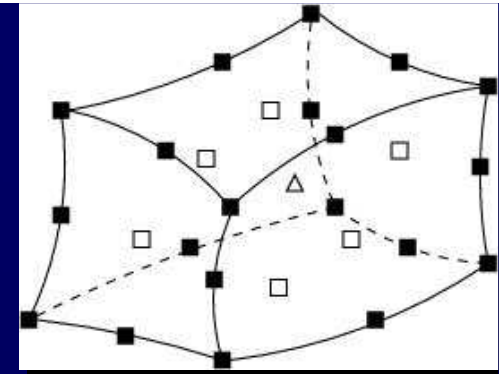
Classical finite-element methods (Lysmer and Drake 1972, Marfurt 1984, Bielak et al 1998) : linear systems, large amount of numerical dispersion



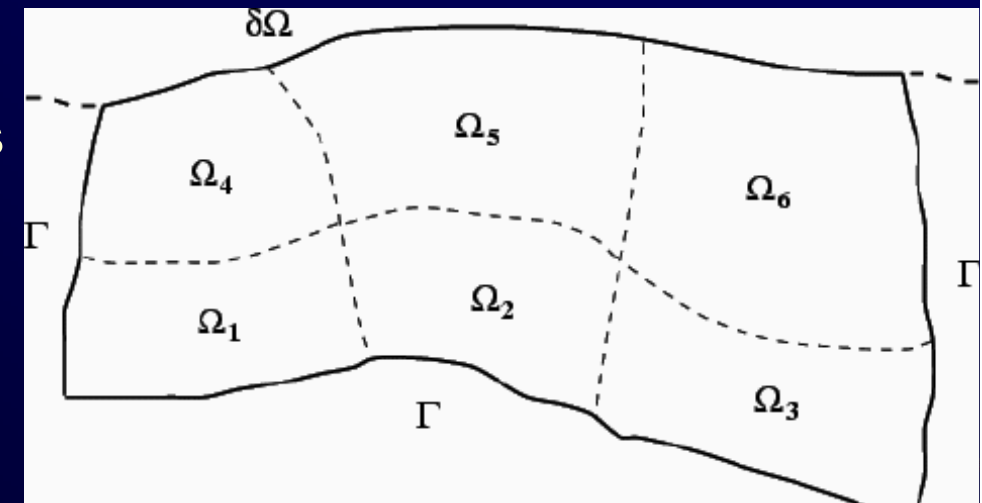
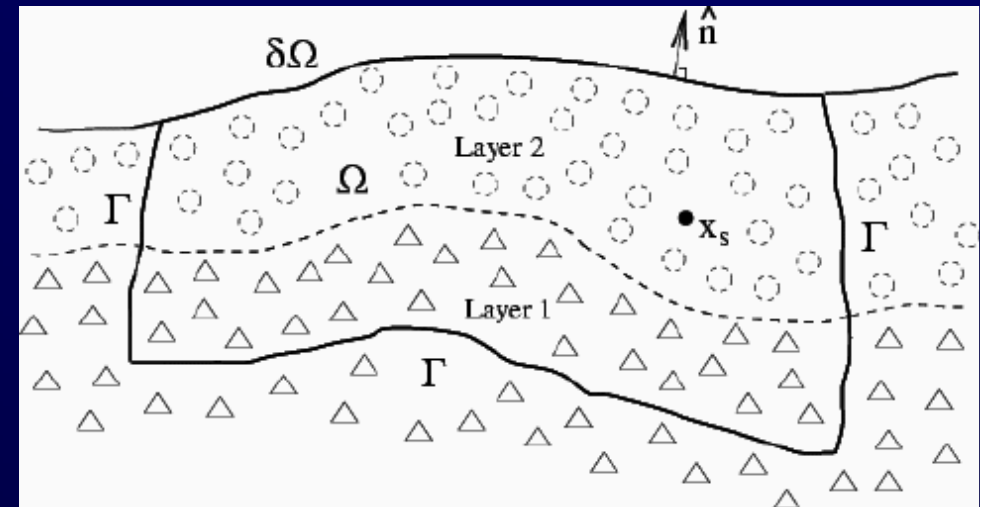
SEM technique
for local or
regional studies



Spectral-Element Method



- Developed in Computational Fluid Dynamics (Patera 1984)
- Accuracy of a pseudospectral method, flexibility of a finite-element method
- Extended by Komatitsch and Tromp, Chaljub et al., Capdeville et al.
- Large curved “spectral” finite-elements with high-degree polynomial interpolation
- Mesh honors the main discontinuities (velocity, density) and topography
- Very efficient on parallel computers, no linear system to invert (diagonal mass matrix)



Equations of Motion (solid)

Differential or *strong* form (e.g., finite differences):

$$\rho \partial_t^2 \mathbf{s} = \nabla \cdot \mathbf{T} + \mathbf{f}$$

We solve the integral or *weak* form:

$$\int \rho \mathbf{w} \cdot \partial_t^2 \mathbf{s} d^3 \mathbf{r} = - \int \nabla \mathbf{w} : \mathbf{T} d^3 \mathbf{r}$$

$$+ \mathbf{M} : \nabla \mathbf{w}(\mathbf{r}_s) S(t)$$

+ **attenuation** (memory variables) and **ocean load**

Equations of Motion (Fluid)

Differential or *strong* form:

$$\rho \partial_t \mathbf{v} = -\nabla p$$

$$\partial_t p = -\kappa \nabla \cdot \mathbf{v}$$

We use a generalized velocity potential χ
the integral or *weak* form is:

$$p = \partial_t \chi$$

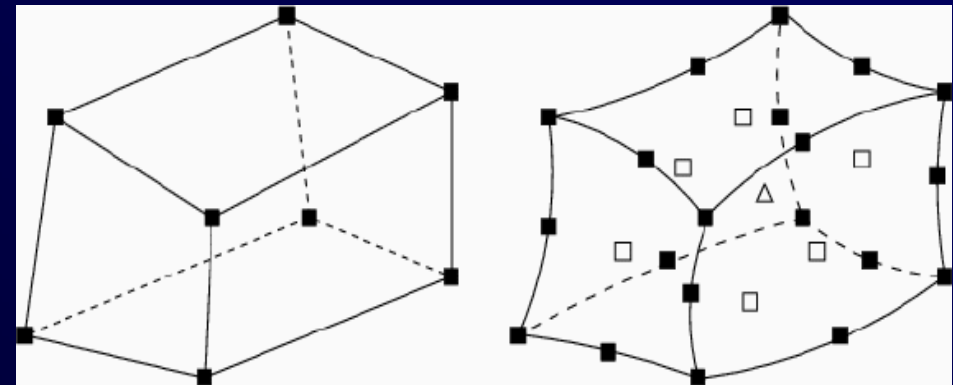
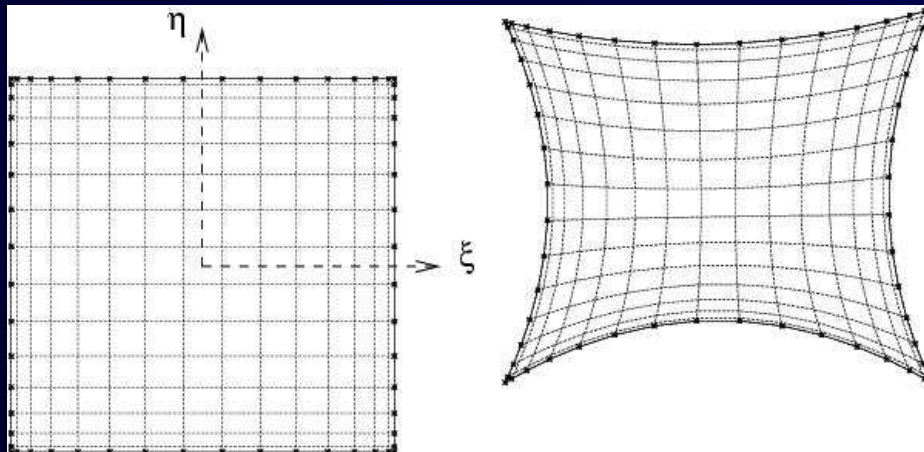
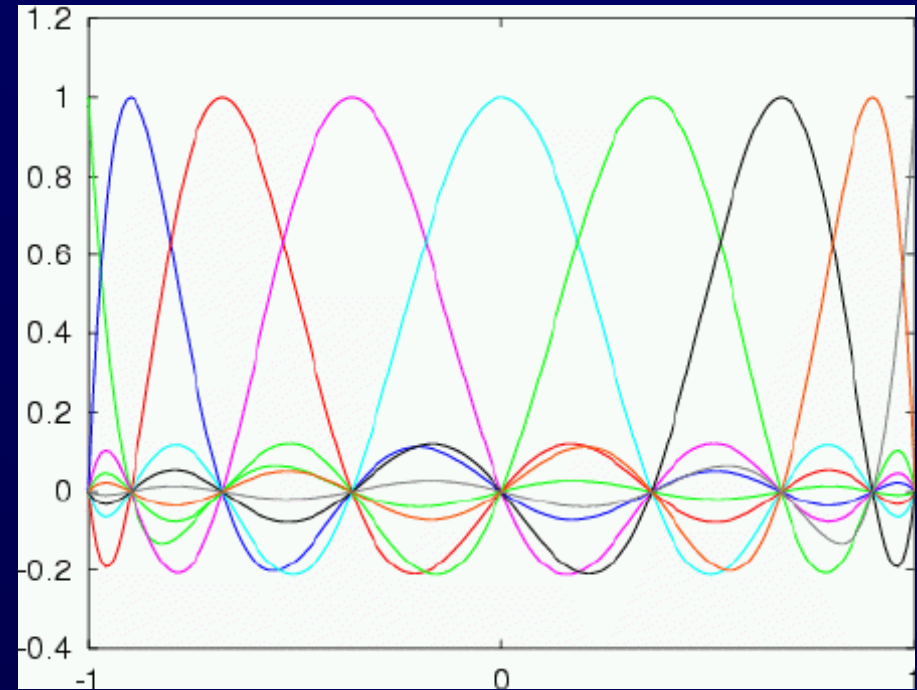
$$\int \kappa^{-1} w \partial_t^2 \chi d^3 \mathbf{r} = - \int \rho^{-1} \nabla w \cdot \nabla \chi d^3 \mathbf{r}$$


⇒ cheap (scalar potential)

⇒ natural coupling with solid


Finite Elements

- High-degree pseudospectral finite elements
- $N = 5$ to 8 usually
- *Exactly* Diagonal mass matrix
- No linear system to invert

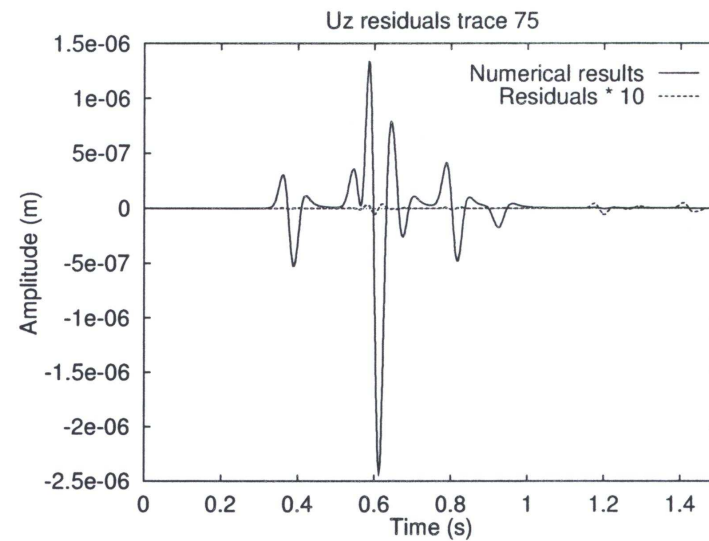
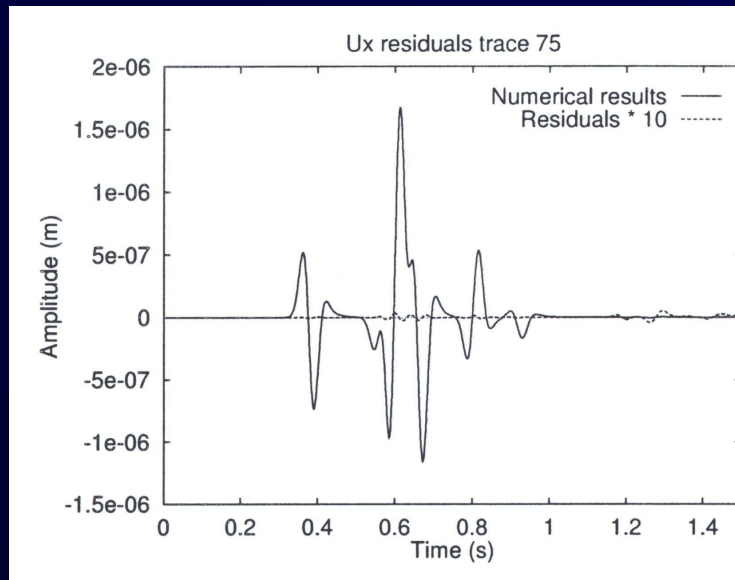
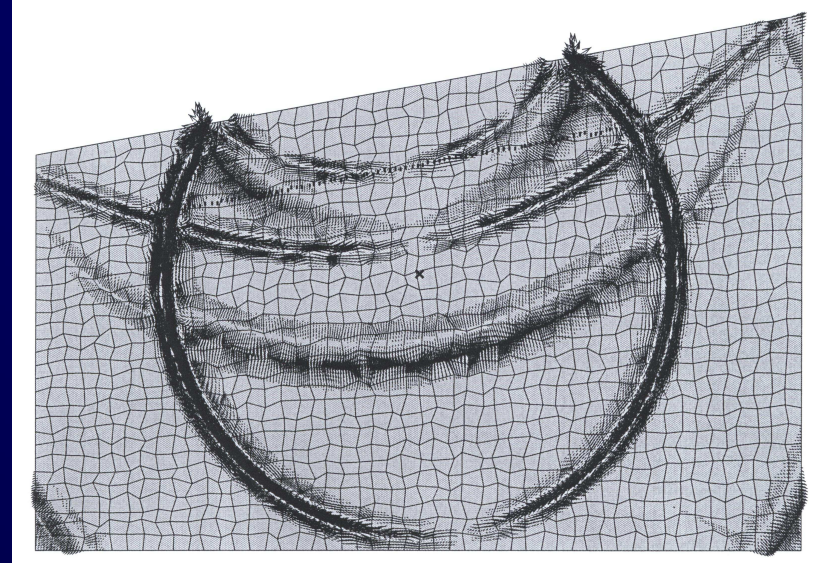
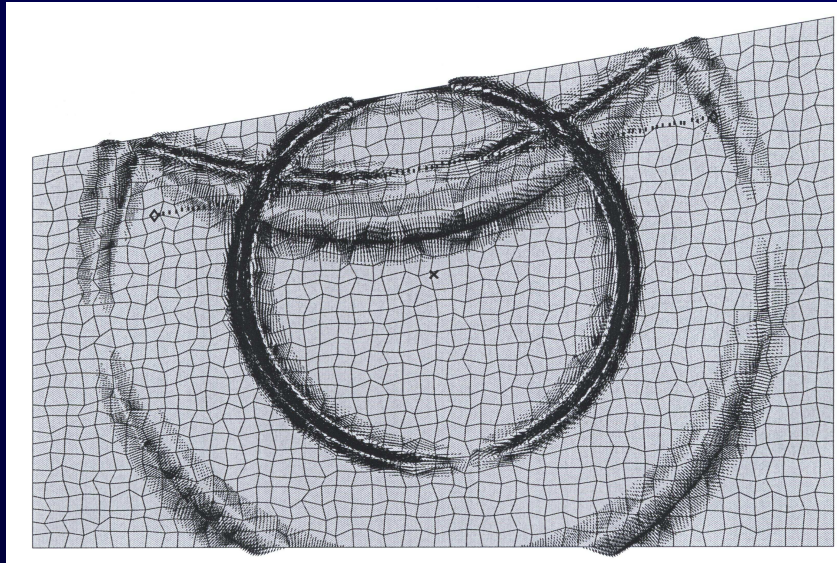




Benchmarks of the SEM at the regional scale

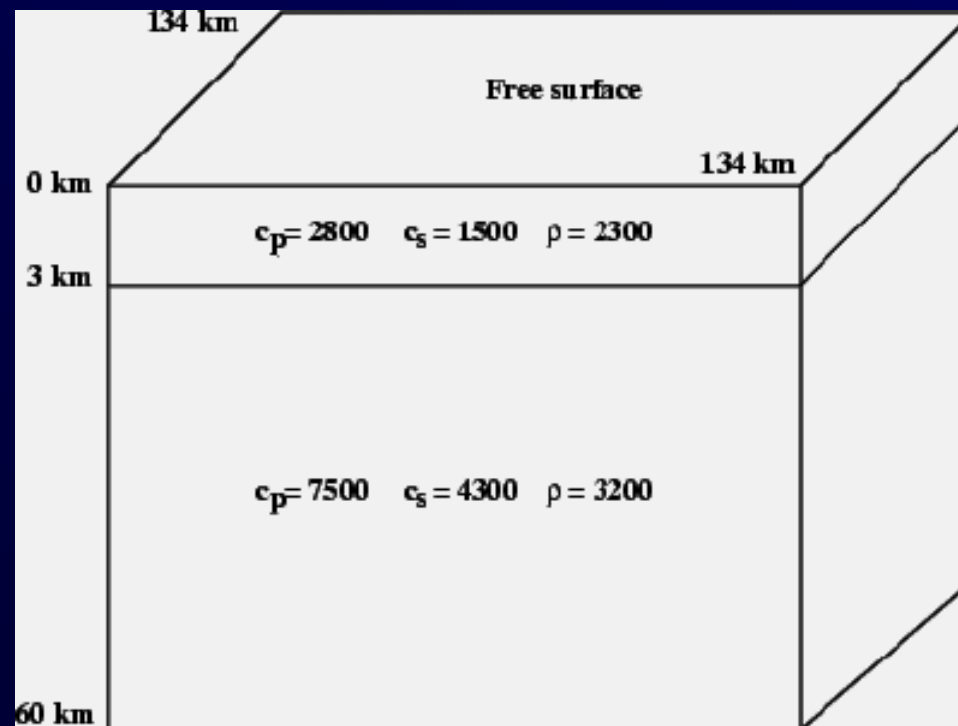


Distorted mesh for Lamb's problem



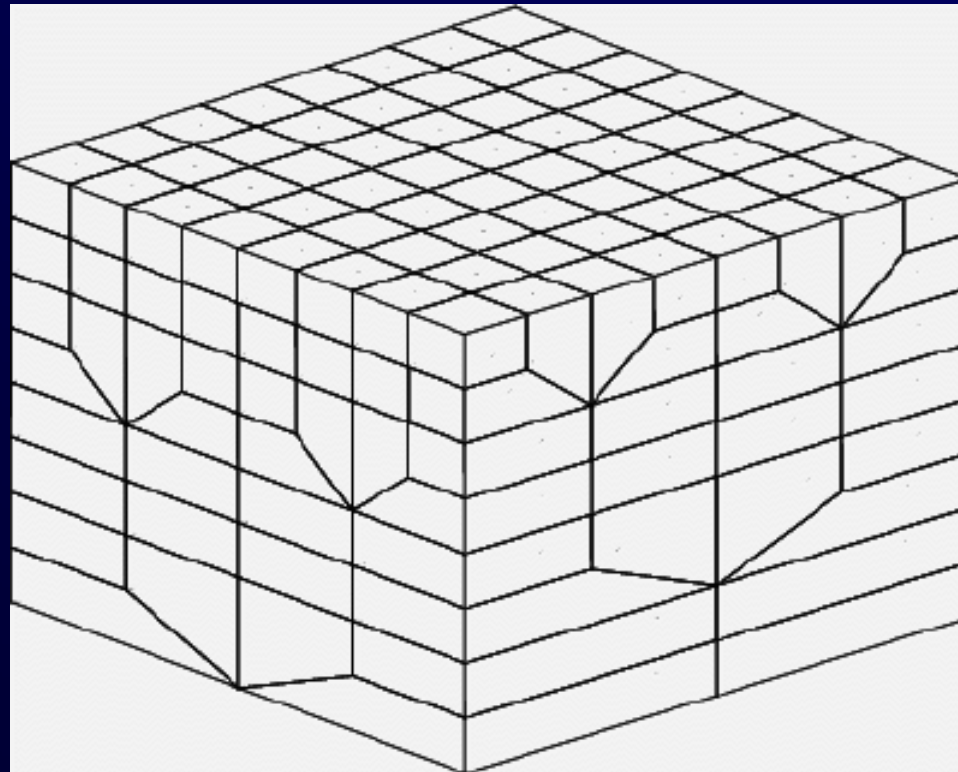
Validation on 3-D models

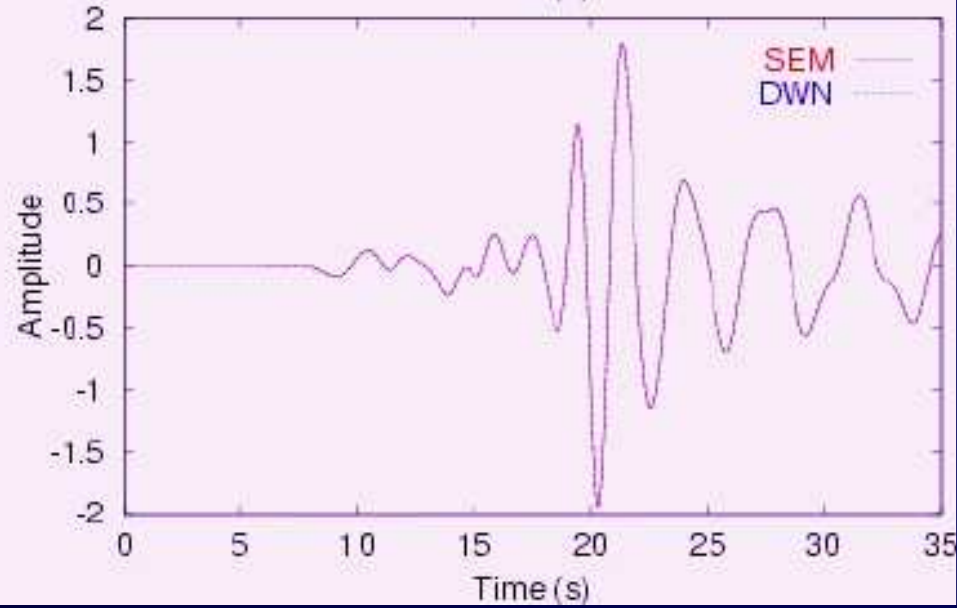
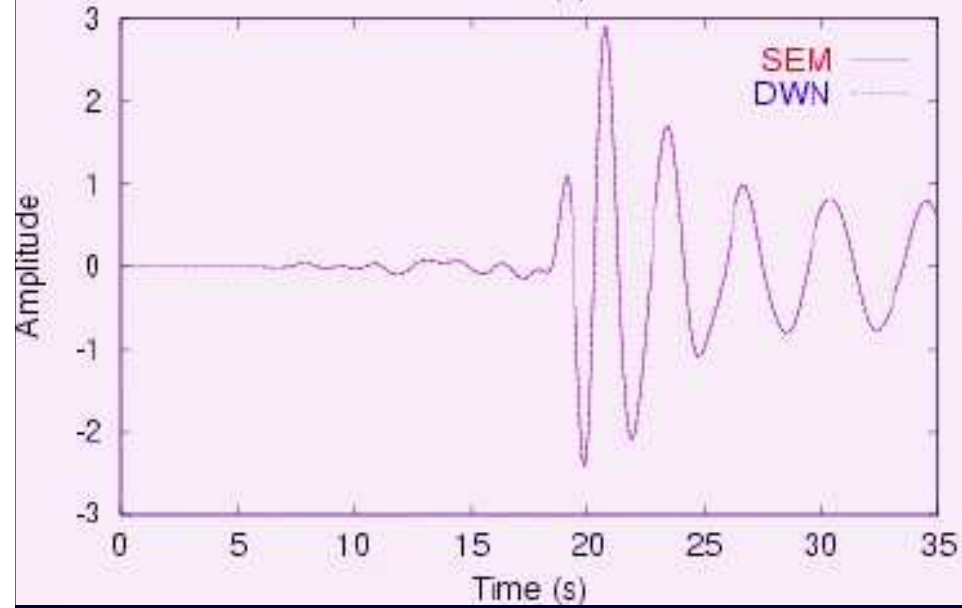
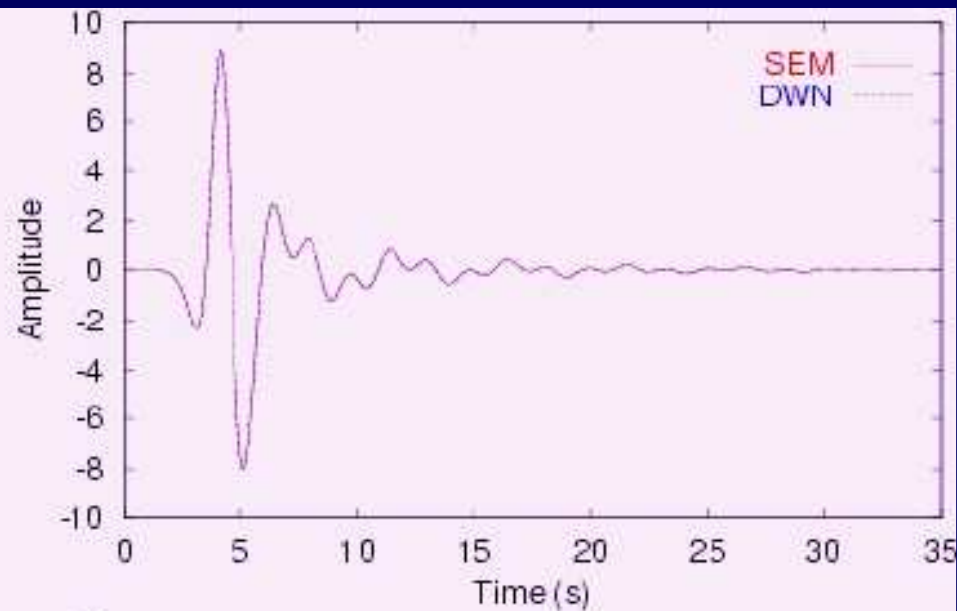
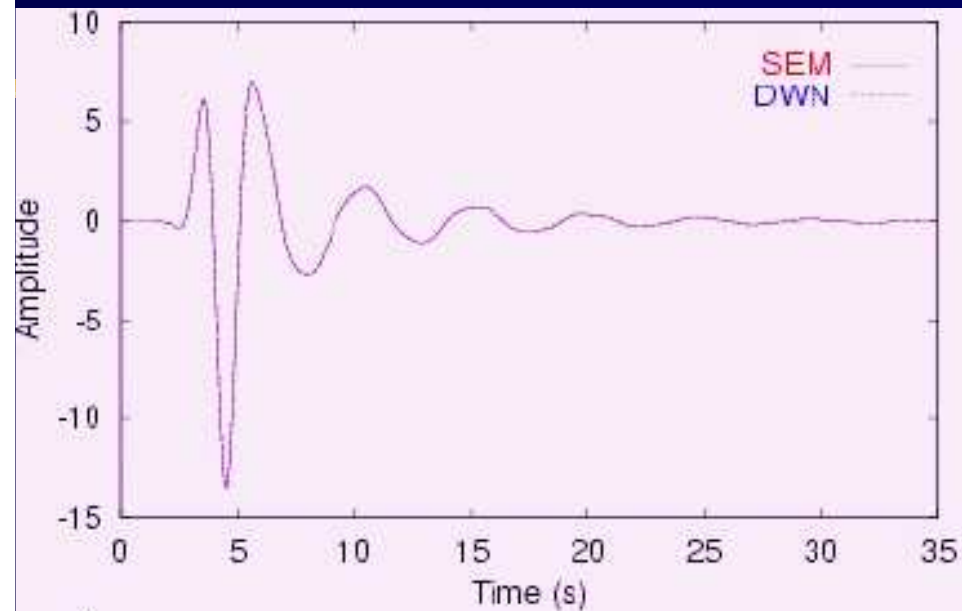
- Layer over a half-space: difficult to accurately model surface waves
- Very precise reference solution: DWNM



Mesh coarsening with depth

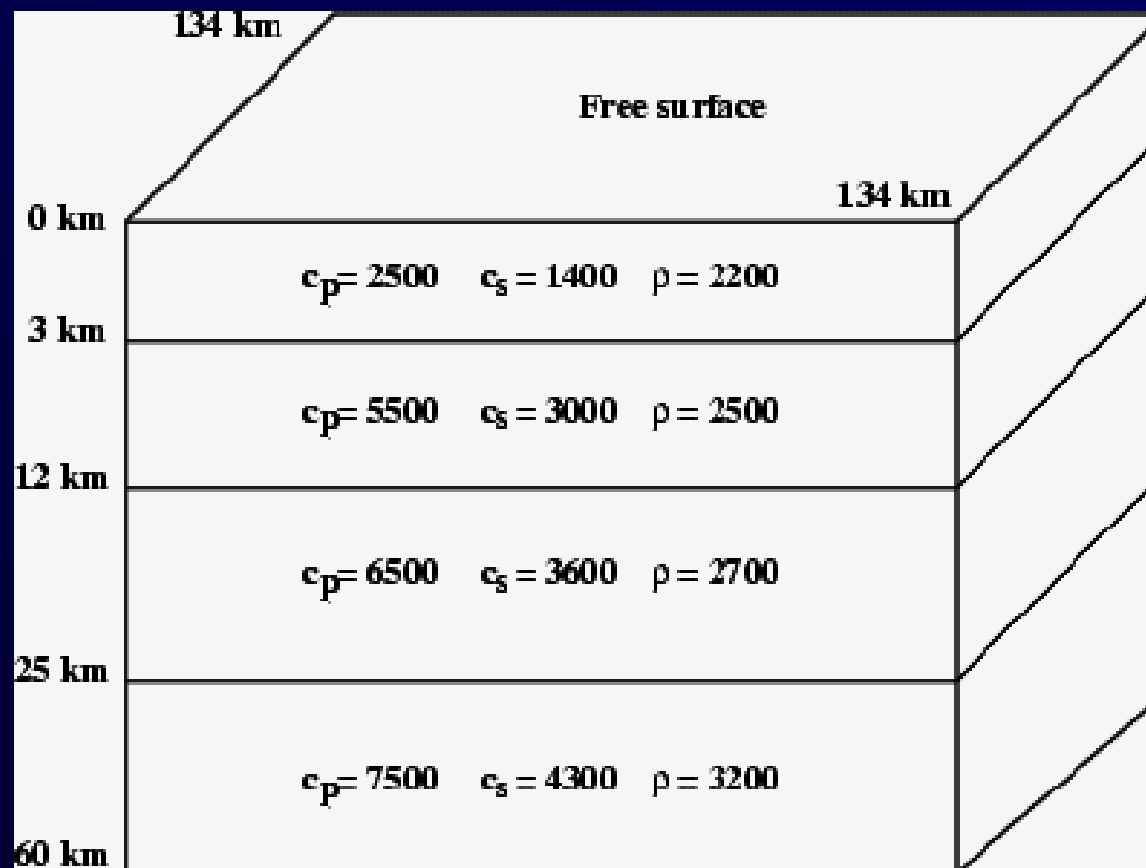
- Adapt the mesh to the velocity structure
- Save a lot of memory and CPU time

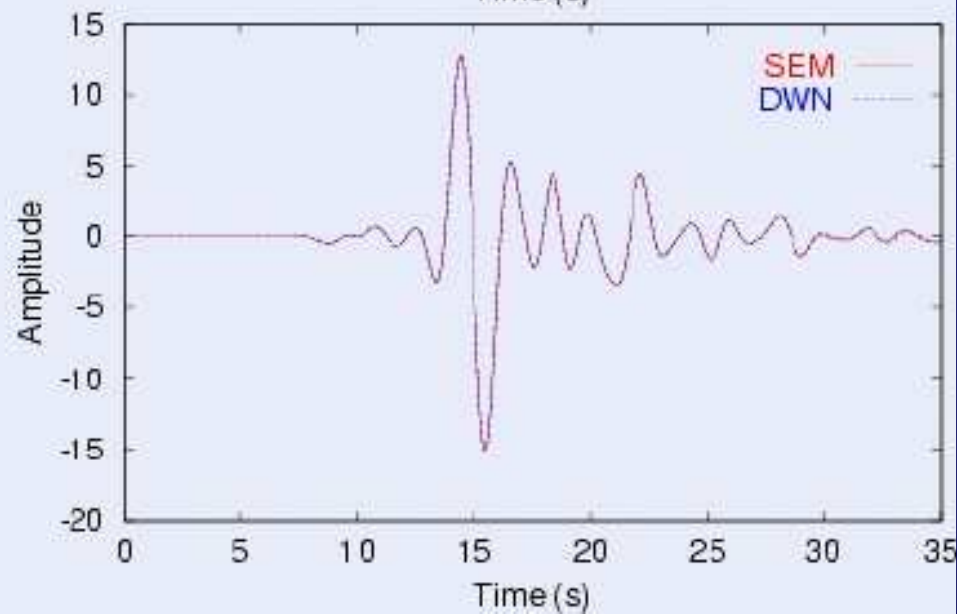
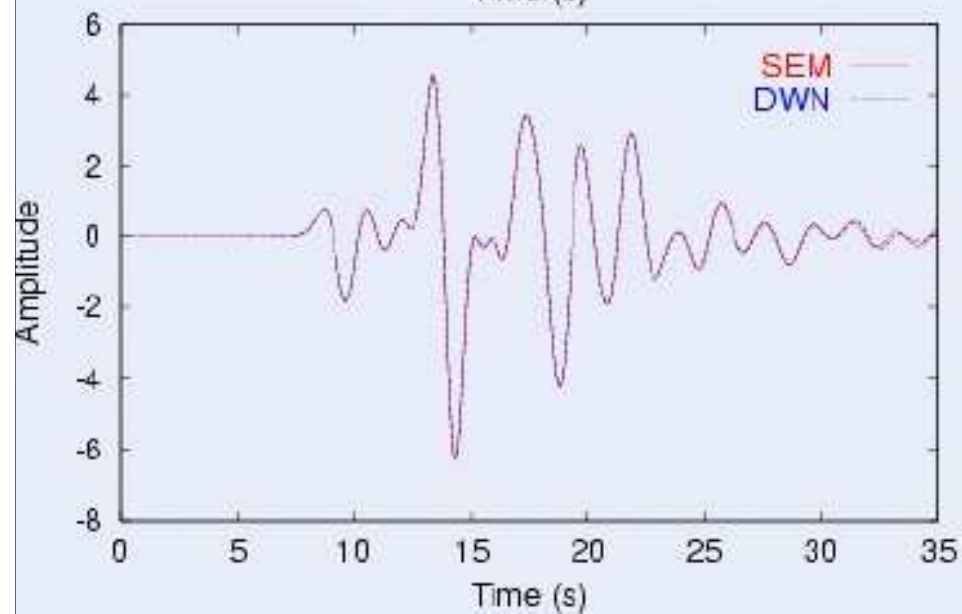
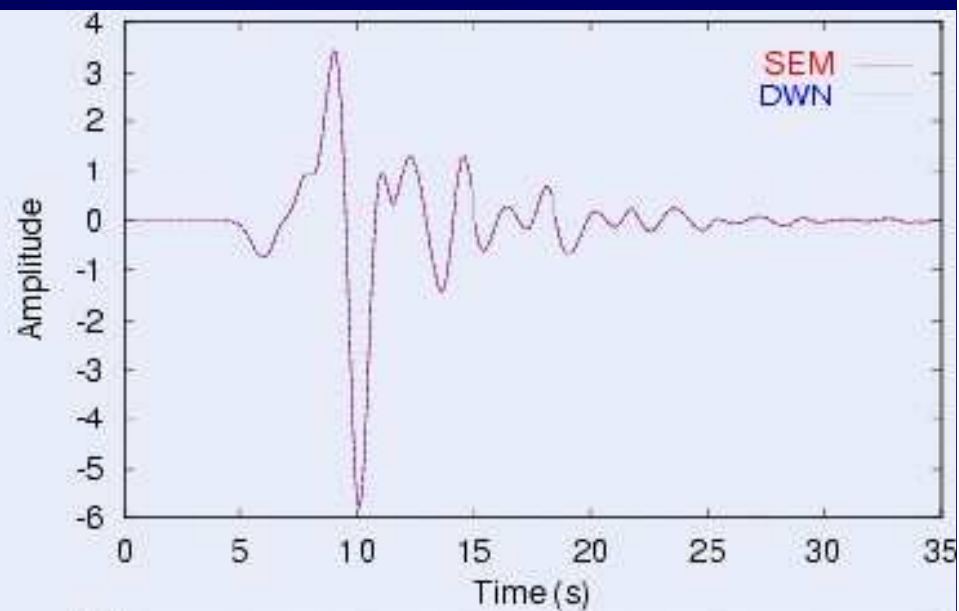
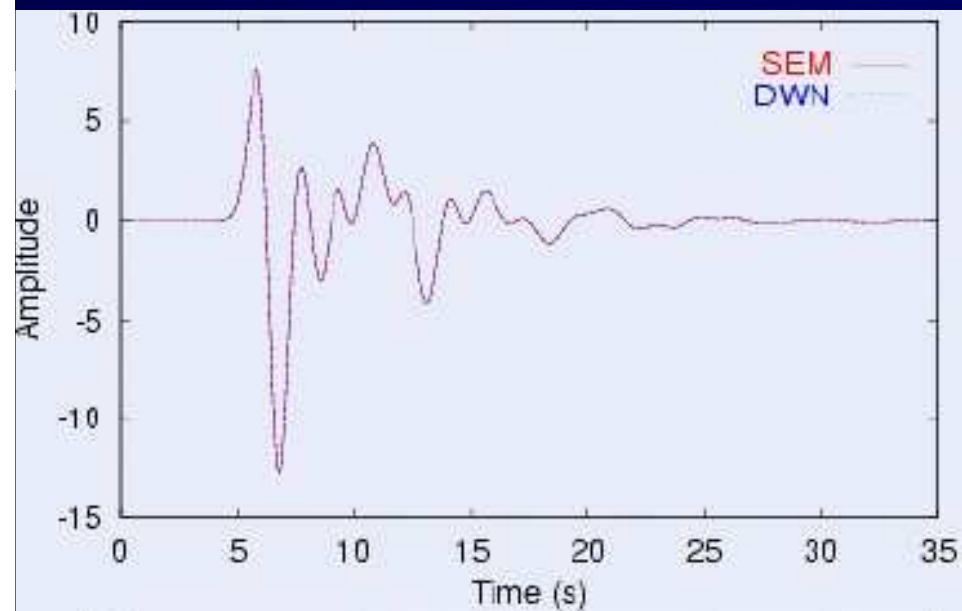




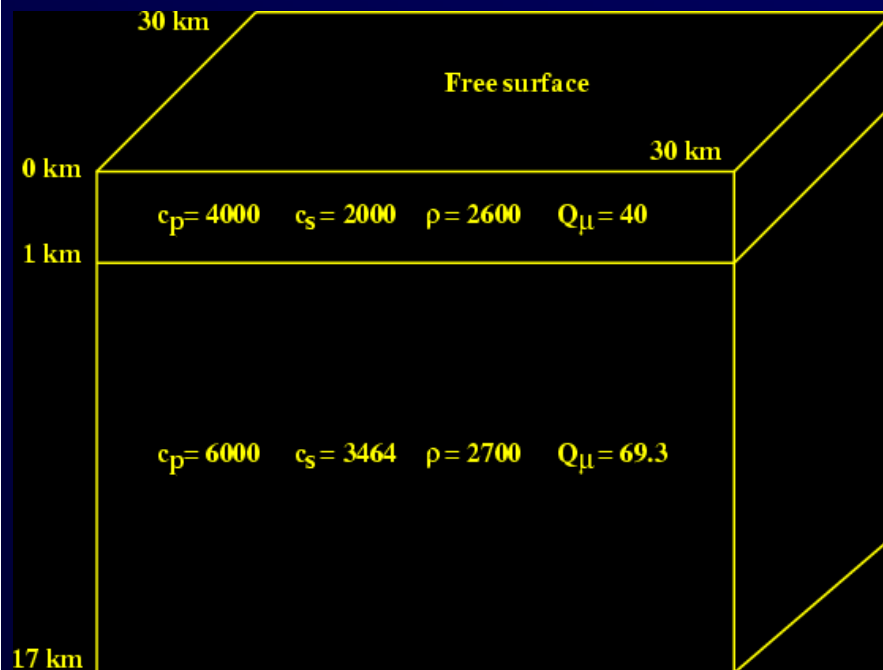
Layer-cake structure

- Body waves and multiples
- Accurate absorbing conditions on edges

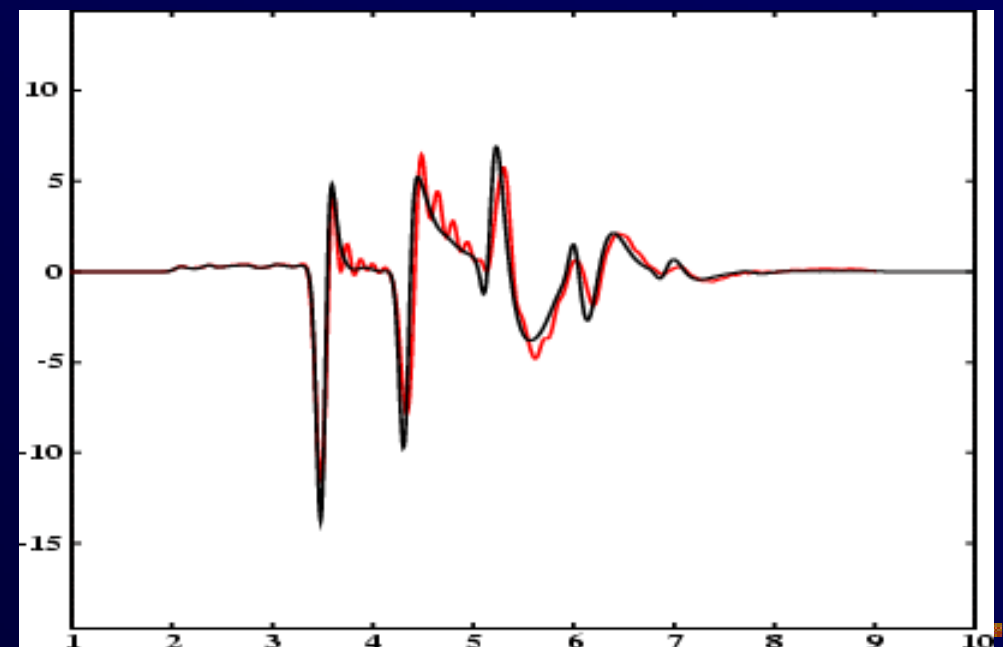
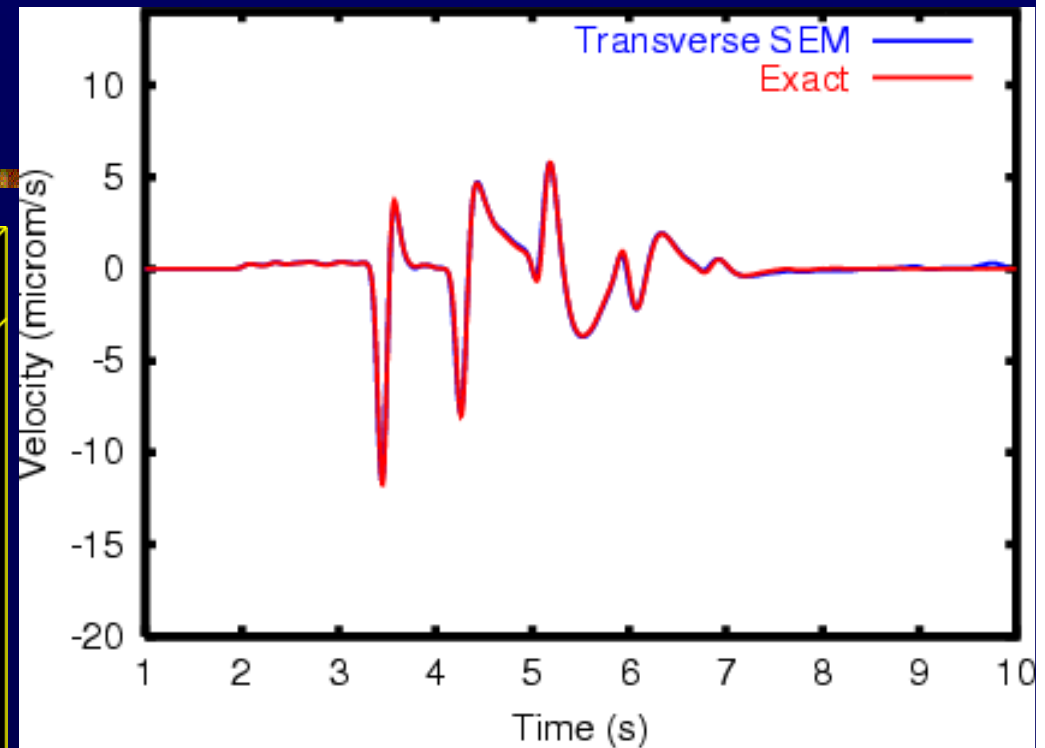





SCEC LOH.3




- Tester ondes de surface, et atténuation avec Q constant
- Comparer aux méthodes classiques de différences finies
- Solution de référence f-k de Apsel et Luco (1983)

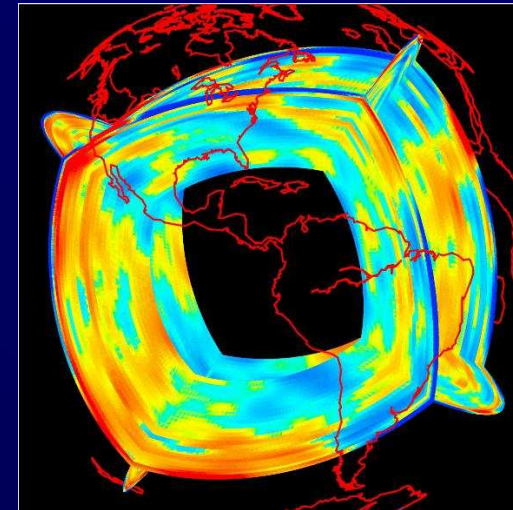
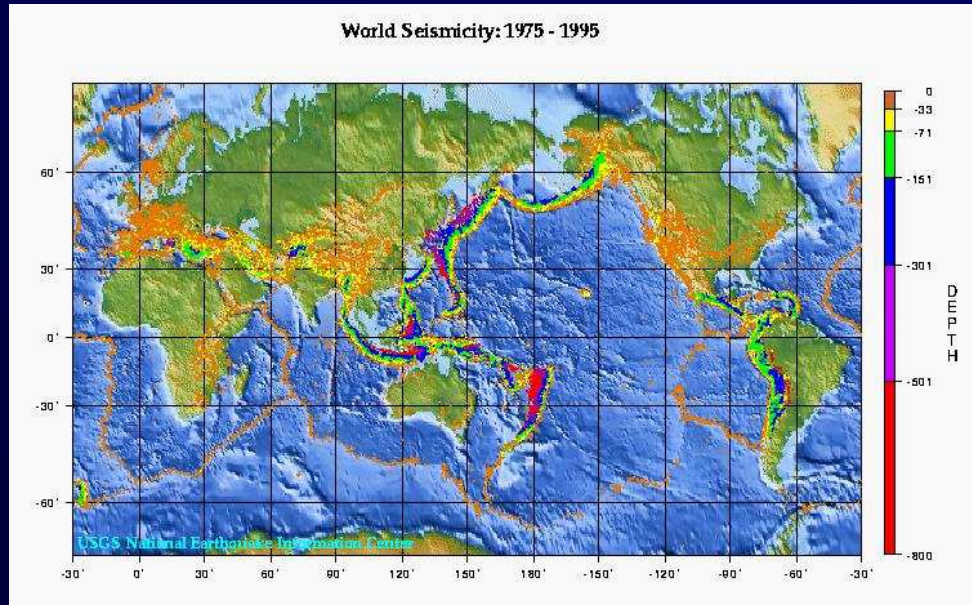




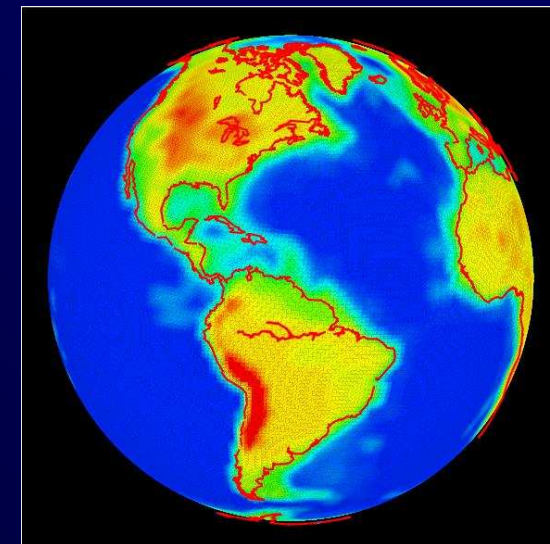
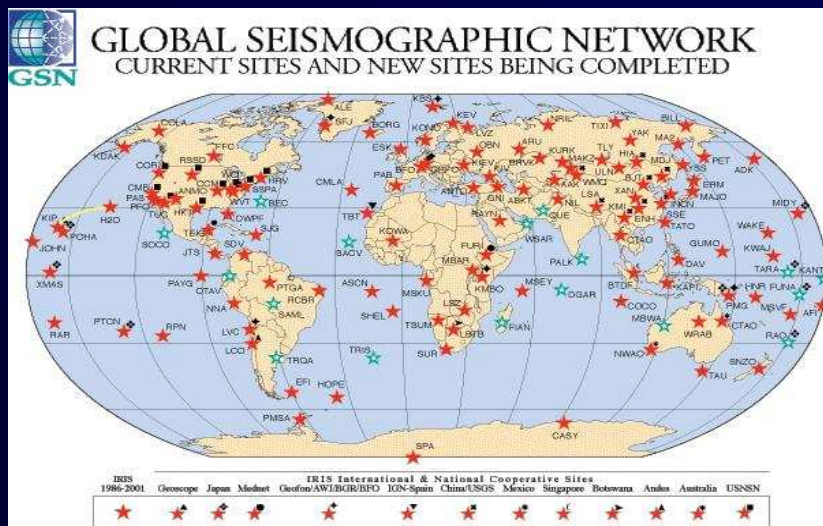
SEM technique for the global Earth



Global 3D Earth



Modèle de manteau S20RTS
(Ritsema et al. 1999)



Crust 5.2 (Bassin et al. 2000)

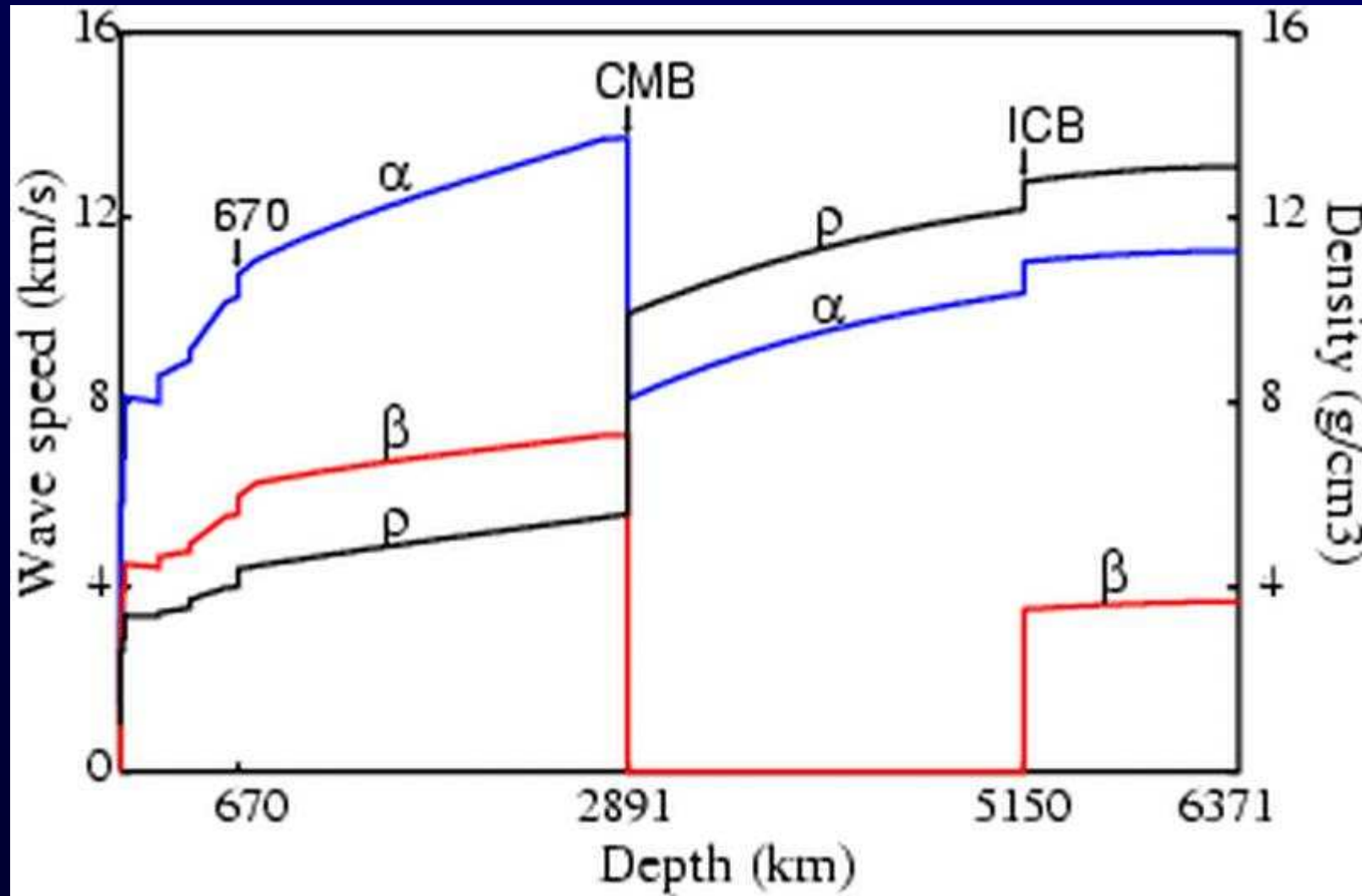
Introduction (Global Earth)

- Need accurate numerical modeling to study Earth structure (global scale)
 - Very large models at high frequency (3D Earth)
 - Complexity: classical methods (ray tracing, finite difference, pseudo-spectral) *do not work* for this problem (surface waves, anisotropy, fluid/solid interfaces, Earth's crust etc.)
-

The Challenge of the Global Earth

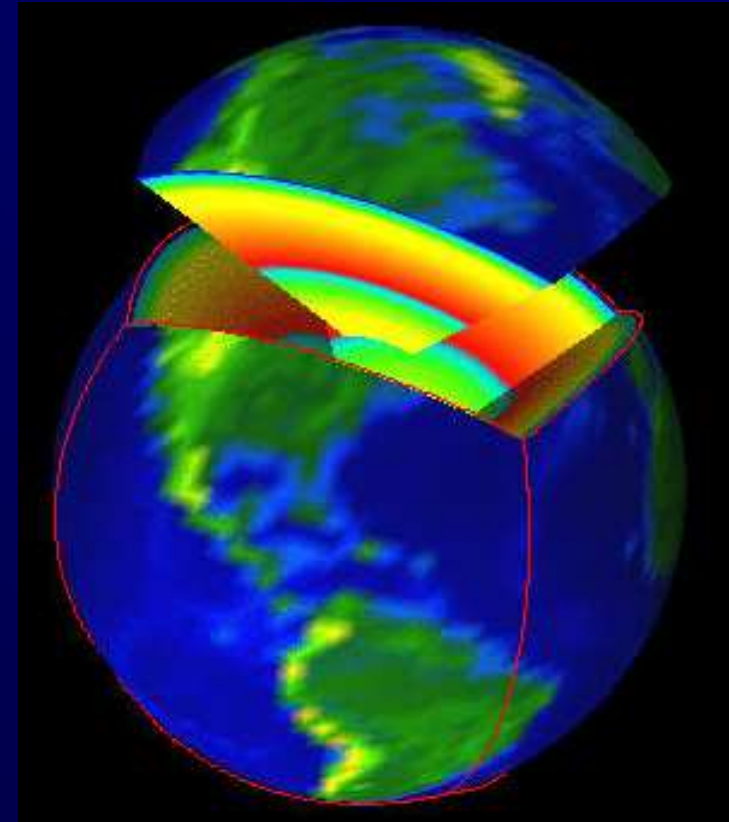
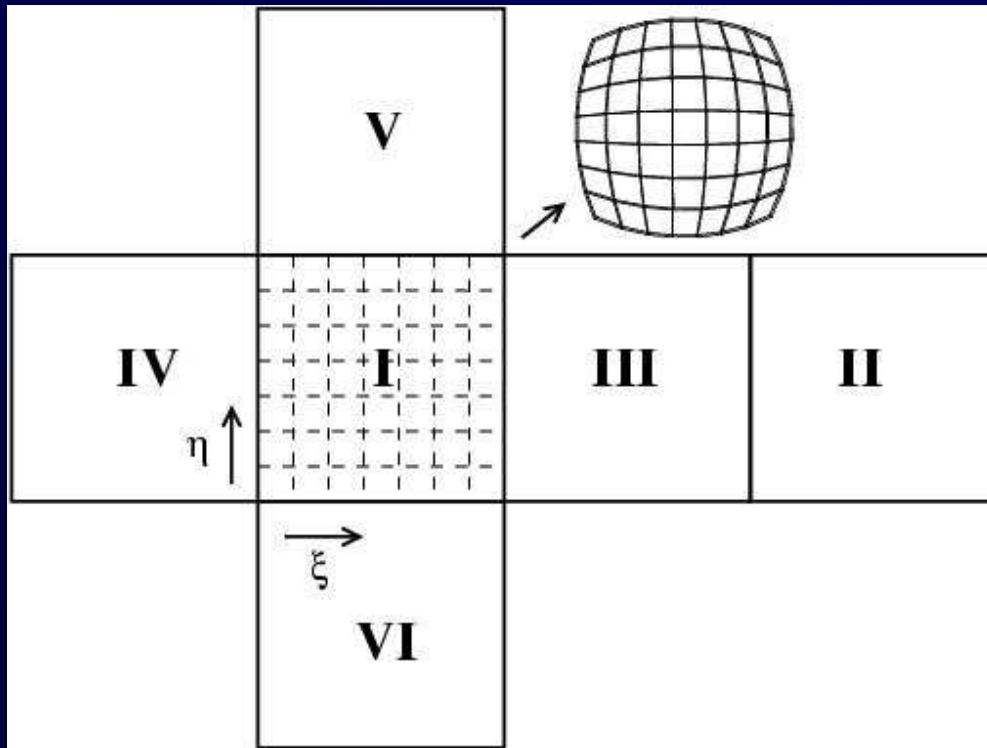
- A slow, thin, highly variable crust
 - Sharp radial velocity and density discontinuities
 - Fluid-solid boundaries (outer core of the Earth)
 - Anisotropy
 - Attenuation
 - Ellipticity, topography and bathymetry
 - Rotation
 - Self-gravitation
 - 3-D mantle and crust models (lateral variations)
-

Sharp Contrasts in Earth Model



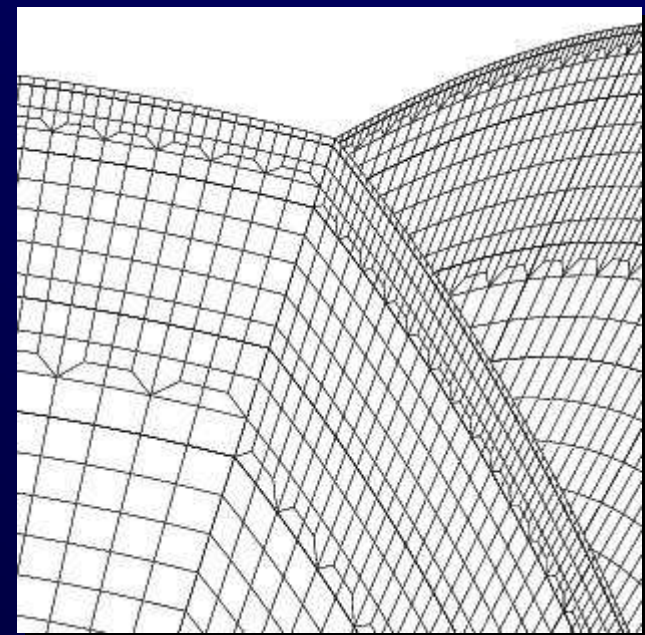
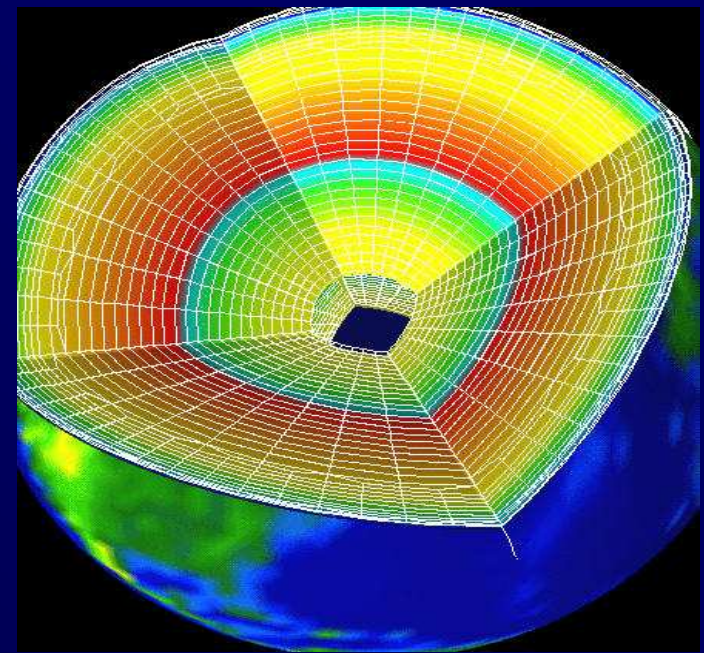
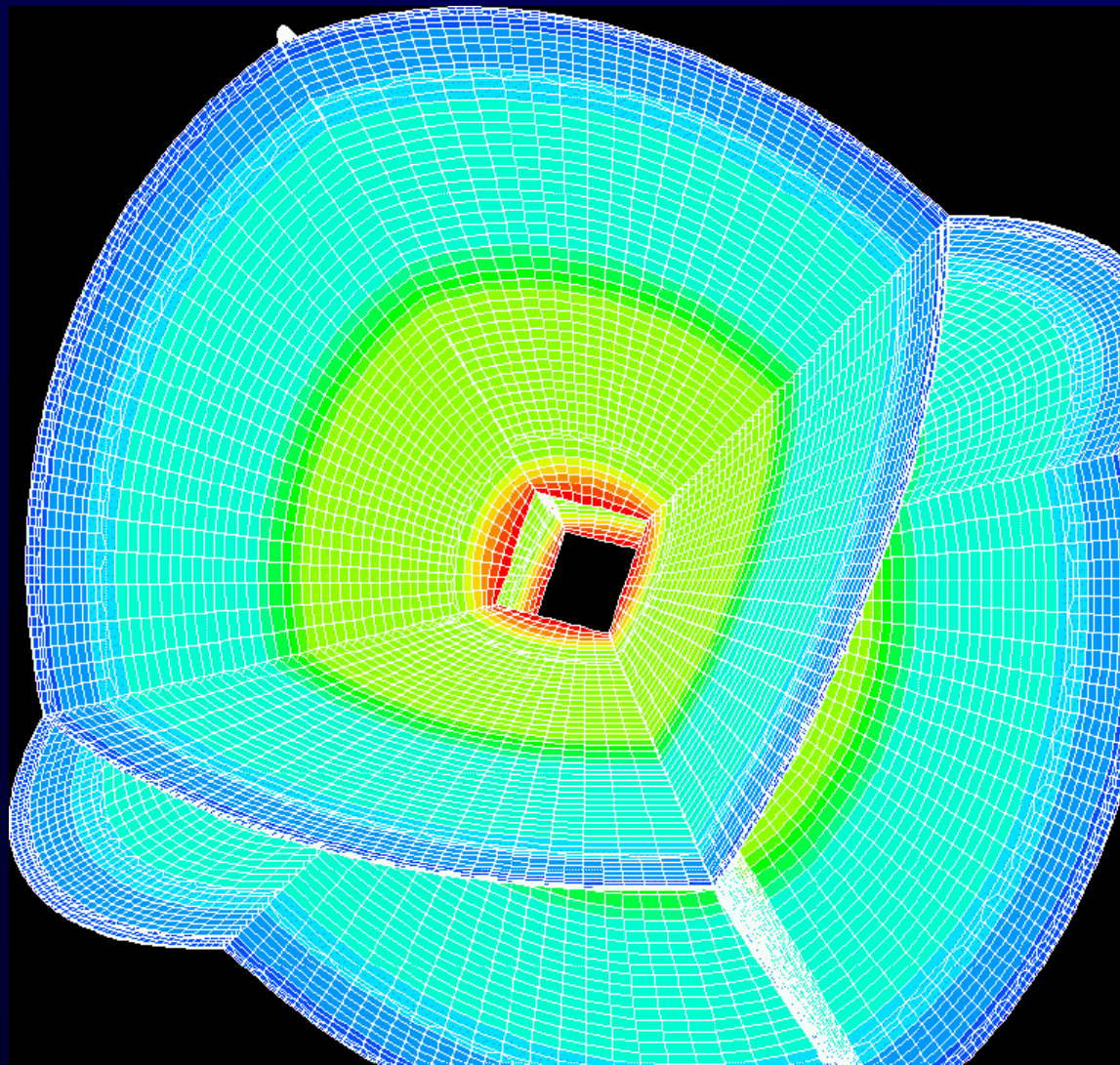
Thin crust, fluid outer core, high Poisson's ratio in inner core

The Cubed Sphere

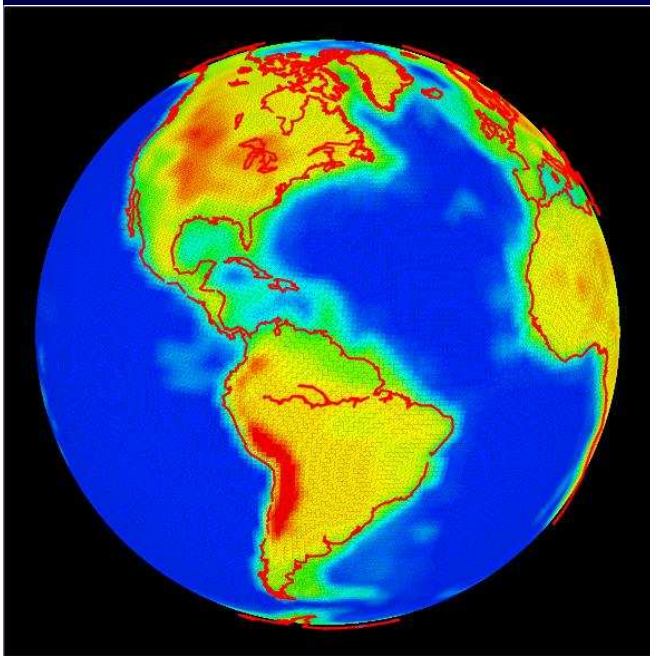


- “Gnomonic” mapping (Sadourny 1972)
- Ronchi et al. (1996), Chaljub (2000)
- Analytical mapping from six faces of cube to unit sphere

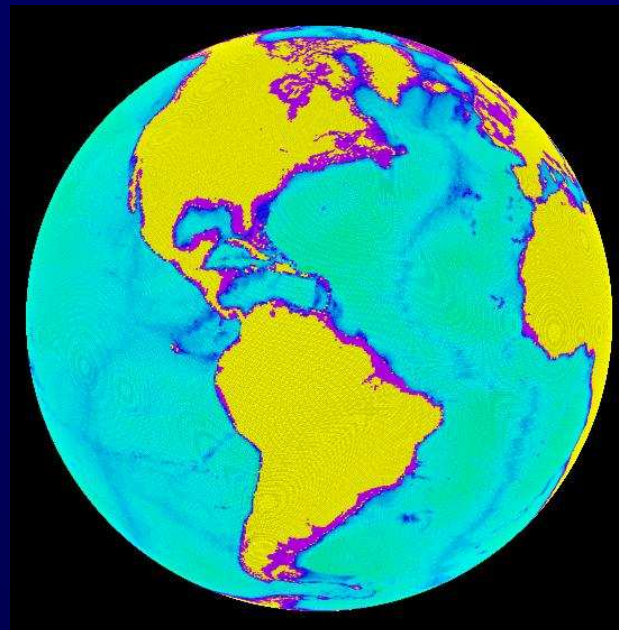
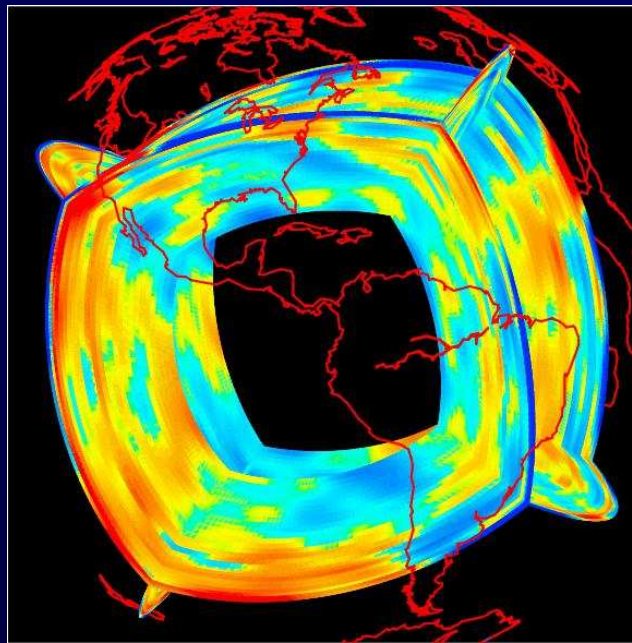
Final Mesh



Global 3-D Earth



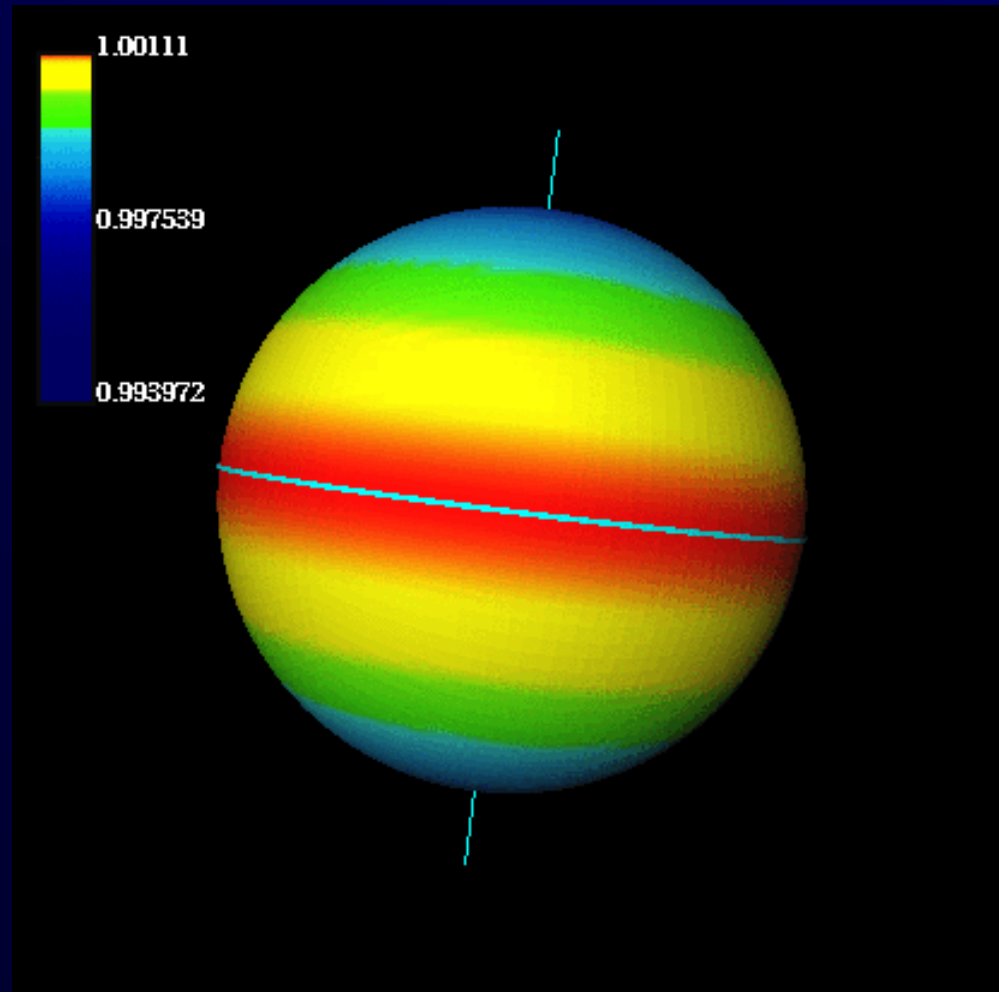
Crust 5.2 (Bassin et al. 2000)
Mantle model S20RTS (Ritsema et al. 1999)



Bathymetry and
ocean load

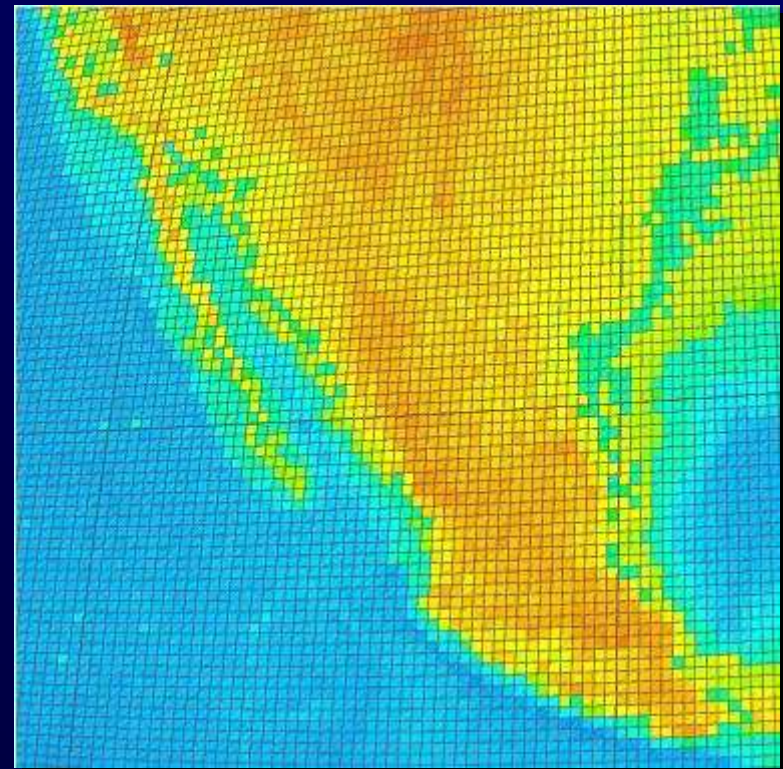
Small modification
of the mesh, no problem

Global 3-D Earth




Ellipticity and topography

Small modification
of the mesh, no problem




Other options for the global Earth

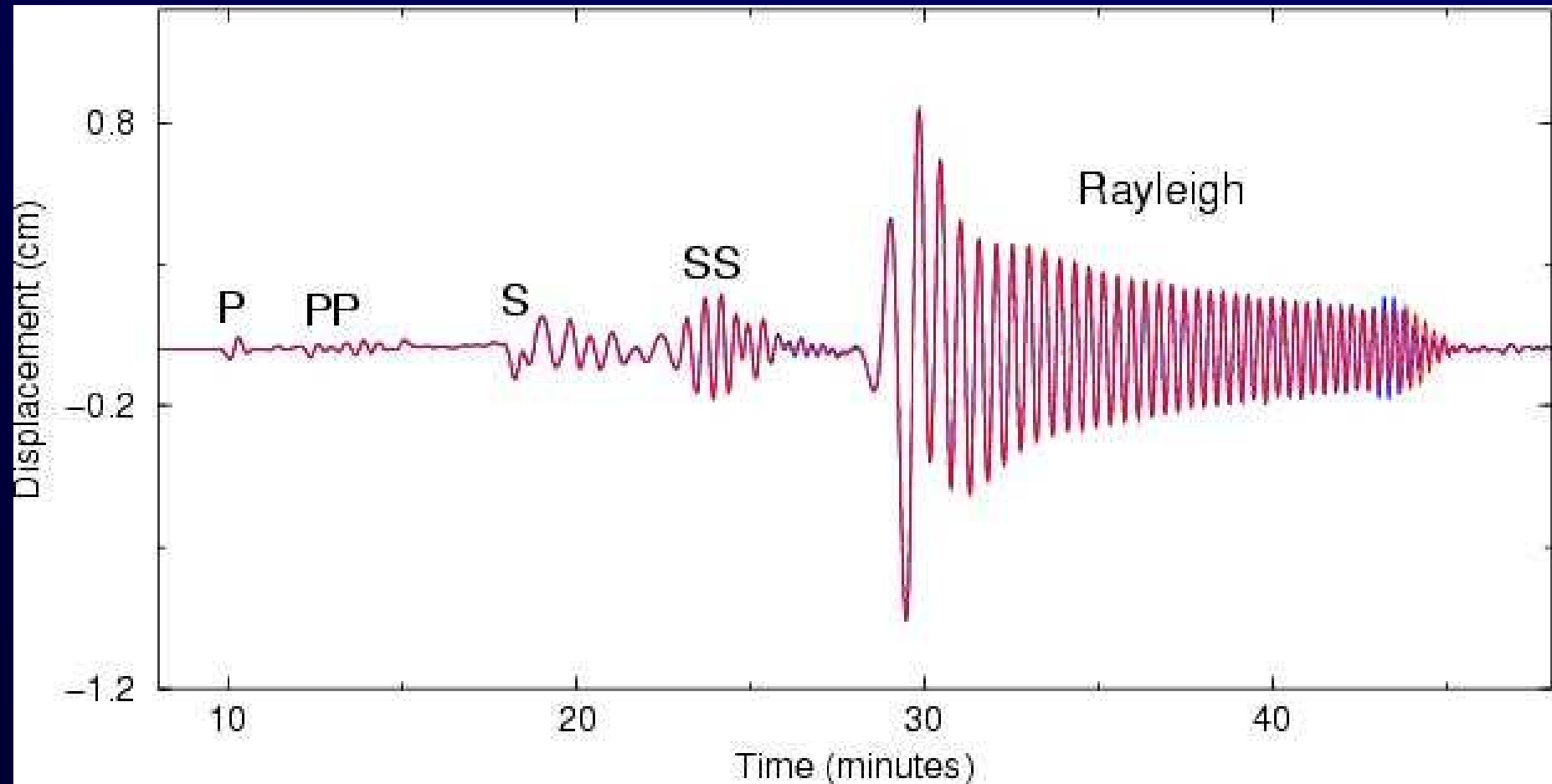
- Non-conforming meshes : Mortar method (Bernardi and Maday 1995, Chaljub 2000)
 - Coupling with normal-modes : Capdeville, Vilotte and Montagner (2000)
-



Benchmarks of the SEM at the global scale

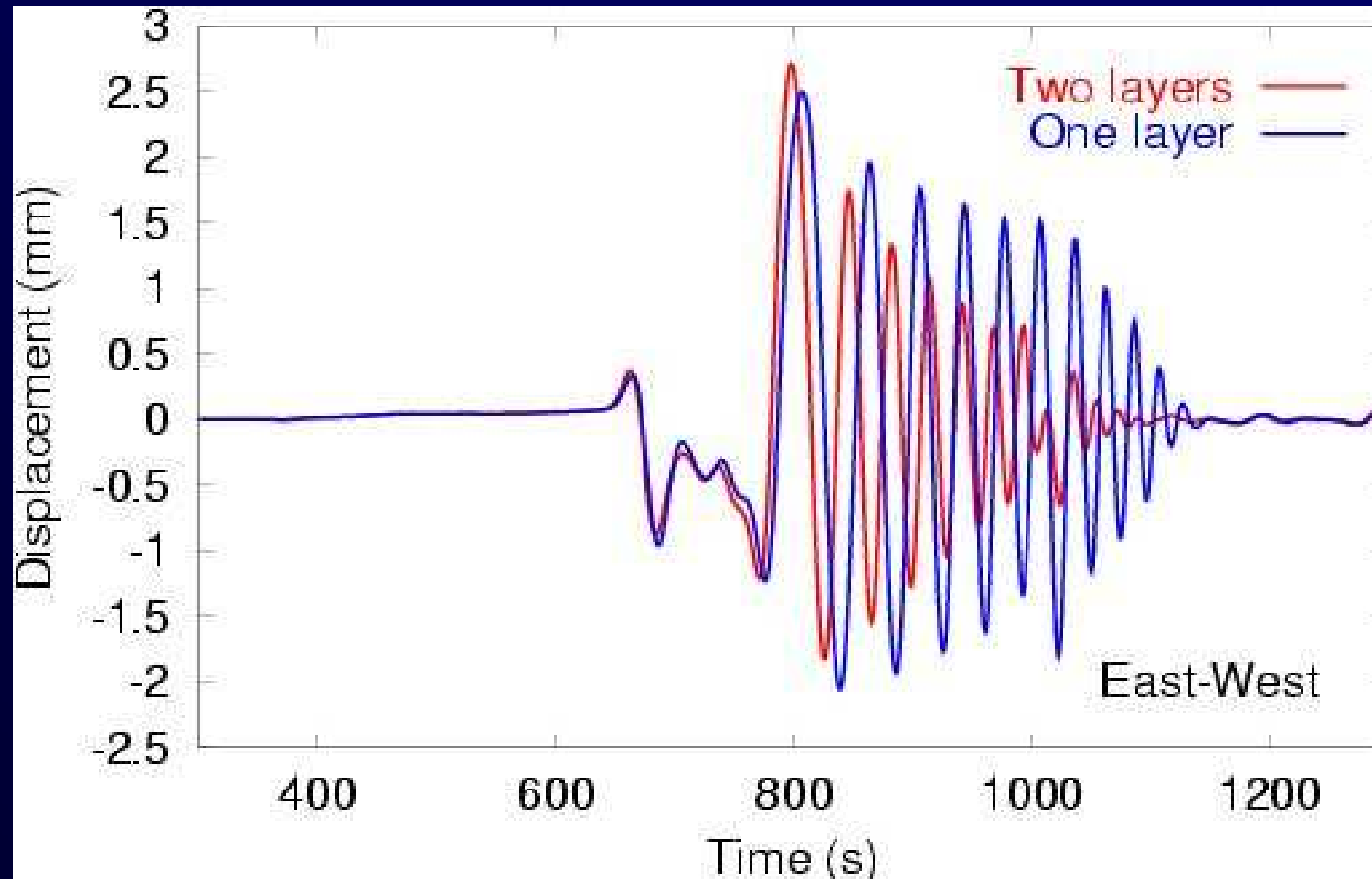


Accurate surface waves



Excellent agreement with normal modes – Depth 15 km
Anisotropy included

Effect of the crust



Large effect on surface waves – dispersion

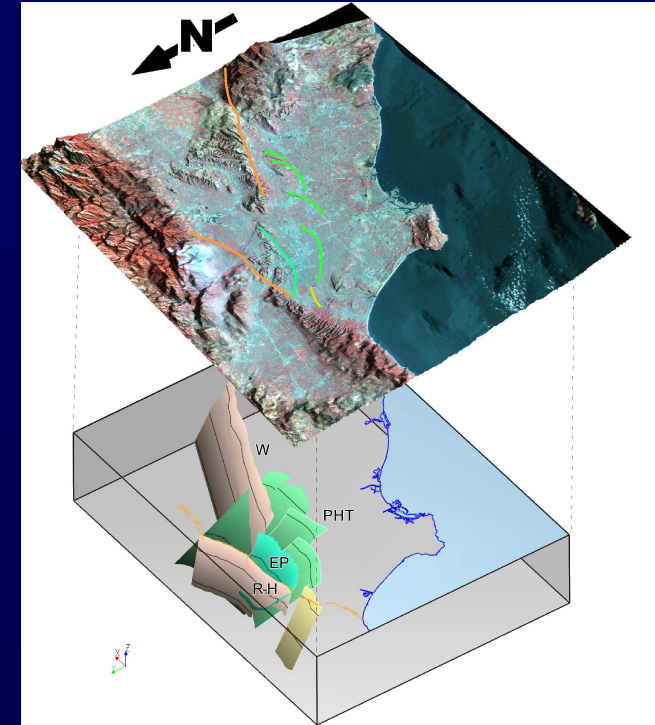
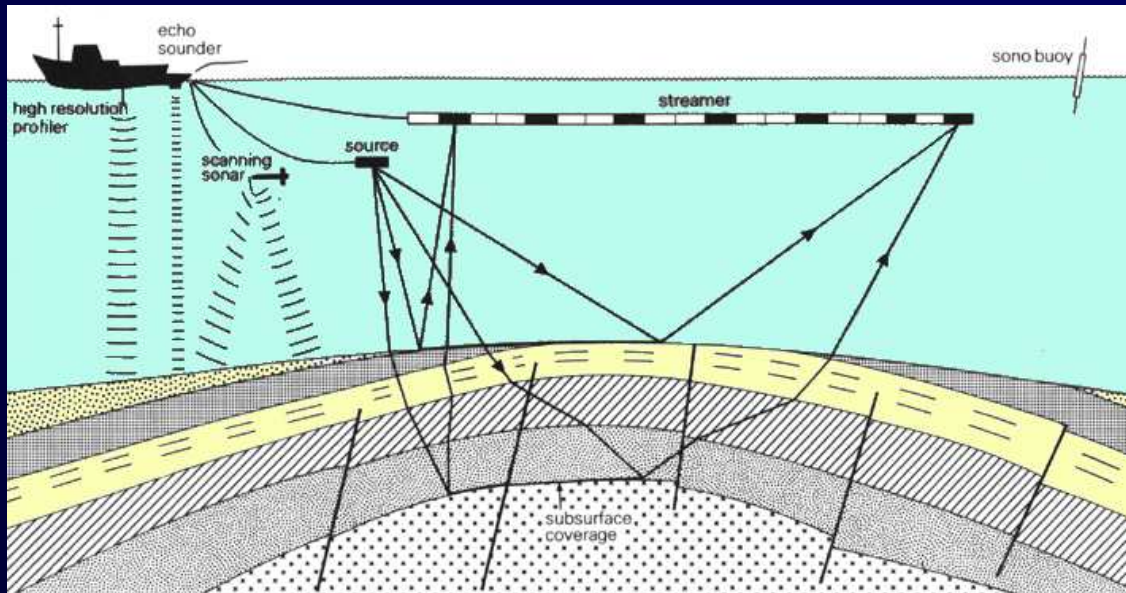
Part II – More complex models or equations



Oil industry applications



Collaboration with the oil industry



Dynamic geophysical technique of imaging subsurface geologic structures by generating sound waves at a source and recording the reflected components of this energy at receivers.

The Seismic Method is the *industry standard* for locating subsurface oil and gas accumulations.

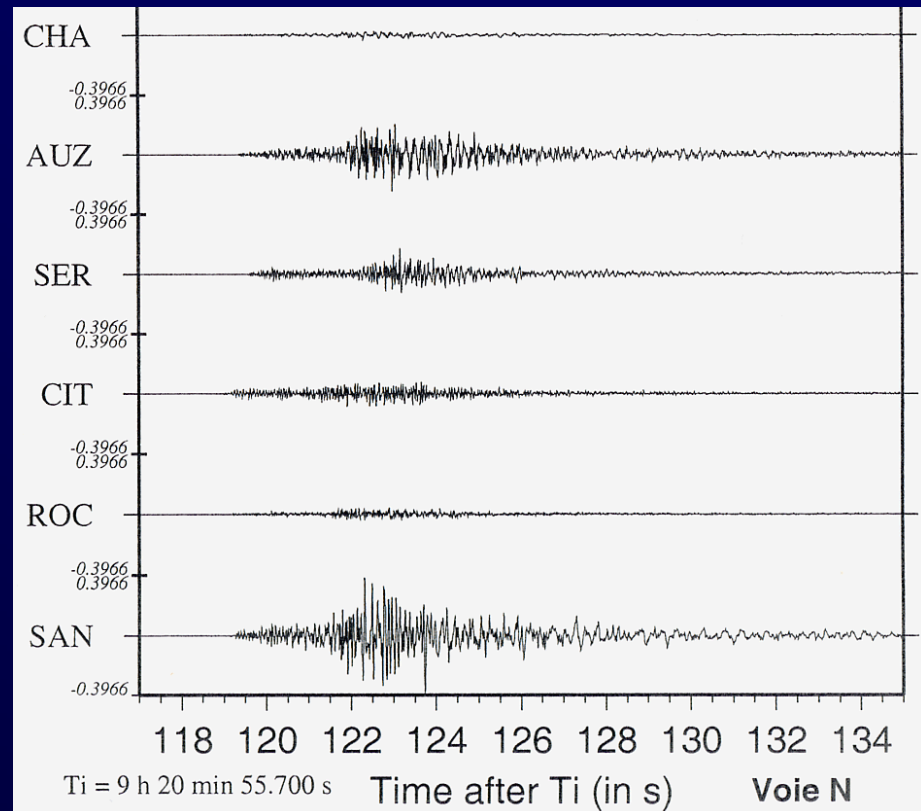
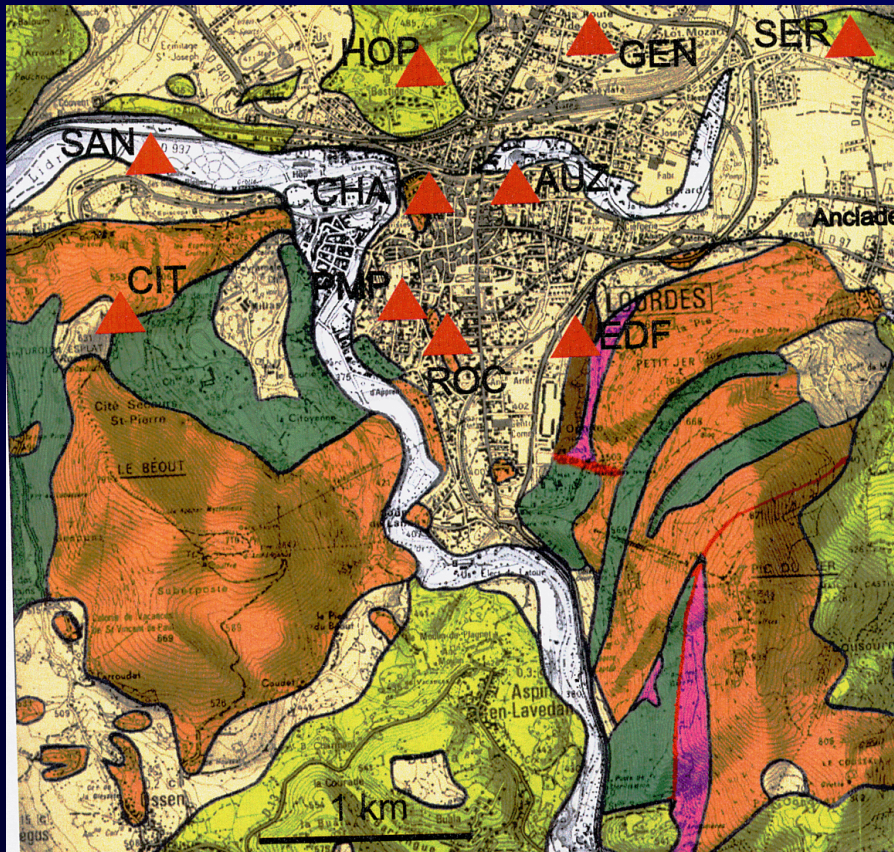


Site effect applications



Échelle locale (effets de site)

- Variations locales très significatives, non reproduites par un calcul 1D (Dubos et Souriau)



Valorisation du réseau accélérométrique permanent (RAP)

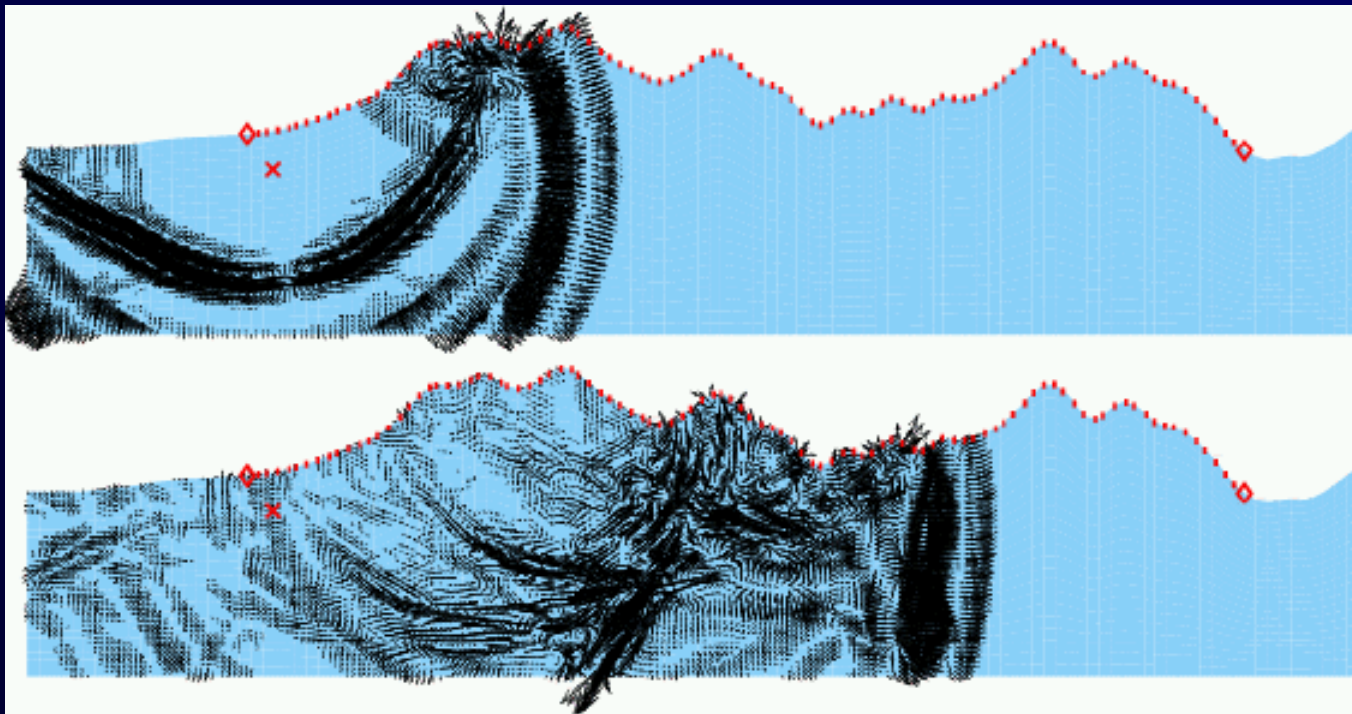


Topography



Topography

- Use flexibility of mesh generation
- Accurate free-surface condition





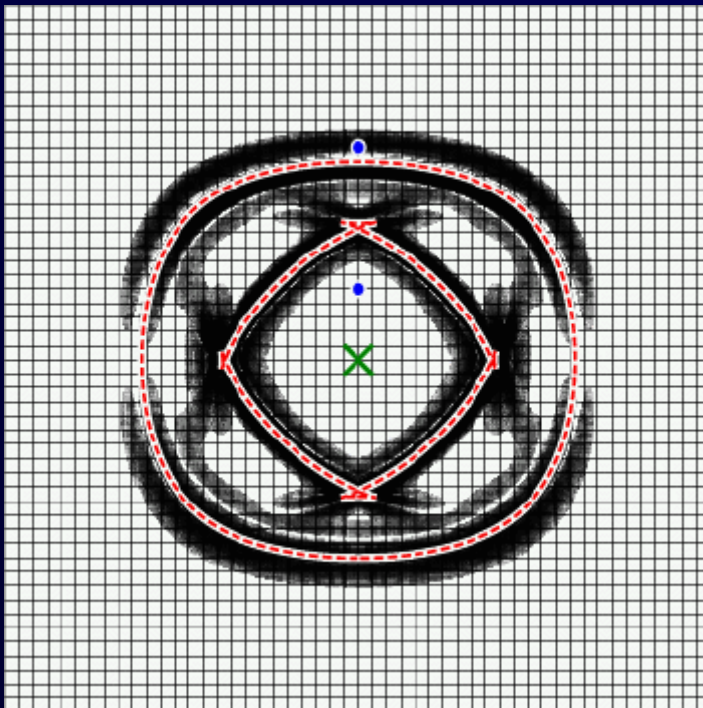
Anisotropy



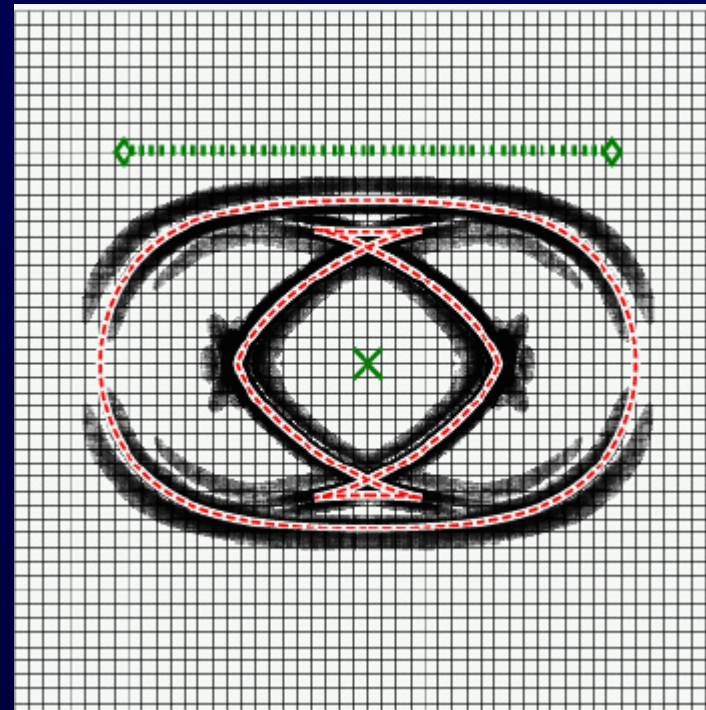
Anisotropy

- Easy to implement up to 21 coefficients
- No interpolation necessary
- Tilted axes can be modeled
- **Attenuation** can also be included

Cobalt

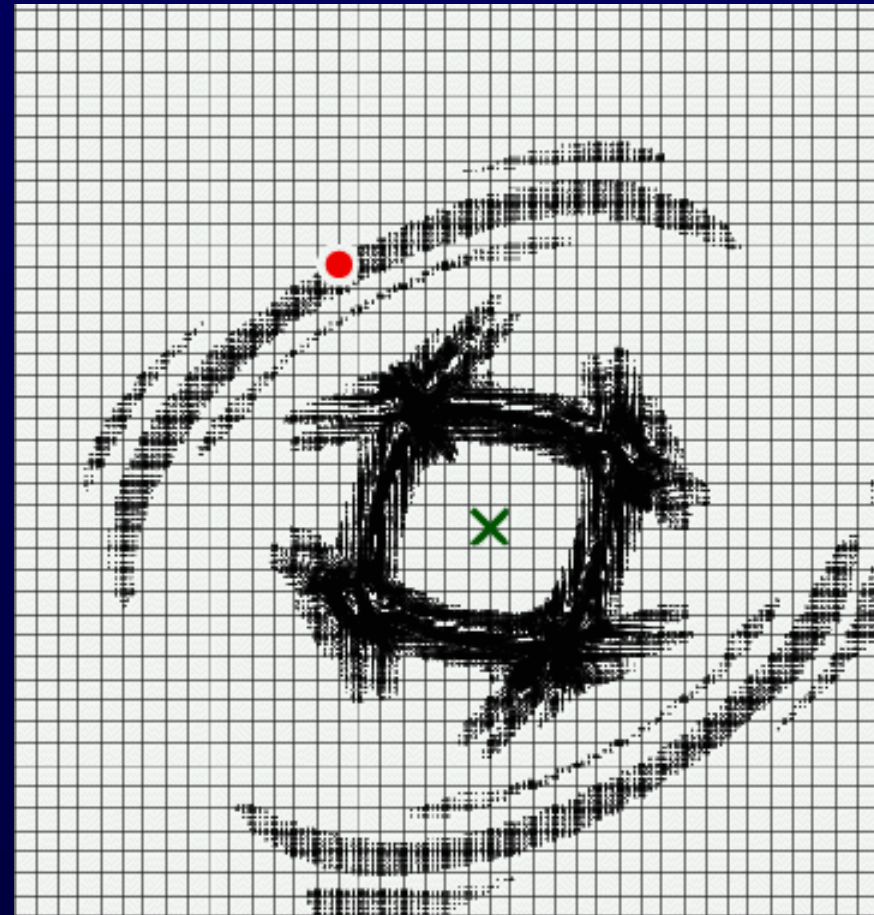


Zinc

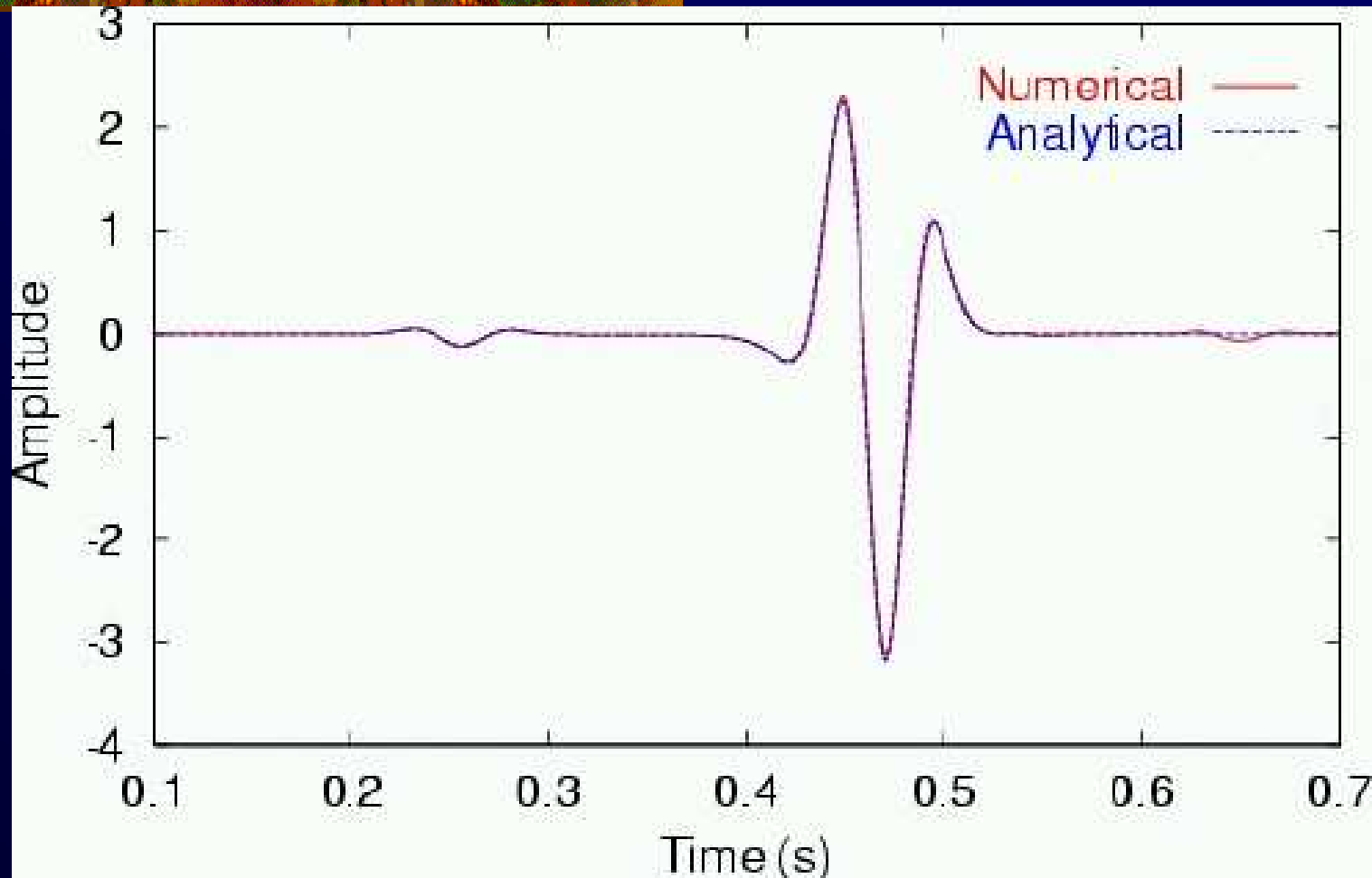


Anisotropy – Tilted 3D case

- Transversely isotropic with rotated axis
- Most of the 21 coefficients $\neq 0$
- Carcione (1988): analytical solution



Tilted 3D case: analytical solution



- Excellent fit for both qP and qS
- Small phase reflected off model edge



Attenuation



Attenuation

- Constitutive relationship:

$$\mathbf{T}(t) = \int_{-\infty}^t \partial_t \mathbf{c}(t - t') : \nabla \mathbf{s}(t') dt'$$

Difficult in time domain methods because of convolution

- Use L standard linear solids to make an absorption-band model:

$$\mu(t) = \mu_R \left[1 - \sum_{\ell=1}^L \left(1 - \tau_{\ell}^{\varepsilon} / \tau_{\ell}^{\sigma} \right) e^{-t/\tau_{\ell}^{\sigma}} \right] H(t)$$

Attenuation

- Constitutive relationship becomes:

$$\mathbf{T} = \mathbf{c}_U : \nabla \mathbf{s} - \sum_{\ell=1}^L \mathbf{R}_\ell$$

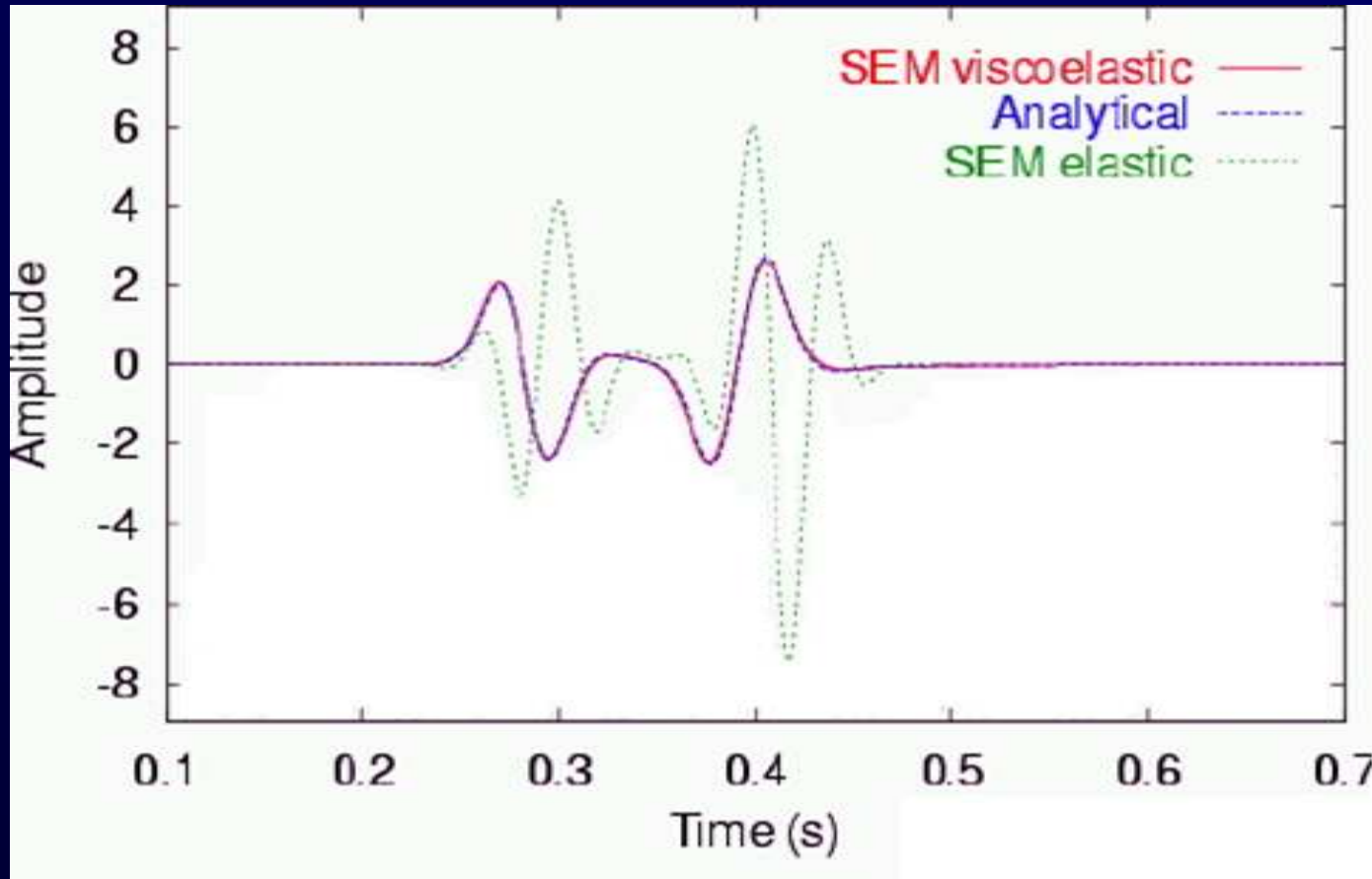
- Memory variable equation:

$$\partial_t \mathbf{R}_\ell = - (\mathbf{R}_\ell - \delta \mu_\ell \mathbf{D}) / \tau_\ell^\sigma$$

where \mathbf{D} is the strain deviator:

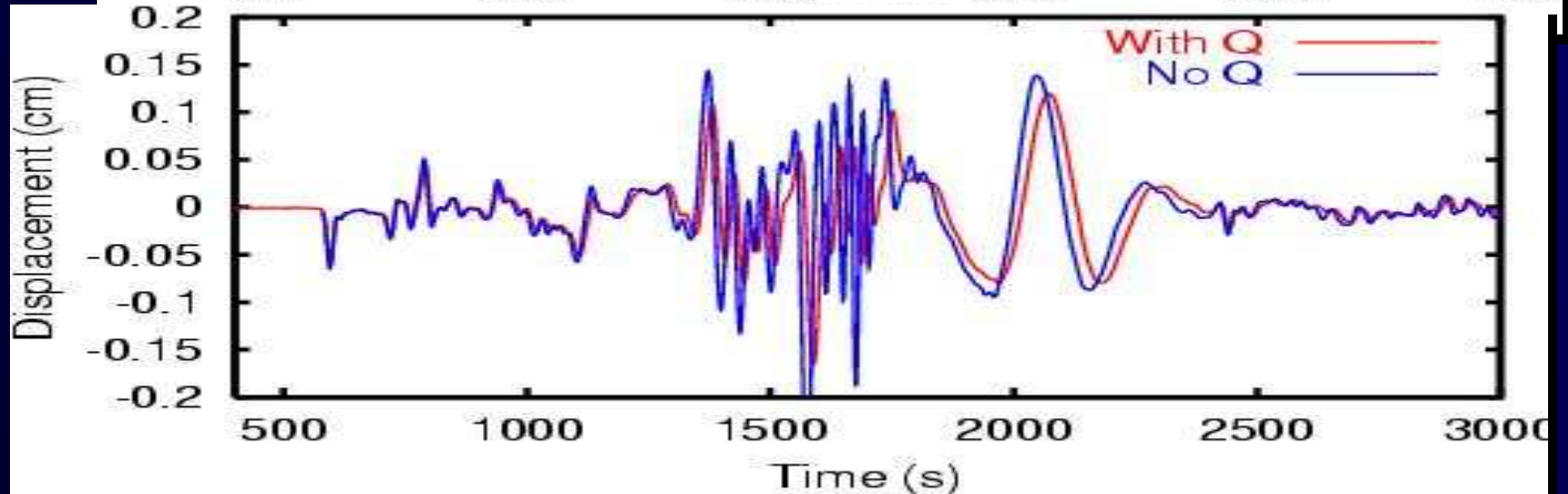
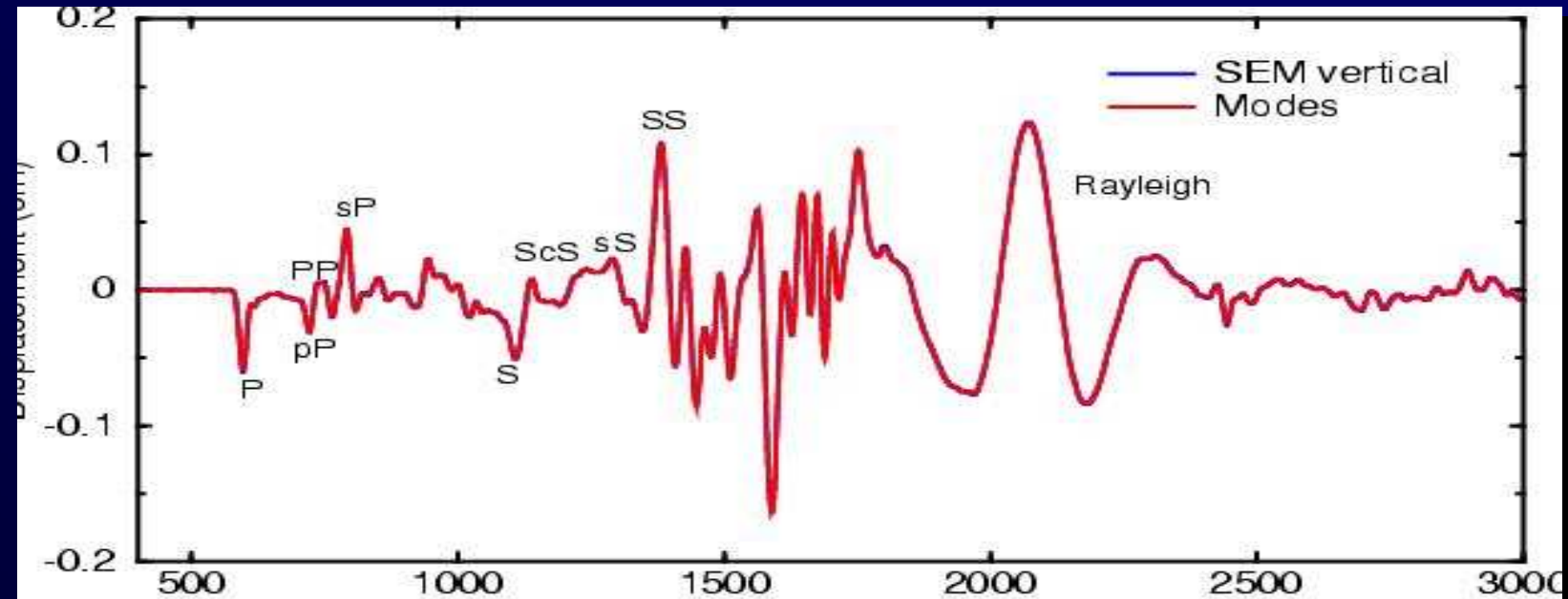
$$\mathbf{D} = \frac{1}{2} \left[\nabla \mathbf{s} + (\nabla \mathbf{s})^T \right] - \frac{1}{3} (\nabla \cdot \mathbf{s}) \mathbf{I}$$


Attenuation




- Problématique en temps – Variables à mémoire
- Difficulté: facteur de qualité Q constant
- Implémenter avec le minimum de mémoire possible

Effect of Attenuation



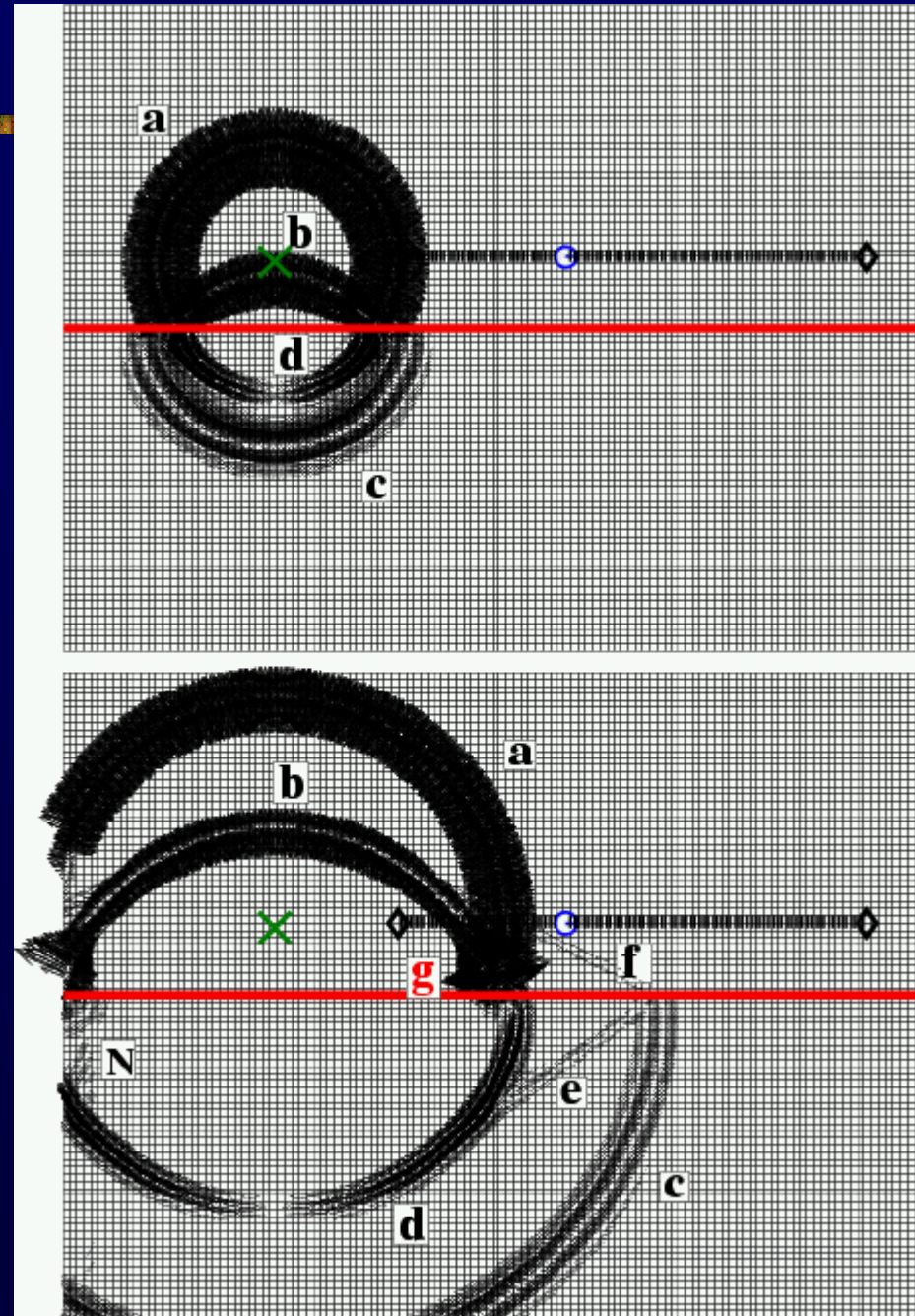


Fluid-solid coupling



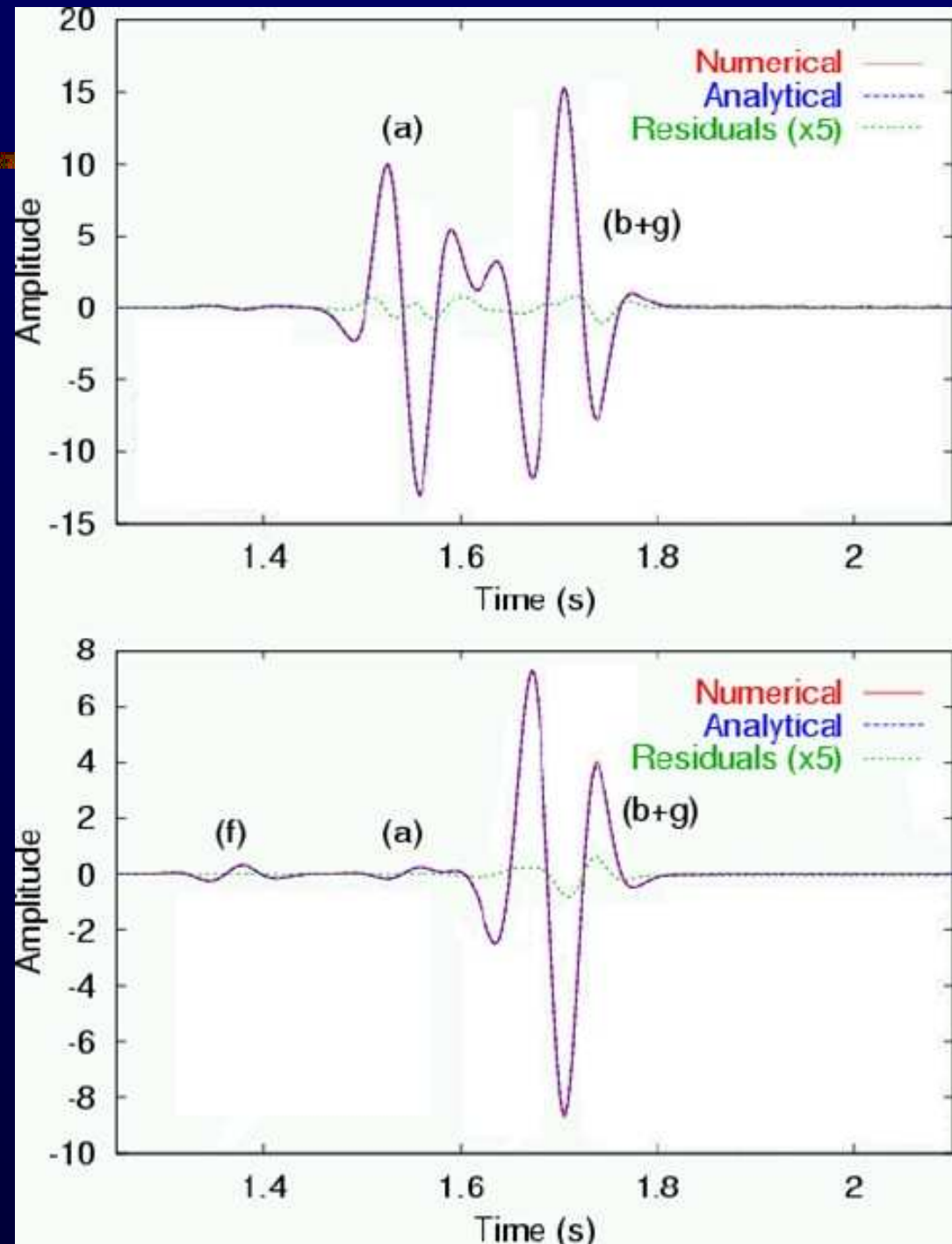
Fluid/solid boundaries

- Difficult with classical finite elements
- We use a velocity potential in the fluid
- Keep diagonal mass matrix



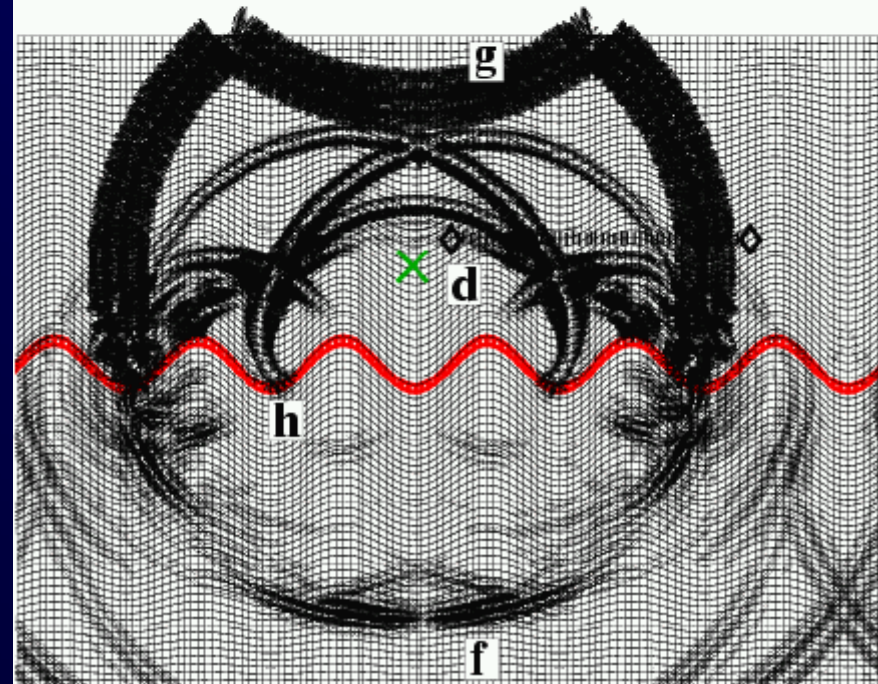
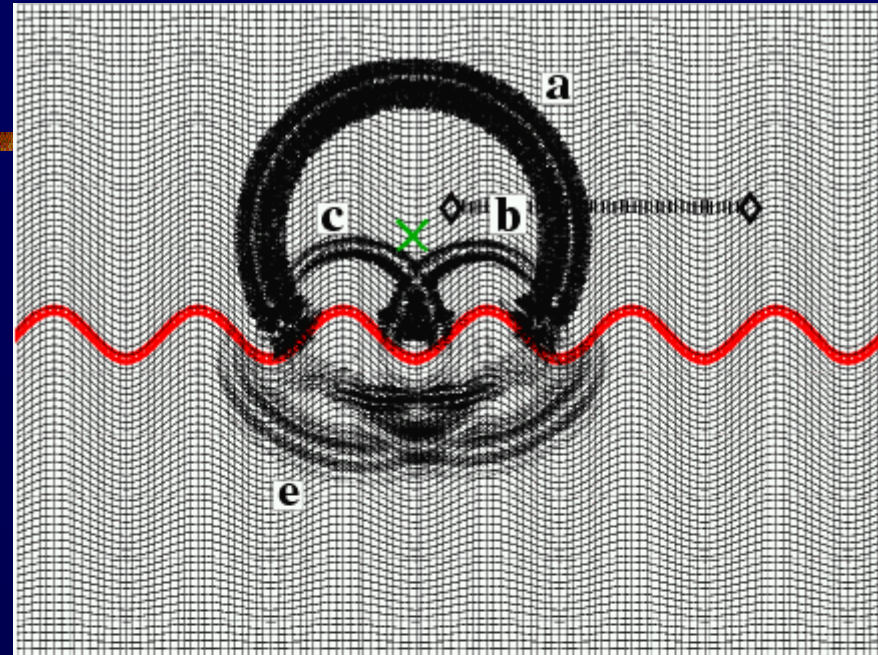
Analytical solution


- Very good fit
- Validation of the method
- Refracted phases accurately modeled




Bathymetry

- Use flexibility of mesh generation process
- Triplications
- Stoneley





Oceans (effect of the ocean load)



Effect of the Oceans

Modified weak form with ocean floor integral:

$$\int \rho \mathbf{w} \cdot \partial_t^2 \mathbf{s} d^3 \mathbf{r} = - \int \nabla \mathbf{w} : \mathbf{T} d^3 \mathbf{r}$$

$$+ \mathbf{M} : \nabla \mathbf{w}(\mathbf{r}_s) S(t) - \int_{F-S} p \mathbf{w} \cdot \hat{\mathbf{n}} d^2 \mathbf{r}$$

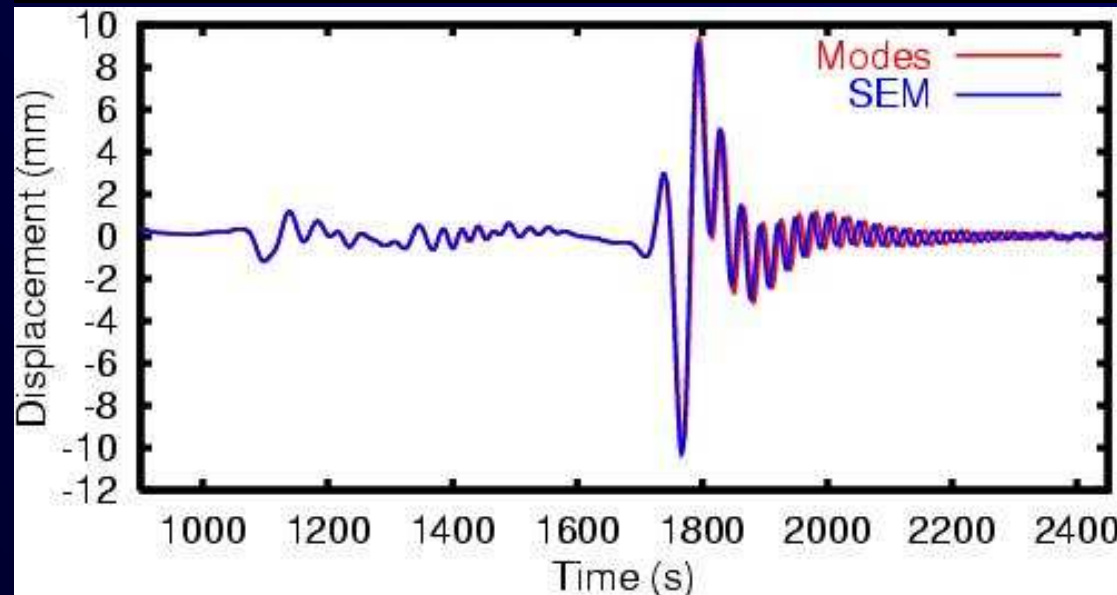
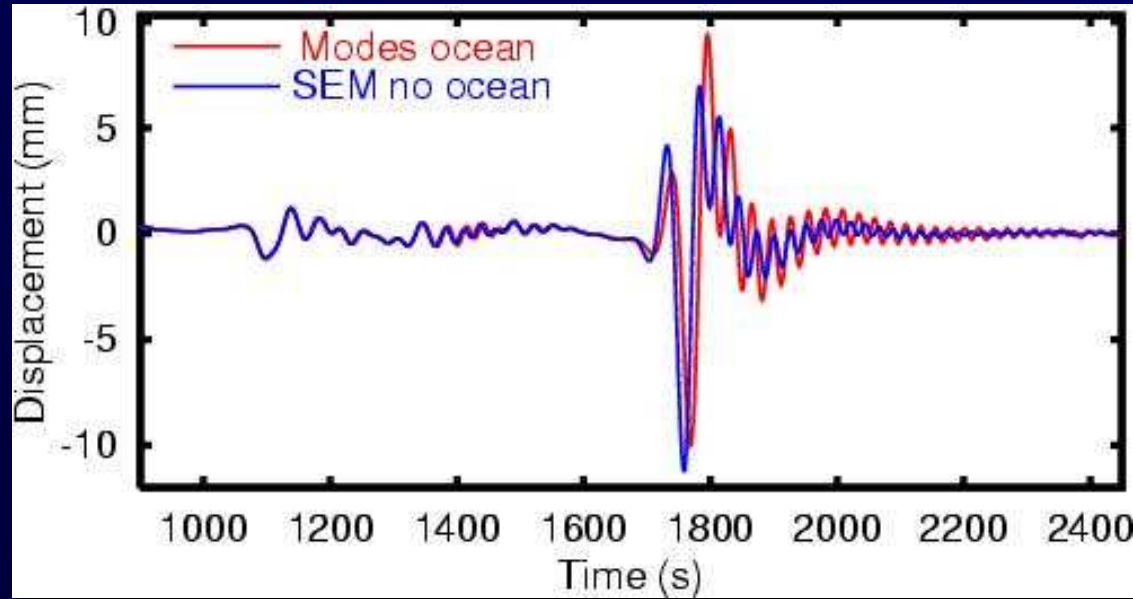
Ocean load:

$$p = \rho_w h \hat{\mathbf{n}} \cdot \partial_t^2 \mathbf{s}$$

weight of column of water,
zero thickness

Good approximation if wavelength \gg thickness of oceans
(good at 20 s, not good at 1 s)

Effect of the Oceans



Depth 18 km

SEM without oceans

Effect of oceans
⇒ on surface waves
is significant for
shallow events

SEM with ocean load



Gravity / rotation



Self-Gravitation and Rotation

- Strong form:

$$\rho \left(\partial_t^2 \mathbf{s} + 2\boldsymbol{\Omega} \times \partial_t \mathbf{s} \right) = \nabla \cdot \mathbf{T} + \nabla (\rho \mathbf{s} \cdot \mathbf{g})$$

$$- \rho \nabla \phi - \nabla \cdot (\rho \mathbf{s}) \mathbf{g} + \mathbf{f}$$

- Neglect mass redistribution - **Cowling approximation** (Valette 1986, Dalhen and Tromp 1998, Chaljub 2000):

$$\rho \left(\partial_t^2 \mathbf{s} + 2\boldsymbol{\Omega} \times \partial_t \mathbf{s} \right) = \nabla \cdot \mathbf{T} + \nabla (\rho \mathbf{s} \cdot \mathbf{g})$$

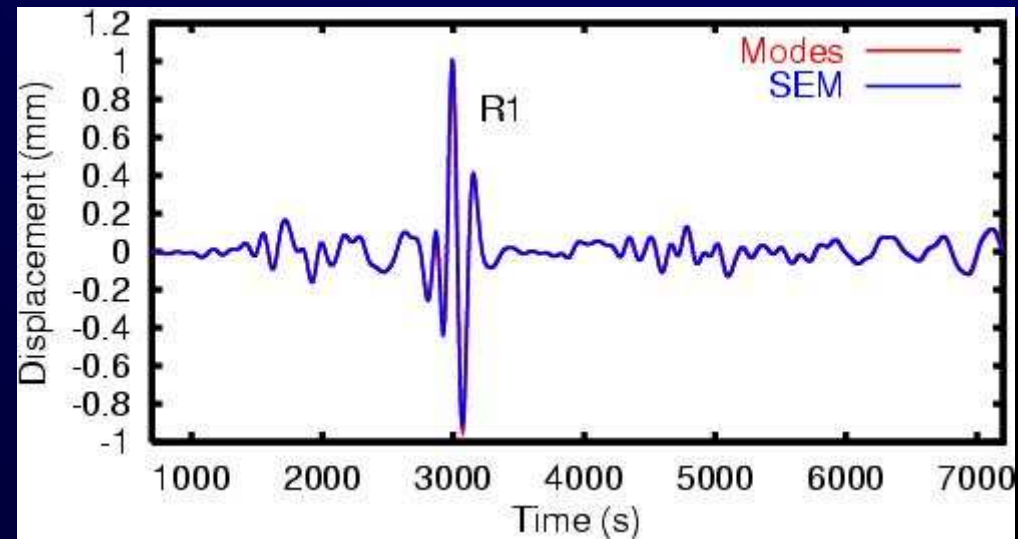
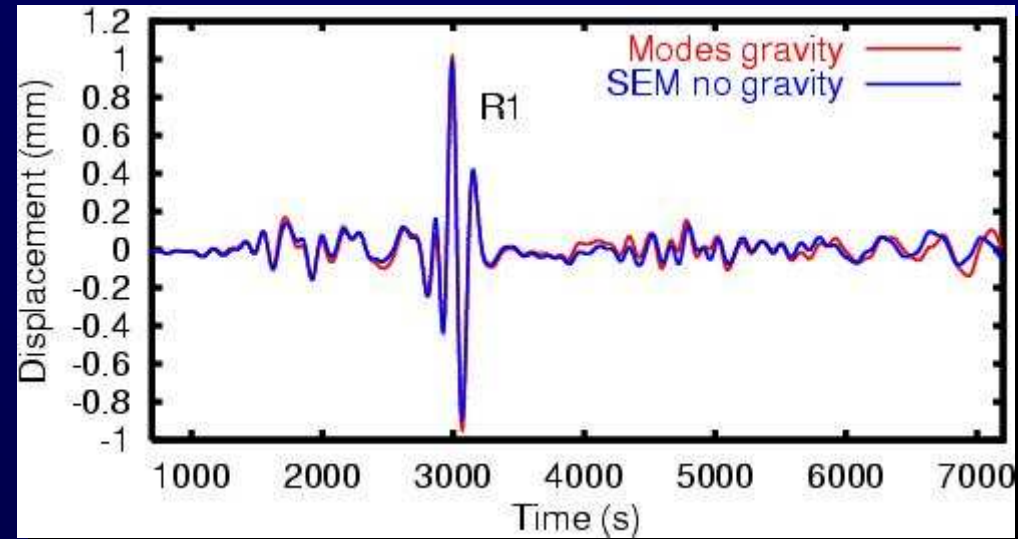
$$- \nabla \cdot (\rho \mathbf{s}) \mathbf{g} + \mathbf{f}$$

Effect of Self-Gravitation

- Main effect is long period oscillation
- Very well reproduced by the spectral-element method



Irian Jaya - depth 15 km





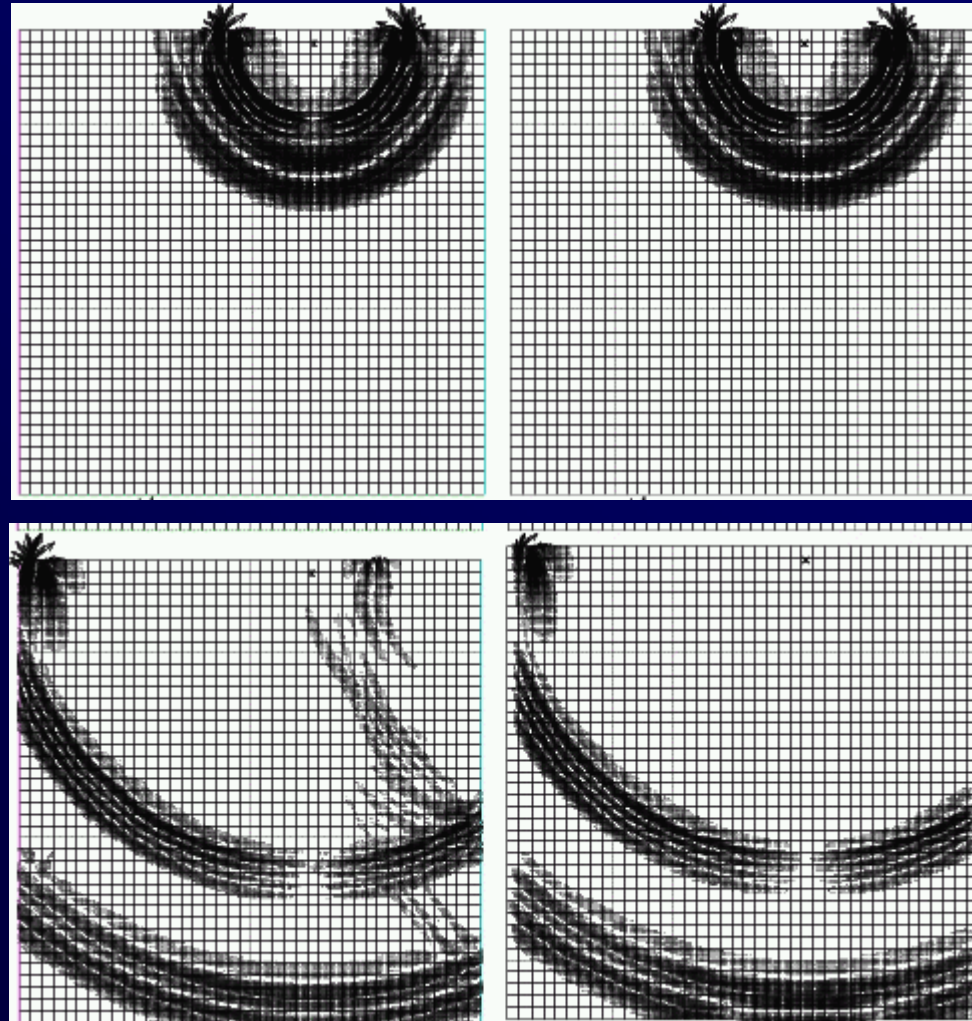
PML

absorbing
conditions



Absorbing conditions

- Used to be a big problem
- Bérenger 1994
- INRIA (Collino, Cohen)
- Extended to second-order systems by Komatitsch and Tromp (2003)



PML (Perfectly Matched Layer) \Rightarrow H el ene Barucq

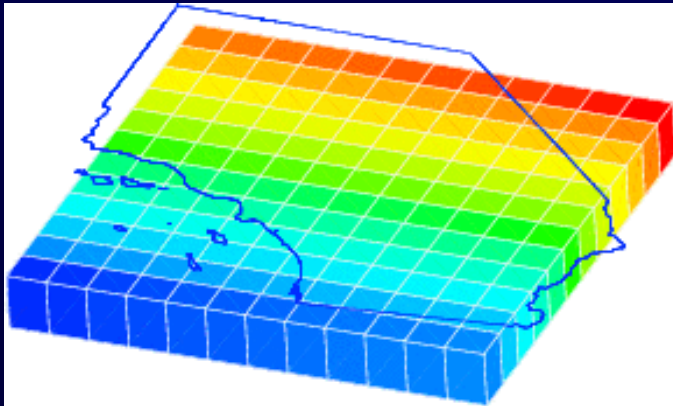


Parallel implementation

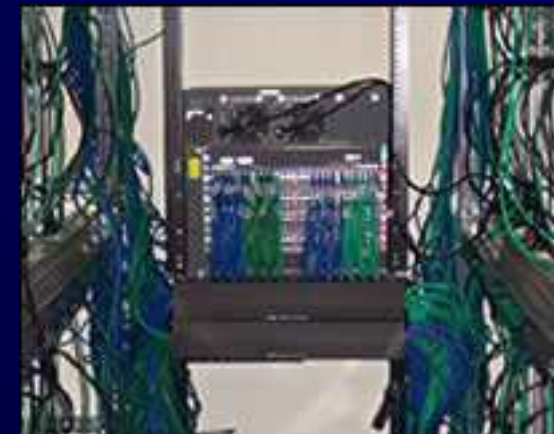
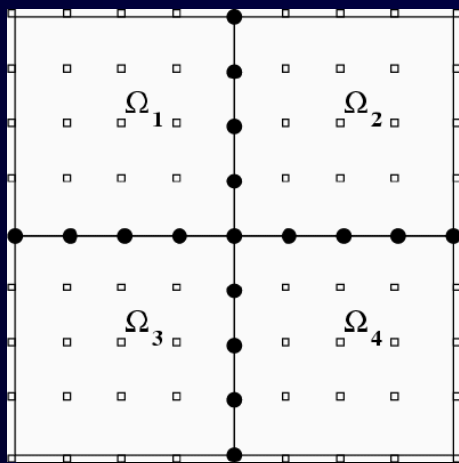


Construction du cluster

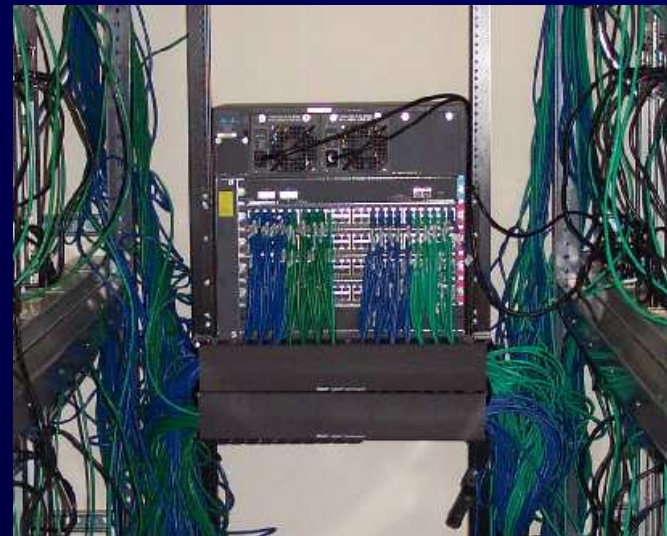
320 processeurs - Linux



160 Gb de mémoire

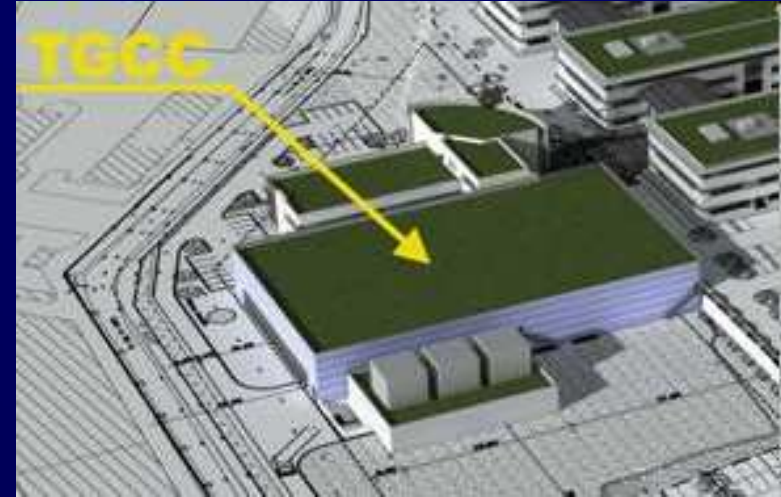


Construction du cluster de Caltech



320 processeurs, 160 Gb de mémoire
Été 2000, maintenant « obsolète », renouvellement en cours

TGCC + PRACE



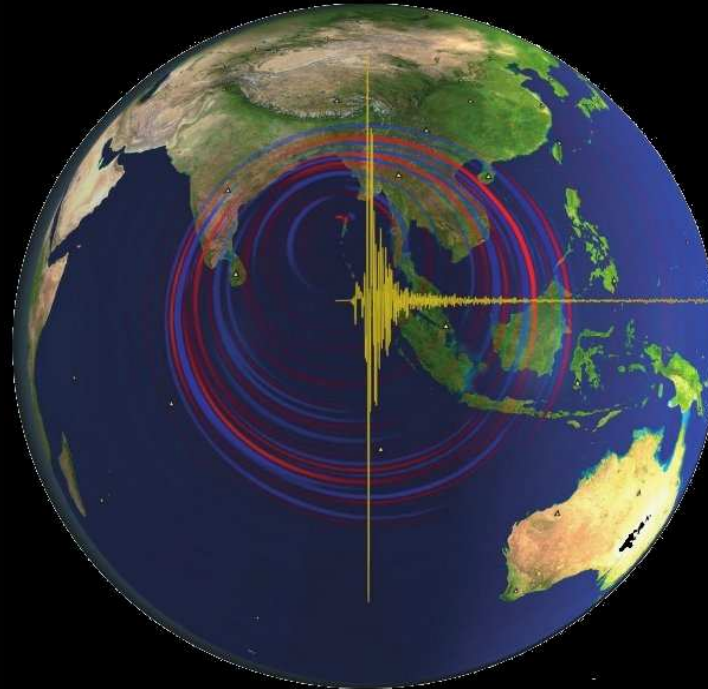
- Salles informatiques : 2600 m²
- Alimentation électrique : ligne de 60 MW
- L'échelle du petaflop pour le calculateur de la future infrastructure Européenne

<http://www.teratec.eu/technopole/tgcc.html>

Le TGCC (Très Grand Centre de Calcul) sera disponible en 2010 pour accueillir la machine Européenne PRACE financée par GENCI.

GENCI (Grand Équipement National de Calcul Intensif)

Our SPECFEM3D software package



Dimitri Komatitsch
Jeroen Tromp
Qinya Liu
David Michéa

Min Chen
Vala Hjörleifsdóttir
Jesús Labarta
Nicolas Le Goff
Pieyre Le Loher
Alessia Maggi
Roland Martin
Brian Savage
Bernhard Schuberth
Carl Tape

...

Goal: modeling seismic wave propagation in the full Earth or in densely populated regions following large earthquakes

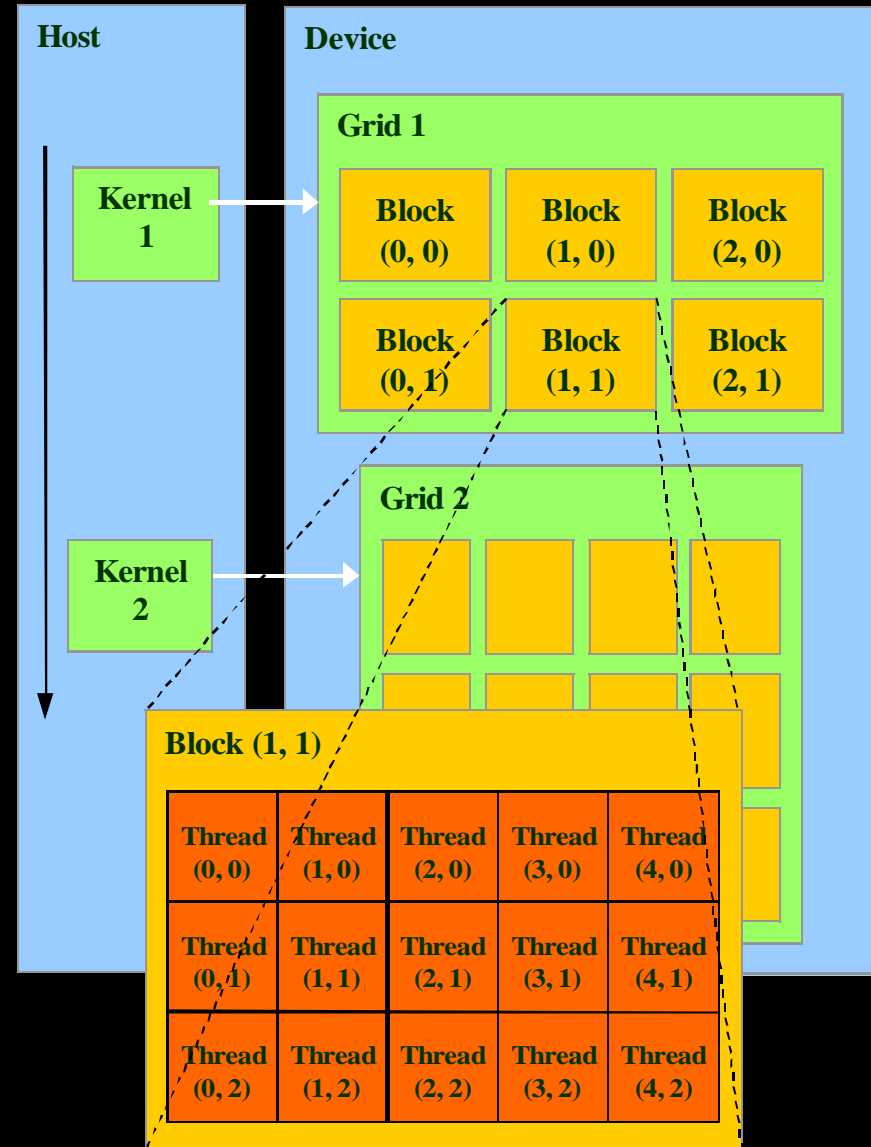
The SPECFEM3D source code is open (GNU GPL v2)

Mostly developed by **Dimitri Komatitsch and Jeroen Tromp** at Harvard University, Caltech and Princeton (USA) and University of Pau (France) since 1996.

Improved with the Barcelona Supercomputing Center, Spain (Jesús Labarta et al.) and David Michéa (INRIA, Pau, HPC-Europa program, 2007), Nicolas Le Goff, Pieyre Le Loher and Roland Martin (CNRS and INRIA, Pau).

Graphics cards

NVIDIA GeForce 8800 GTX

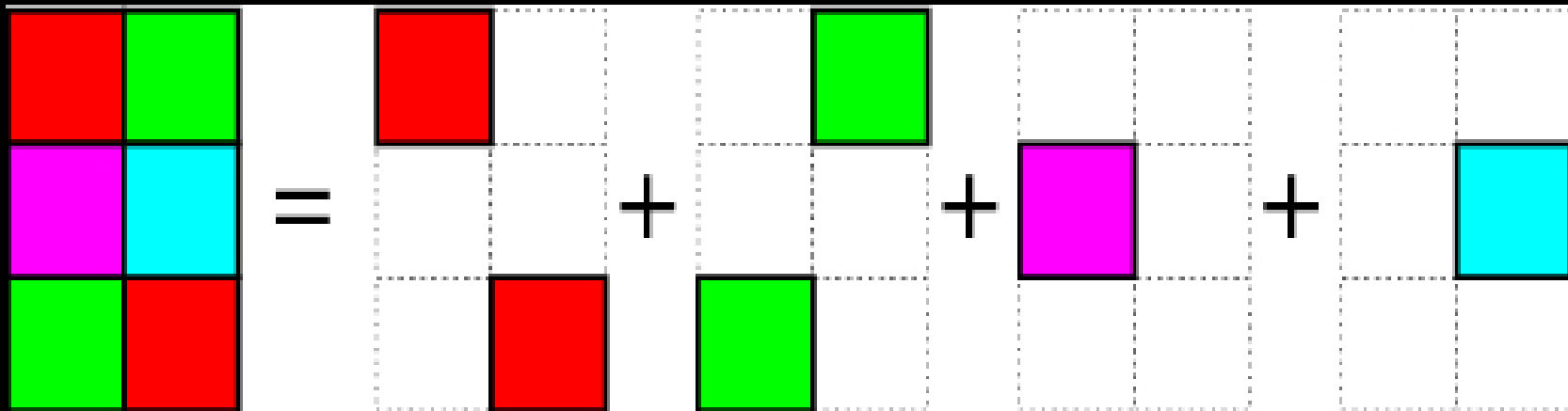
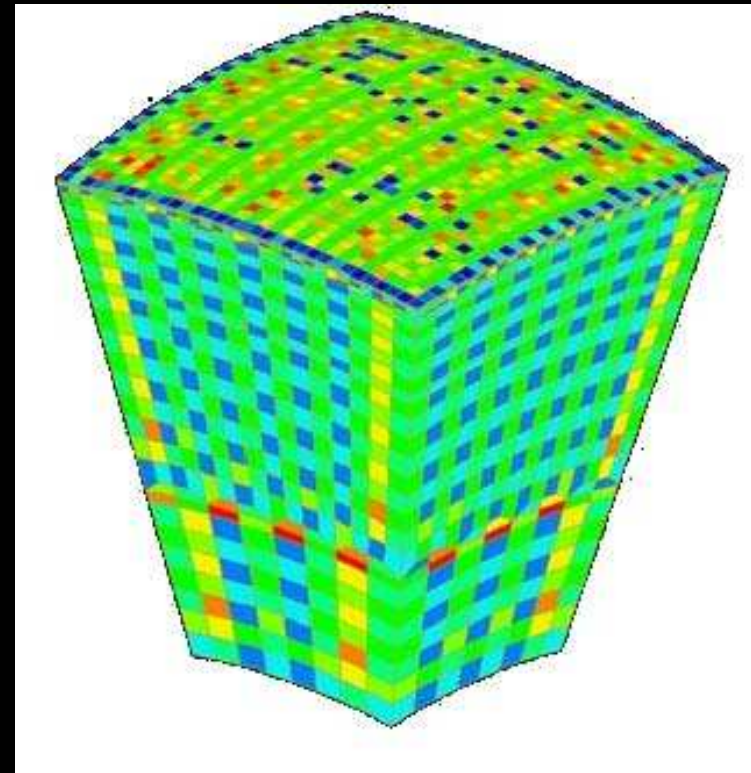


Minimize CPU ↔ GPU data transfers

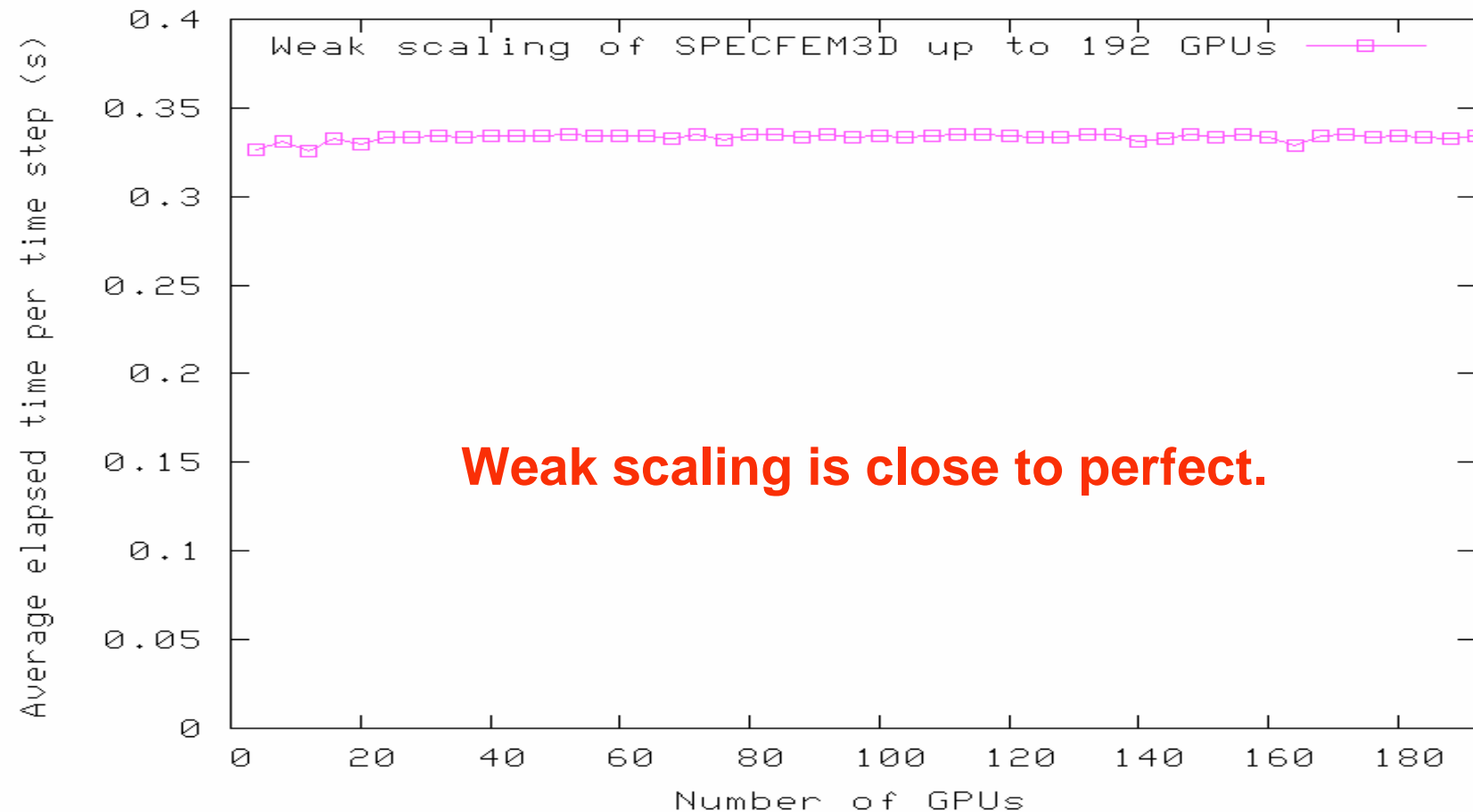
- CPU ↔ GPU memory bandwidth much lower than GPU memory bandwidth
 - Use page-locked host memory (`cudaMallocHost()`) for maximum CPU ↔ GPU bandwidth
- Minimize CPU ↔ GPU data transfers by moving more code from CPU to GPU
 - Even if that means running kernels with low parallelism computations
 - Intermediate data structures can be allocated, operated on, and deallocated without ever copying them to CPU memory
- Group data transfers
 - One large transfer much better than many small ones
- Fit all the arrays on the GPU card to avoid costly CPU ↔ GPU data transfers
- But of course the MPI buffers must remain on the CPU, therefore we can not avoid a small number of transfers (of 2D cut planes)

Porting SPECFEM3D on CUDA: mesh coloring

- Key challenge: ensure that contributions from two local nodes never update the same global value from different warps
- **Use of mesh coloring:** suppress dependencies between mesh points inside a given kernel



Multi-GPU weak scaling (up to 192 GPUs)



- It is difficult to define speedup: versus what?
- For us, on the CEA/CCRT/GENCI GPU/Nehalem cluster, about 20x for one GPU versus one CPU core.

Part III

Some real

3D cases studied



Los Angeles basin



The Basin Challenge

- Slow, laterally variable sedimentary layers
- Sharp transitions between sediments and basement, with complex shape (Magistrale et al. 1996, 2000, SCEC)
- Significant topography/bathymetry
- Shape of Moho (Zhu and Kanamori, 2000)
- Attenuation (very poorly constrained)
- Complex source models for large events (Wald et al.)
- Effect of oceans for Channel island stations (small)

Classically computed based on **finite-difference** (Olsen et al. 1996, Graves et al 1996, Peyrat et al 2001) or **finite-element** techniques (Bao et al., Bielak 1998, Moczo). **Not all of above effects included.**

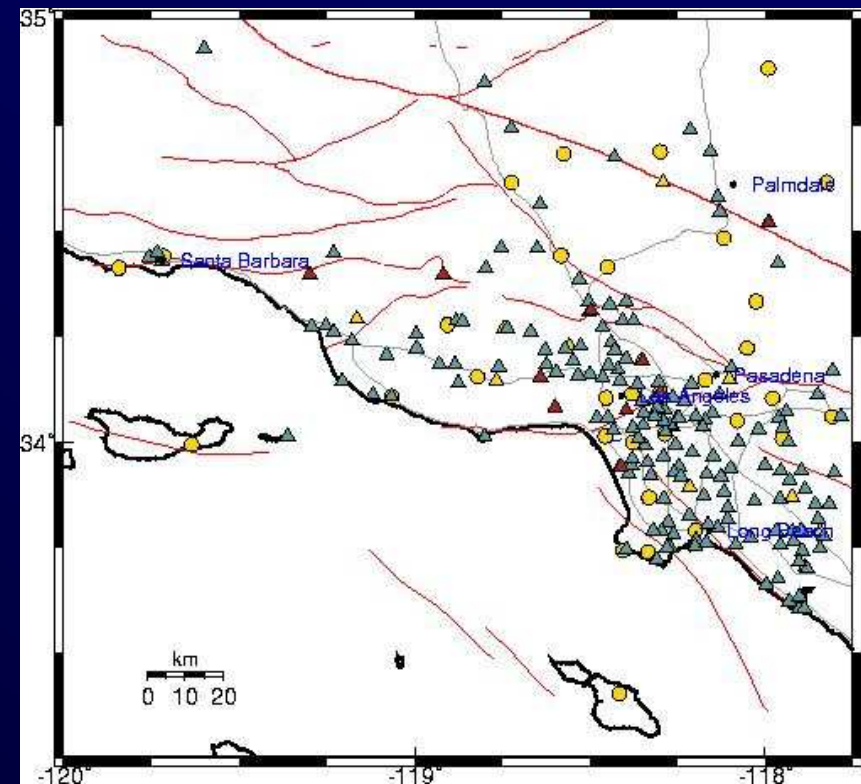
The Los Angeles region



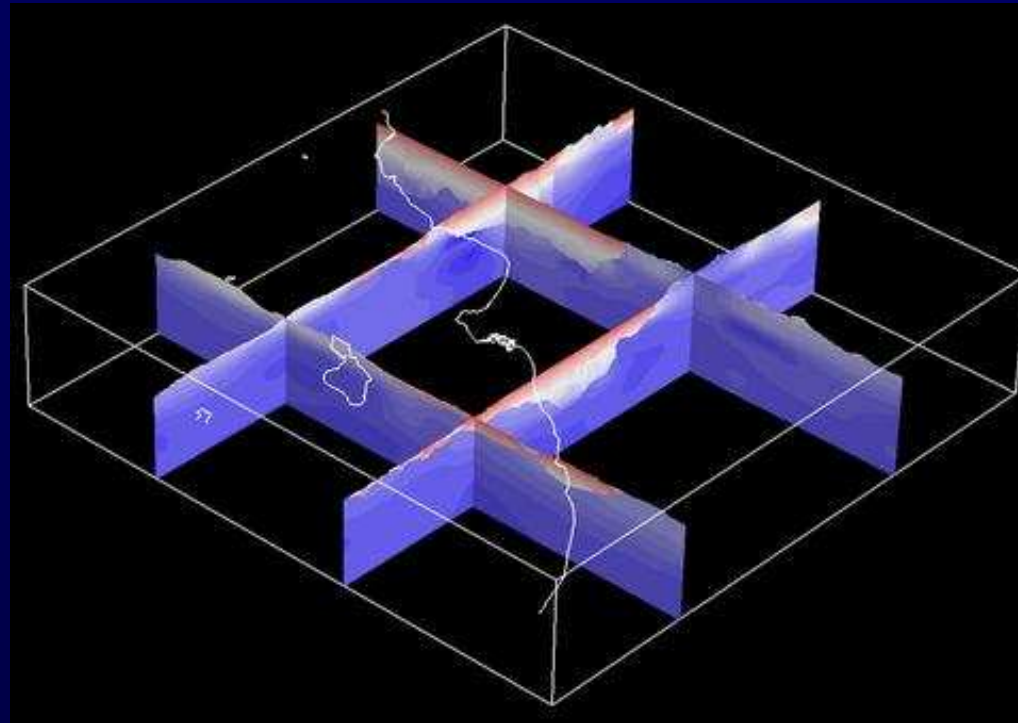
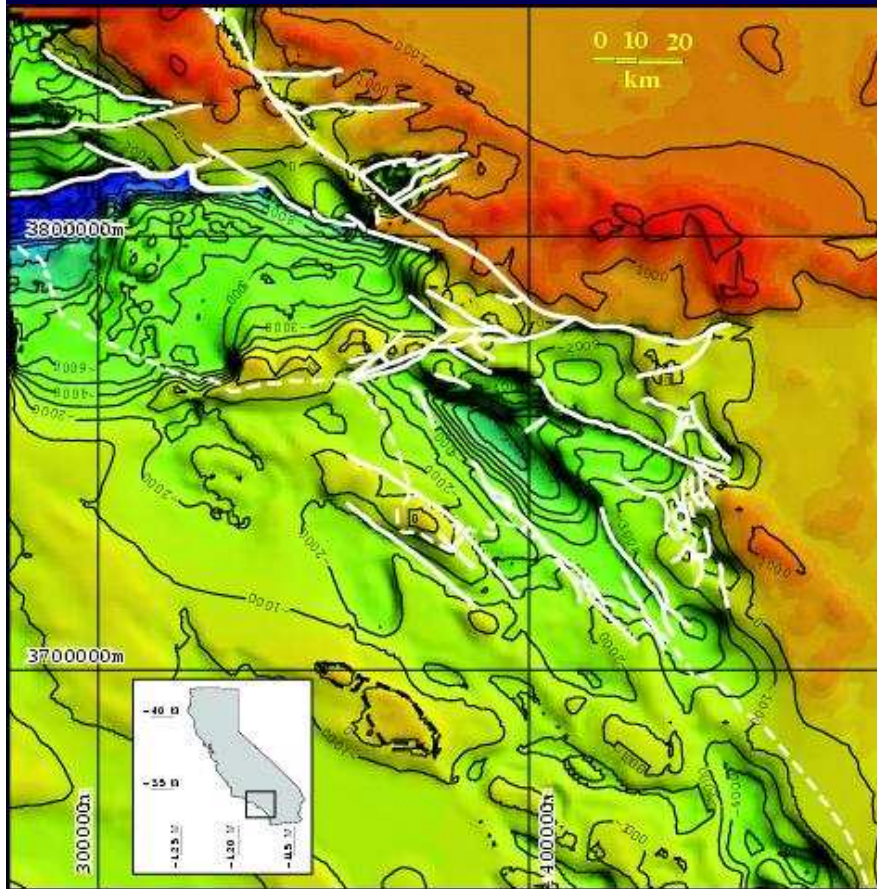
- Large region
- L.A. basin, San Fernando valley, Ventura basin
- Mountains, bathymetry
- ECSZ
- Blue rectangles
- Large number of stations (TriNet)

Introduction (Basins)

- Need accurate numerical methods to model seismic hazard – very densely populated areas
- Large and complex 3D models (e.g., L.A., Tokyo, Mexico)
- Wealth of high-quality data (TriNet)

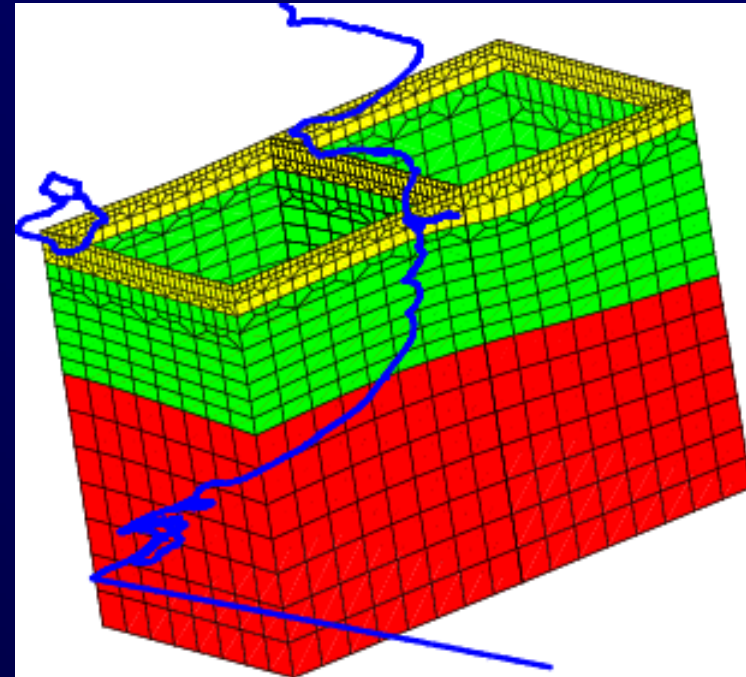
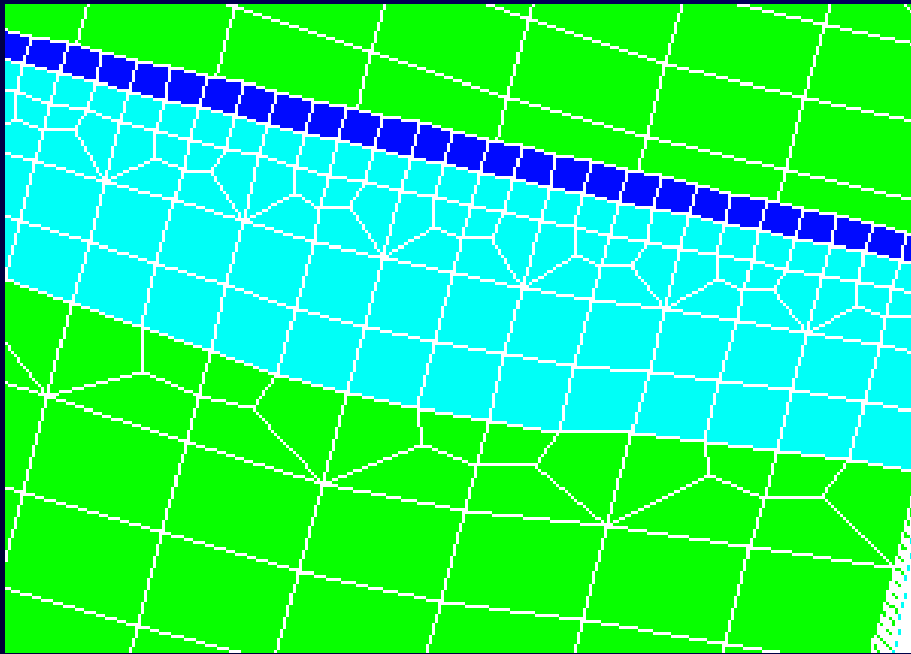
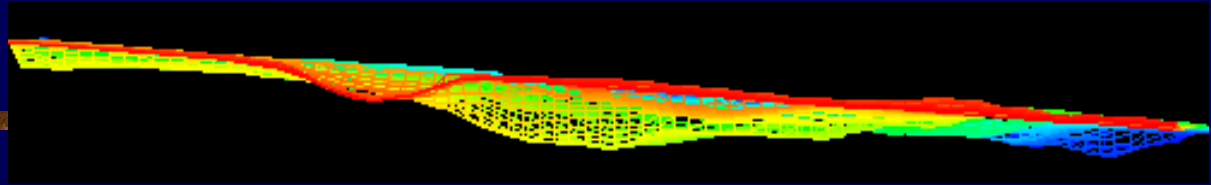


Harvard LA basin model



- 20,000 km of petroleum industry profiles
- 300+ well logs (*Süss and Shaw, JGR, 2003*)
- 85,000 direct velocity measurements

Final Mesh



Difficulties:

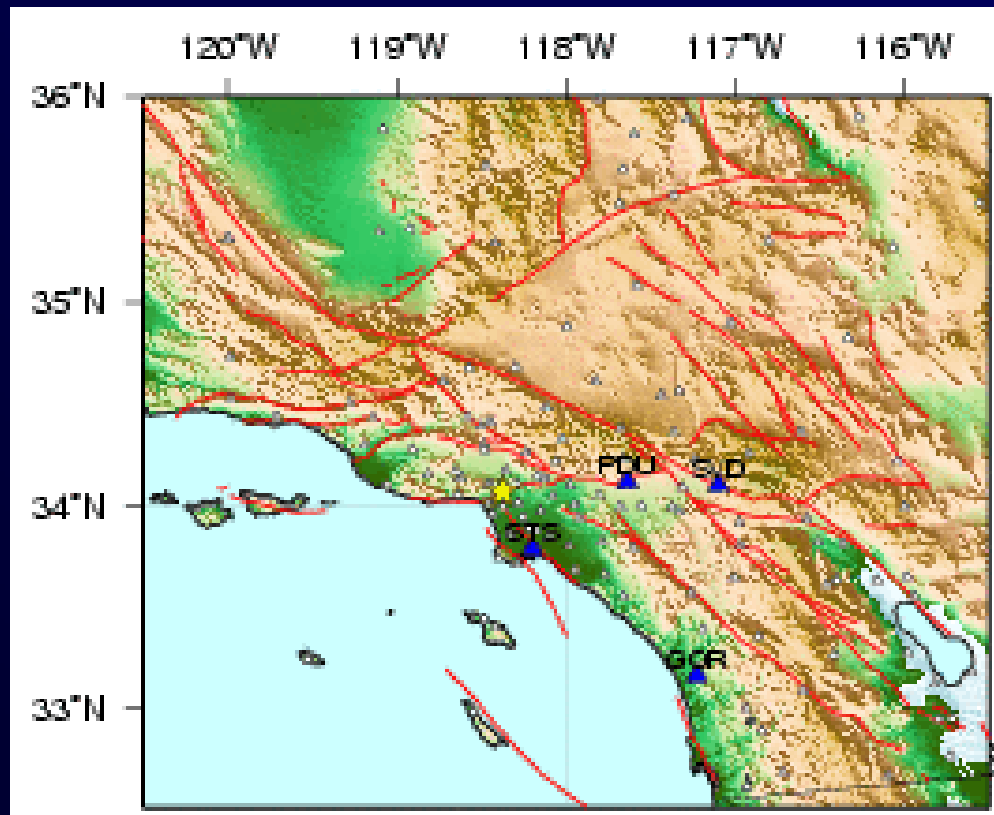
- Adapt the mesh to topography, bathymetry, bottom part of basement, and 3D shape of Moho
- Implement coarsening with depth to save CPU and memory

Hollywood Earthquake

Hollywood
September 9, 2001 $M_w = 4.2$

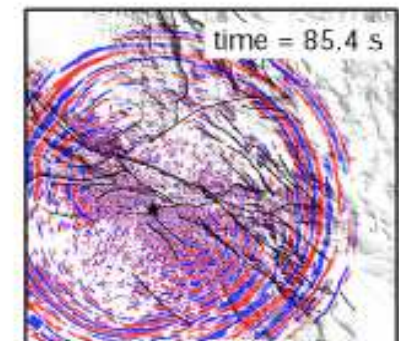
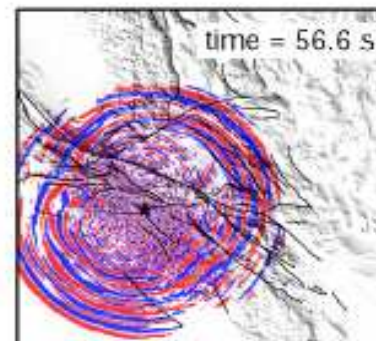
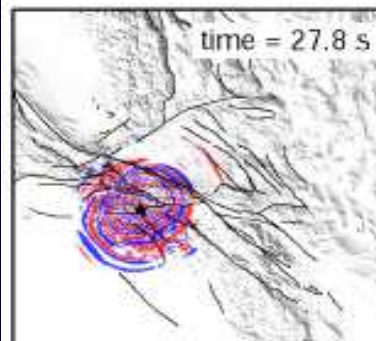
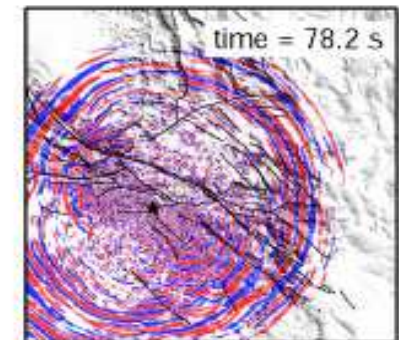
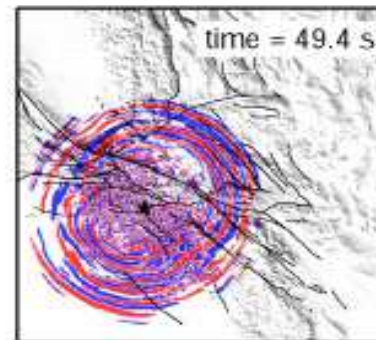
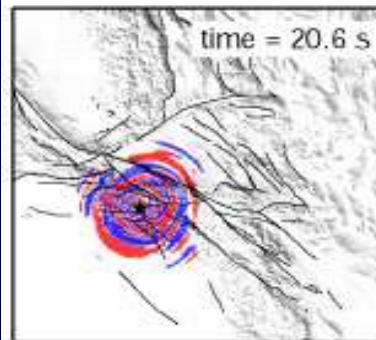
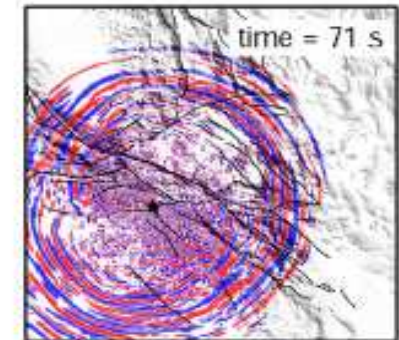
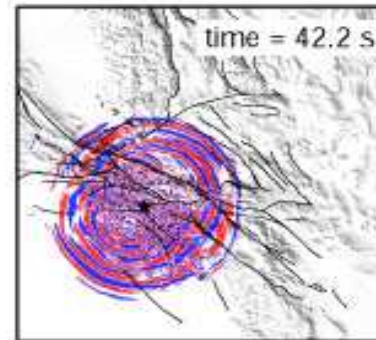
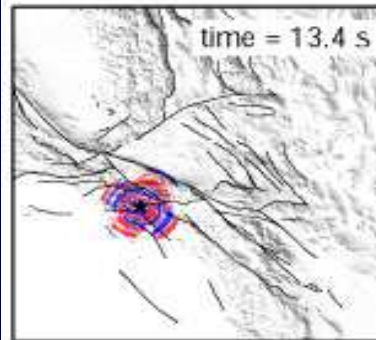
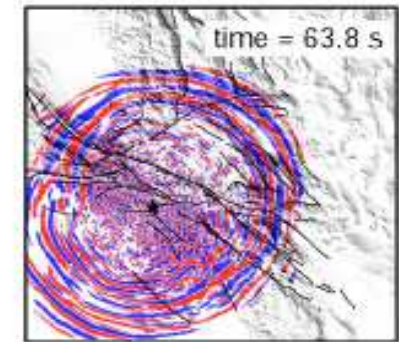
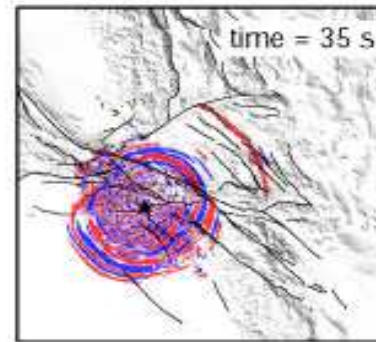
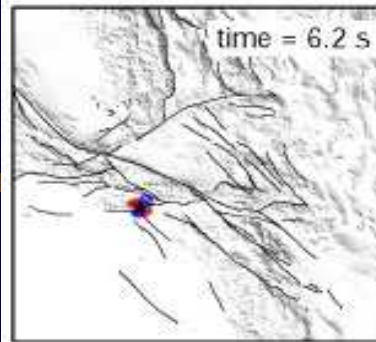


Small M 4.2 earthquake on Sept 9, 2001

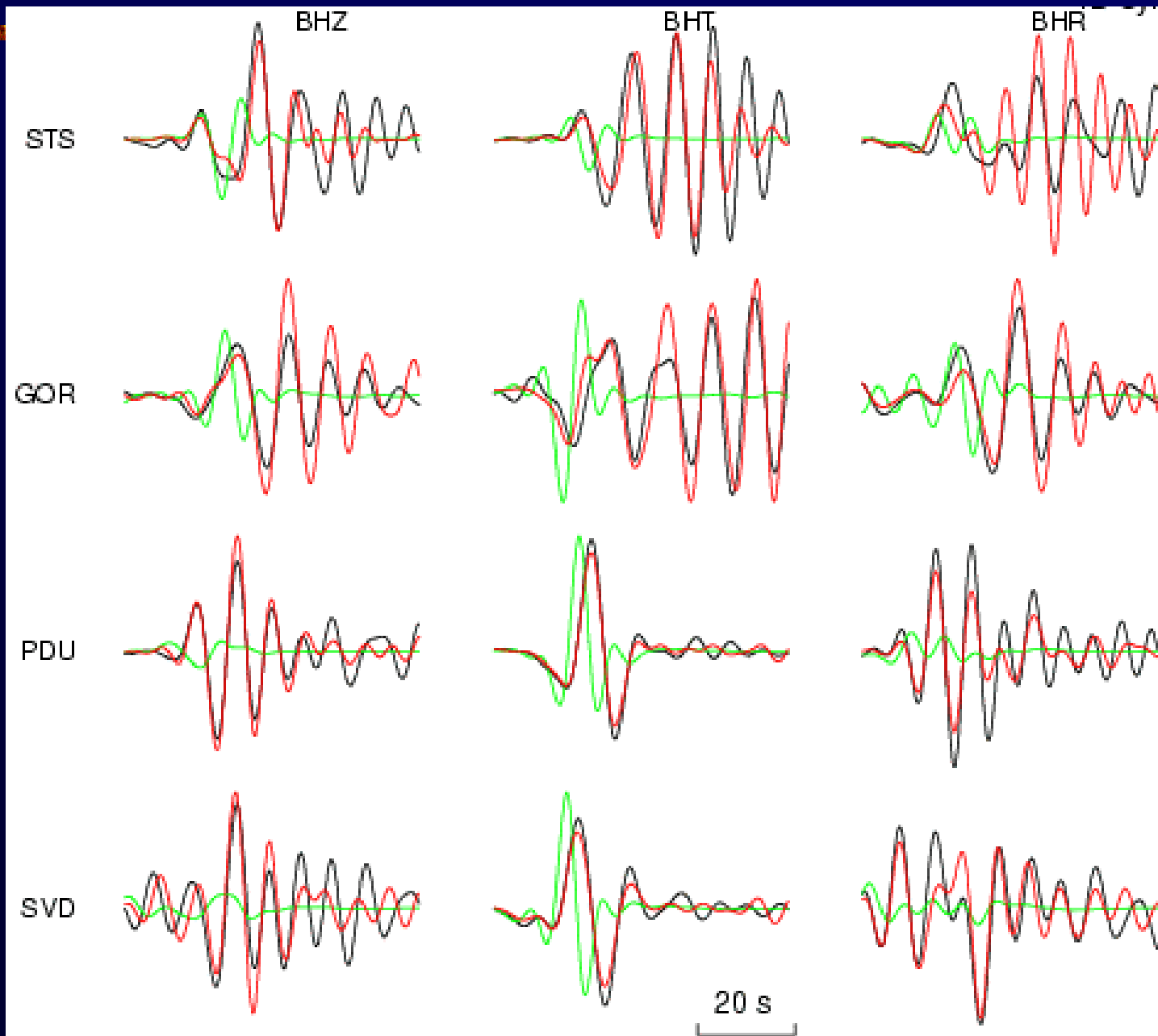


Amplification in basin

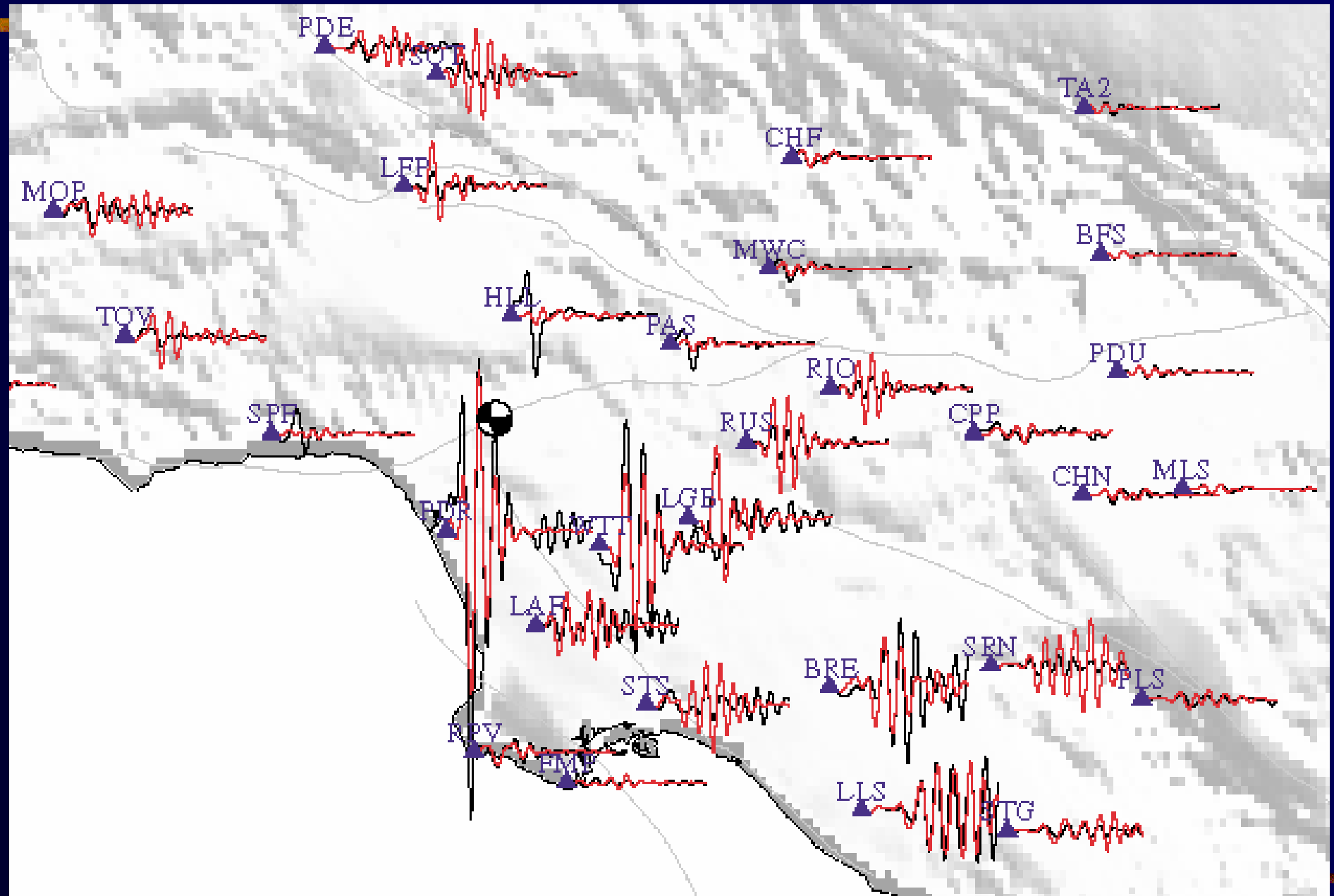
Snapshots



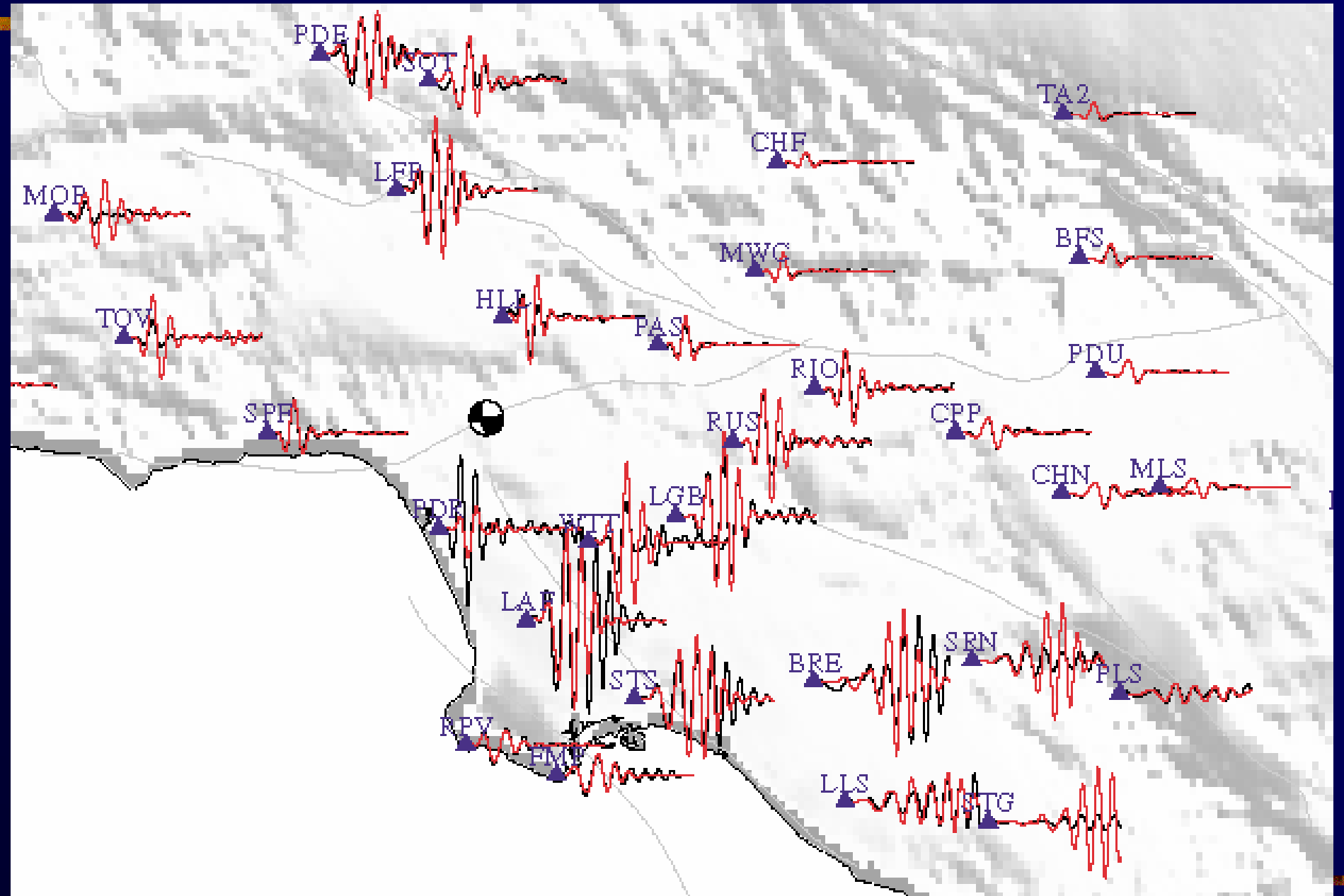
Data vs. 3D and 1D at 6 sec.



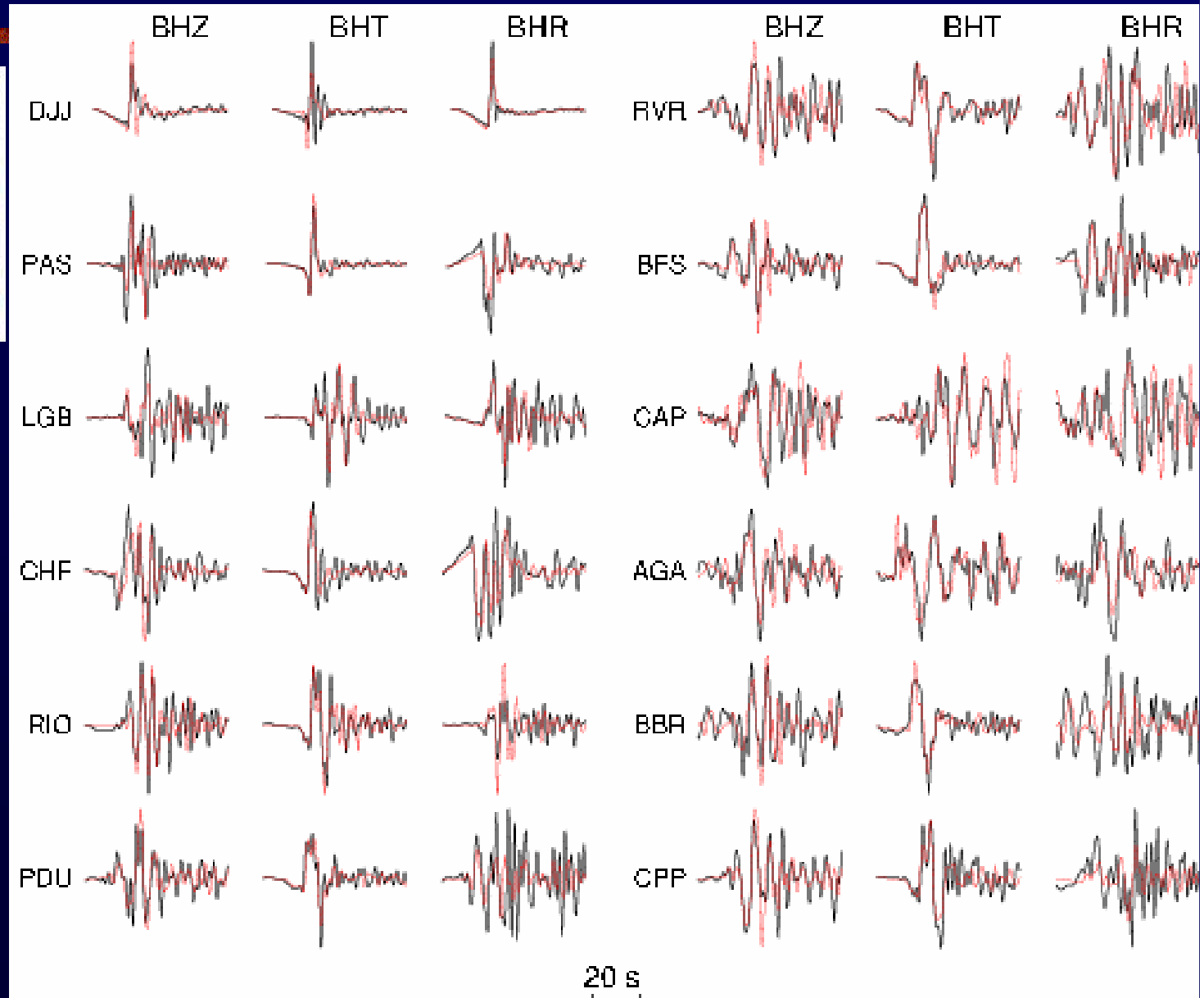
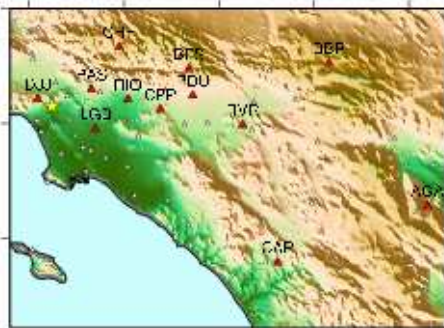
Hollywood radial



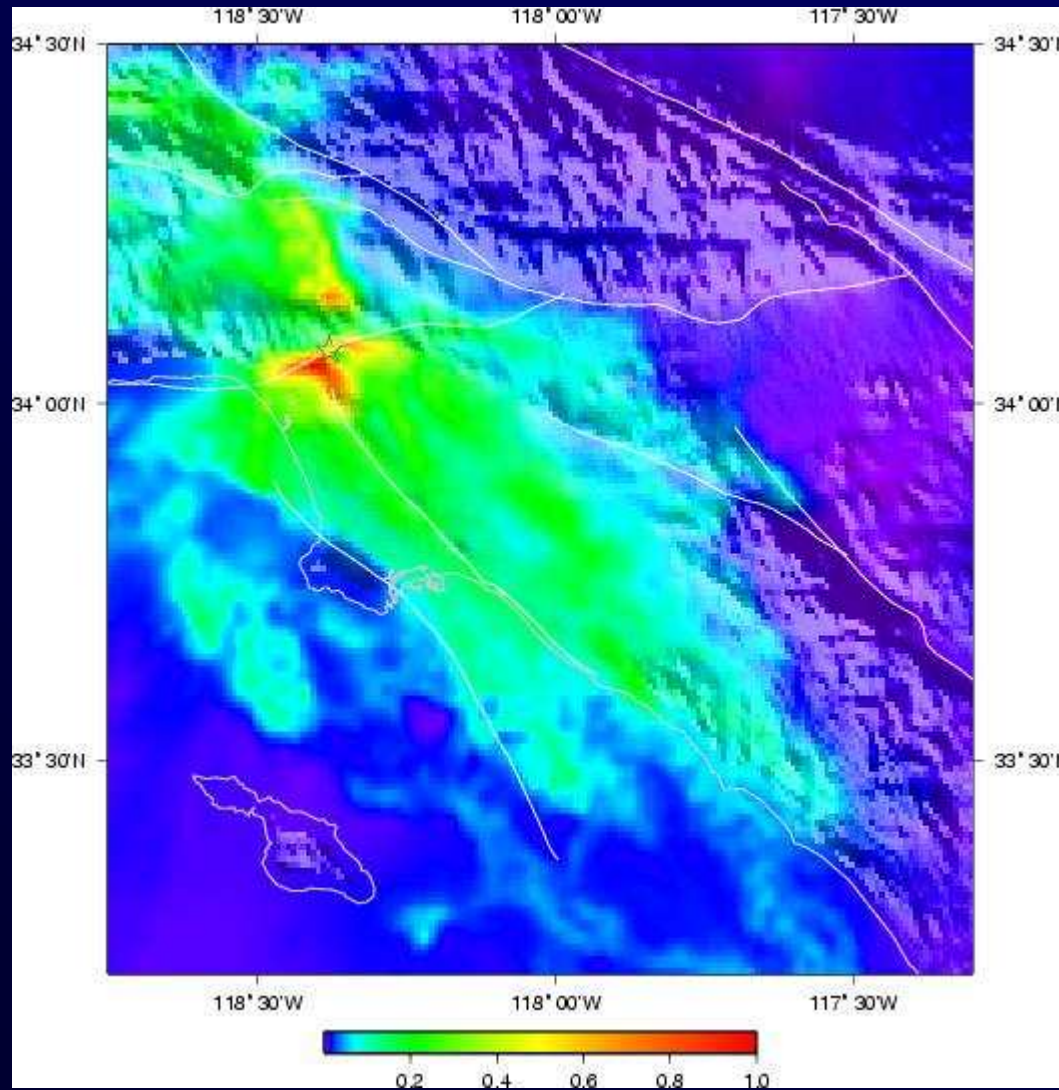
Hollywood transverse



Hollywood 2 s at 12 stations

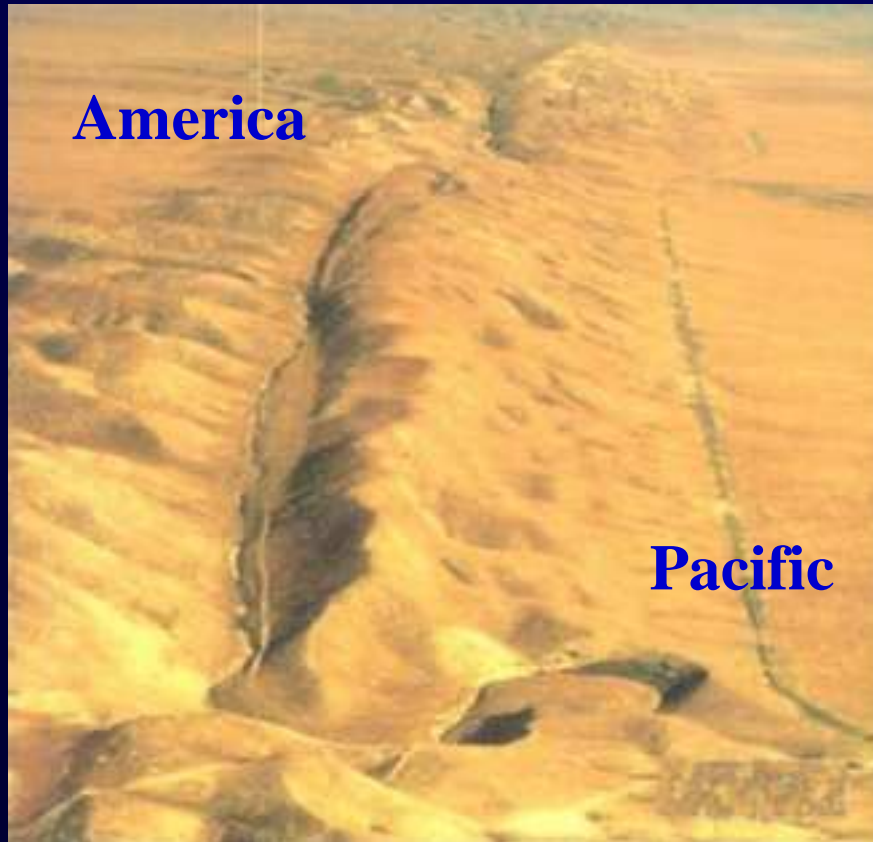


Peak ground acceleration



- Maximum of norm of acceleration
- Consistent with shape of basin
- Transfer from L.A. basin to San Fernando
- Almost no shaking in Palos Verdes
- Nothing in mountains

San Andreas – January 9, 1857

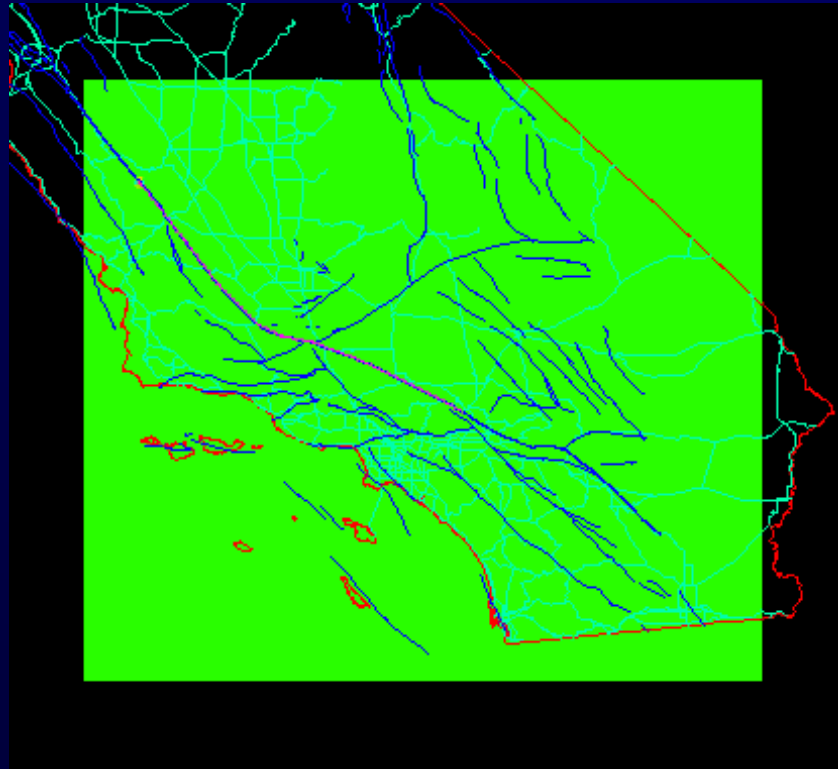


Carrizo Plain, USA, horizontal scale \cong 200 m

Vertical scale approximately 1 km

Carrizo Plain, San Andreas Fault, California, USA

Earthquakes at the regional scale




Scale approximately 500 km


3D spectral-element method (SEM)

Conclusions (Basins)

- We have demonstrated the flexibility and accuracy of the spectral-element method for seismic wave propagation in 3D basins models
- Relatively easy to implement on parallel computers, and very efficient – e.g., PC Beowulf cluster
- Three components down to 2 seconds, good fit
- Can handle complex 3D models, attenuation, topography, 3D shape of Moho, oceans
- We are now limited by knowledge of model, not by the method
 - ⇒ Will give us the ability to test and improve models
 - ⇒ Will improve our ability to assess seismic hazard



Global Earth: large earthquake in Vanuatu

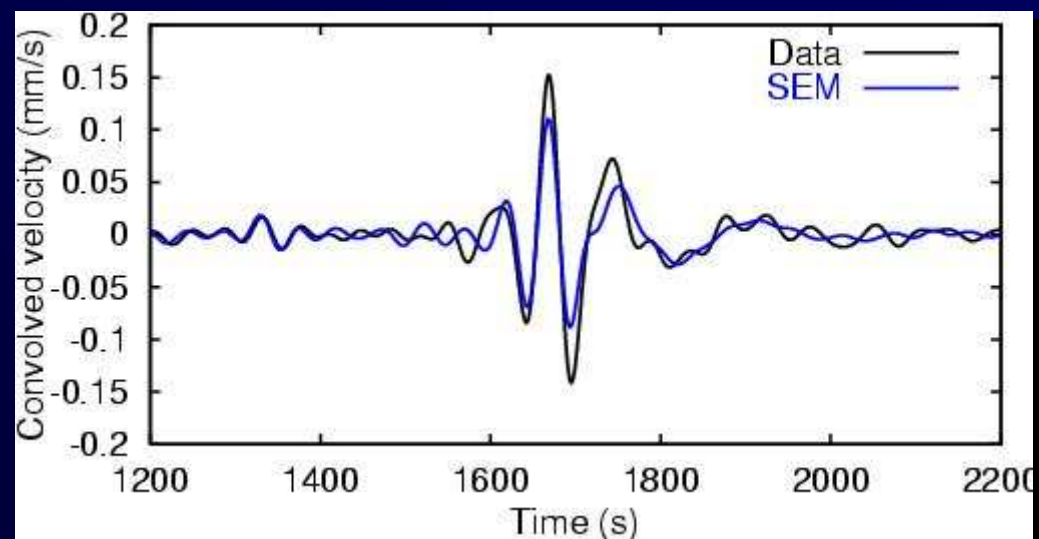
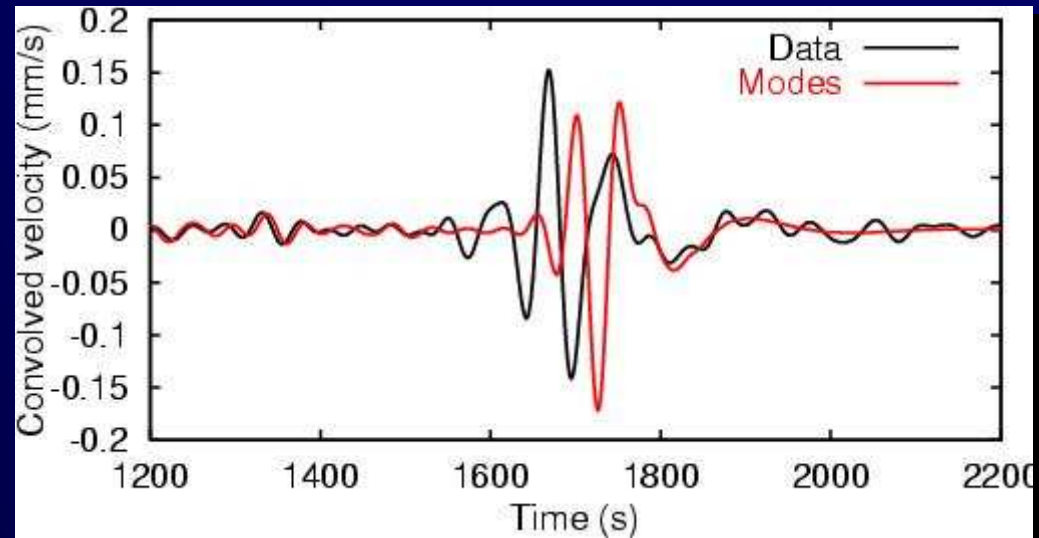
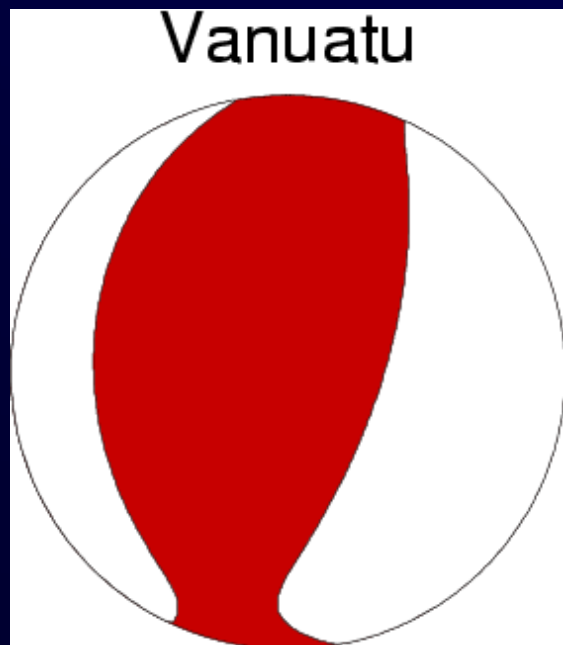


Vanuatu Earthquake in Japan

- Vertical component (Rayleigh wave)

Mostly oceanic path

Depth 15 km

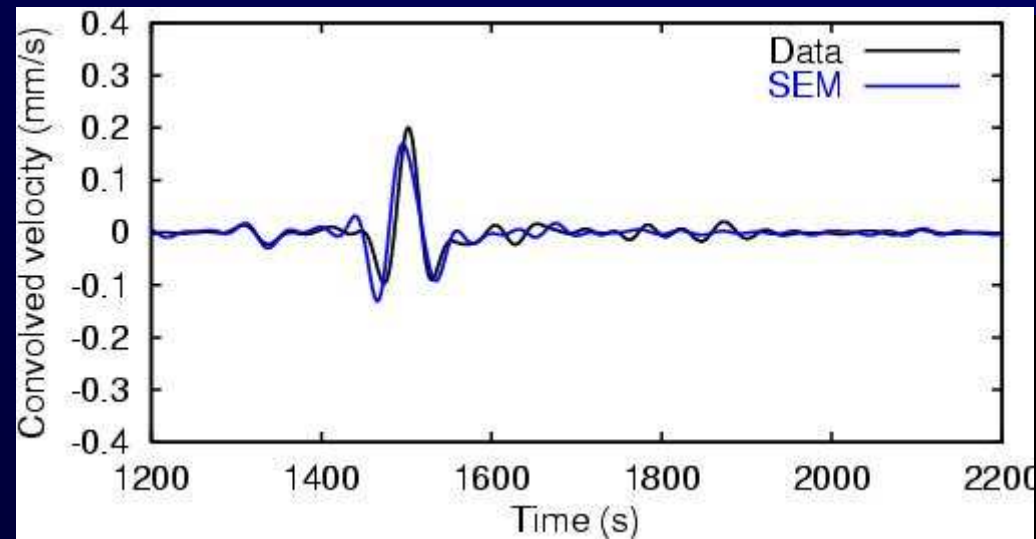
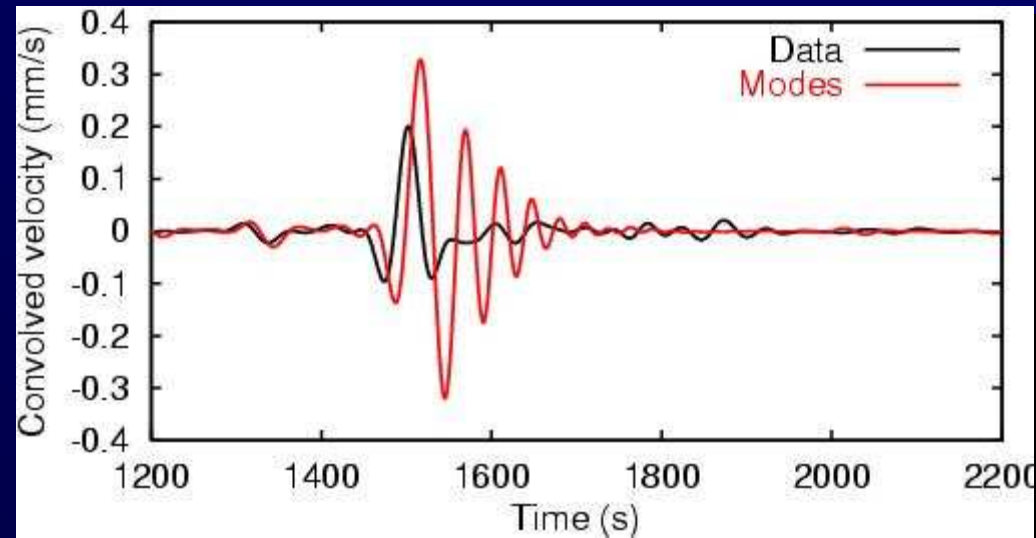
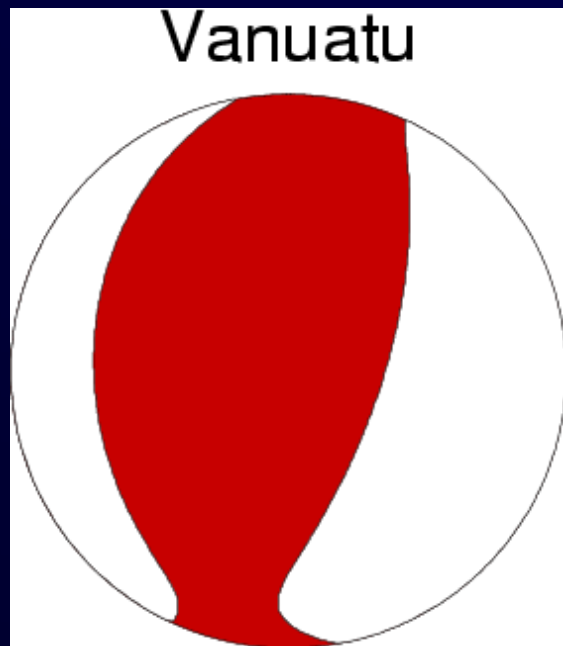


Vanuatu Earthquake in Japan

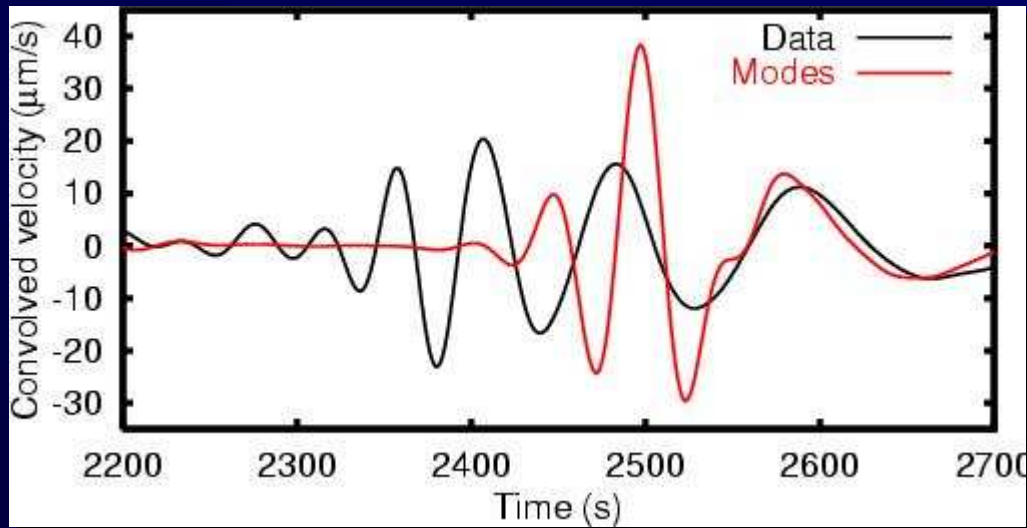
- Transverse component (Love wave)

Mostly oceanic path

Depth 15 km

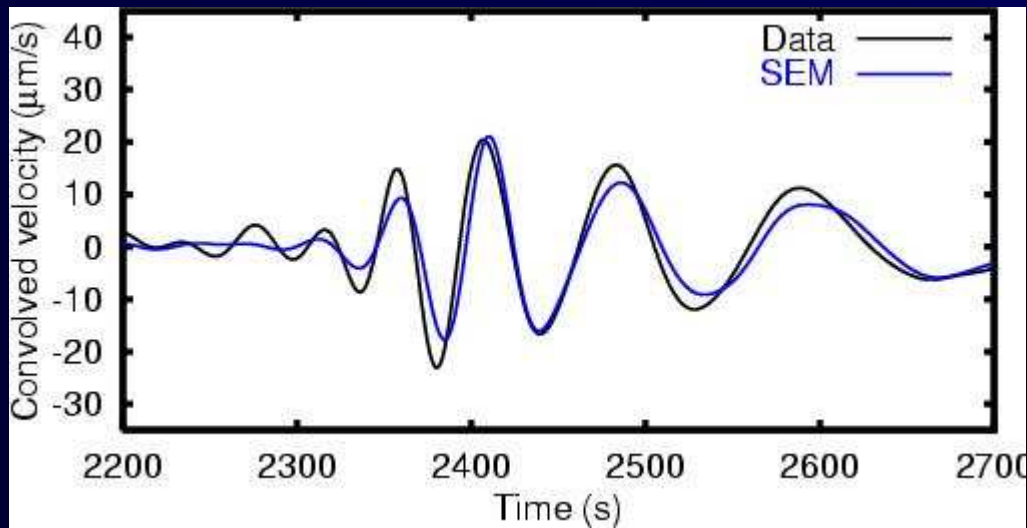


Vanuatu Earthquake in Pasadena




Mostly oceanic path

Delay is 85 s
for Rayleigh wave




Conclusions (Global Earth)

- Large machines like the EarthSimulator allow us to compute global 3D models with full complexity down to a few seconds
 - Earth models are not accurate enough
 - Worse for surface waves, crustal model not well known
 - Will ultimately need to perform tomographic inversion based upon fully 3D synthetics
 - Relatively easy to implement on parallel computers, and very efficient – e.g., PC Beowulf cluster
-



Solving inverse problems in 3D





Adjoint Method (Waveforms)

Tromp et al. (2006, 2008, 2009), Princeton

$$\chi_1(\mathbf{m}) = \frac{1}{2} \sum_{r=1}^{N_r} \int_0^T w_r(t) \|s(\mathbf{x}_r, t; \mathbf{m}) - \mathbf{d}(\mathbf{x}_r, t)\|^2 dt,$$

$$\delta\chi_1 = \int_V [K_\rho(\mathbf{x}) \delta \ln \rho(\mathbf{x}) + K_\mu(\mathbf{x}) \delta \ln \mu(\mathbf{x}) + K_\kappa(\mathbf{x}) \delta \ln \kappa(\mathbf{x})] d^3 \mathbf{x},$$

$$K_\rho(\mathbf{x}) = - \int_0^T \rho(\mathbf{x}) \partial_t s^\dagger(\mathbf{x}, T-t) \cdot \partial_t s(\mathbf{x}, t) dt,$$

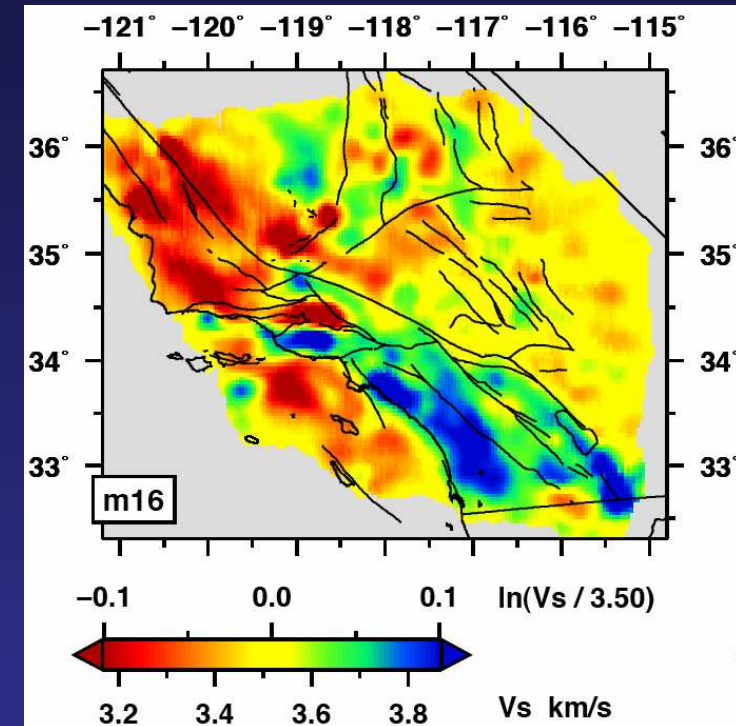
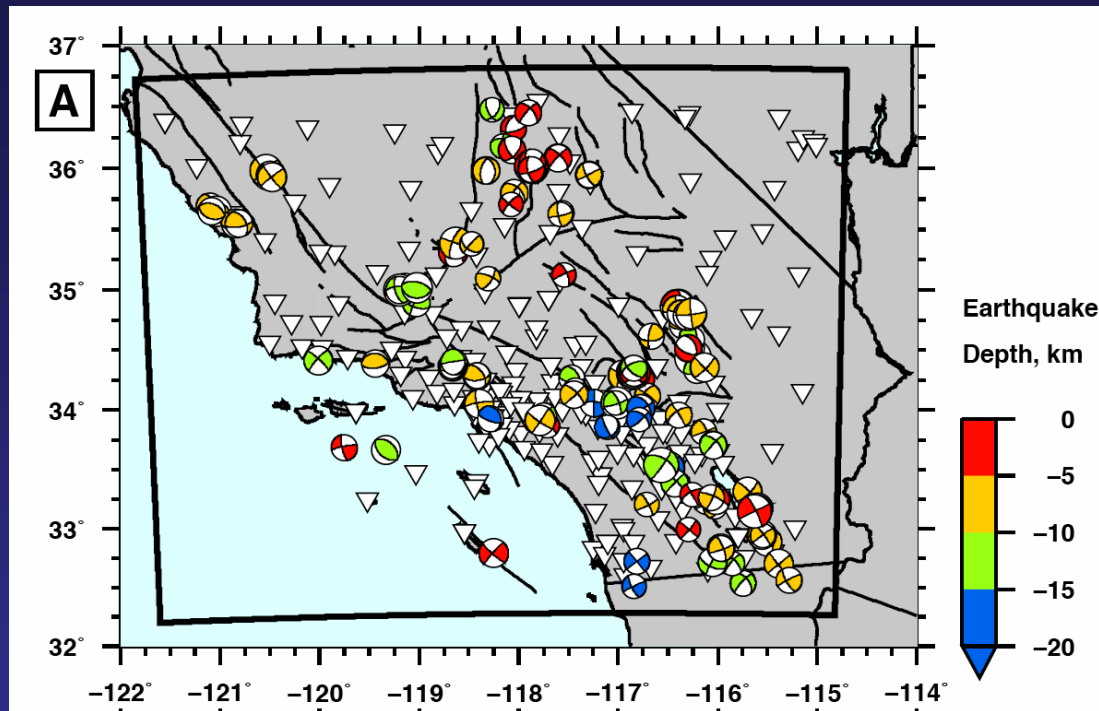
$$K_\mu(\mathbf{x}) = - \int_0^T 2\mu(\mathbf{x}) \mathbf{D}^\dagger(\mathbf{x}, T-t) : \mathbf{D}(\mathbf{x}, t) dt,$$

$$K_\kappa(\mathbf{x}) = - \int_0^T \kappa(\mathbf{x}) [\nabla \cdot \mathbf{s}^\dagger(\mathbf{x}, T-t)] [\nabla \cdot \mathbf{s}(\mathbf{x}, t)] dt,$$

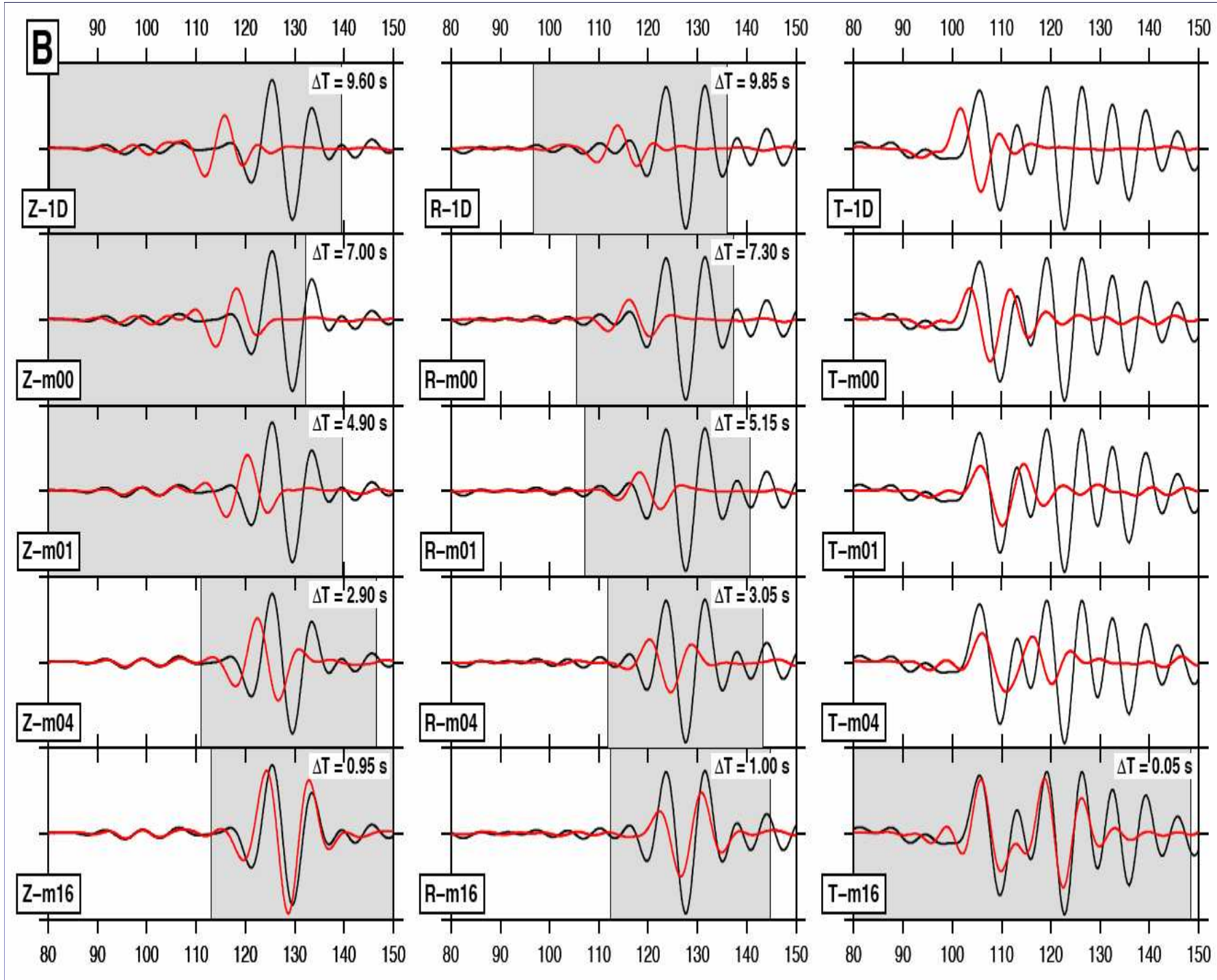
$$\mathbf{f}_1^\dagger(\mathbf{x}, t) = \sum_{r=1}^{N_r} w_r(t) [s(\mathbf{x}_r, T-t) - \mathbf{d}(\mathbf{x}_r, T-t)] \delta(\mathbf{x} - \mathbf{x}_r),$$

‘Banana-Donut’ kernels (Tony Dahlen et al.)

143 earthquakes used in inversion (Tape et al., 2009, Princeton Univ.)



- 3 simulations per earthquake per iteration
 - 16 iterations
 - 6,864 simulations
 - 168 processor cores per simulation
 - 45 minutes of wall-clock time per simulation
 - 864,864 processor core hours
- Depth 10 km





Denali (Alaska) earthquake



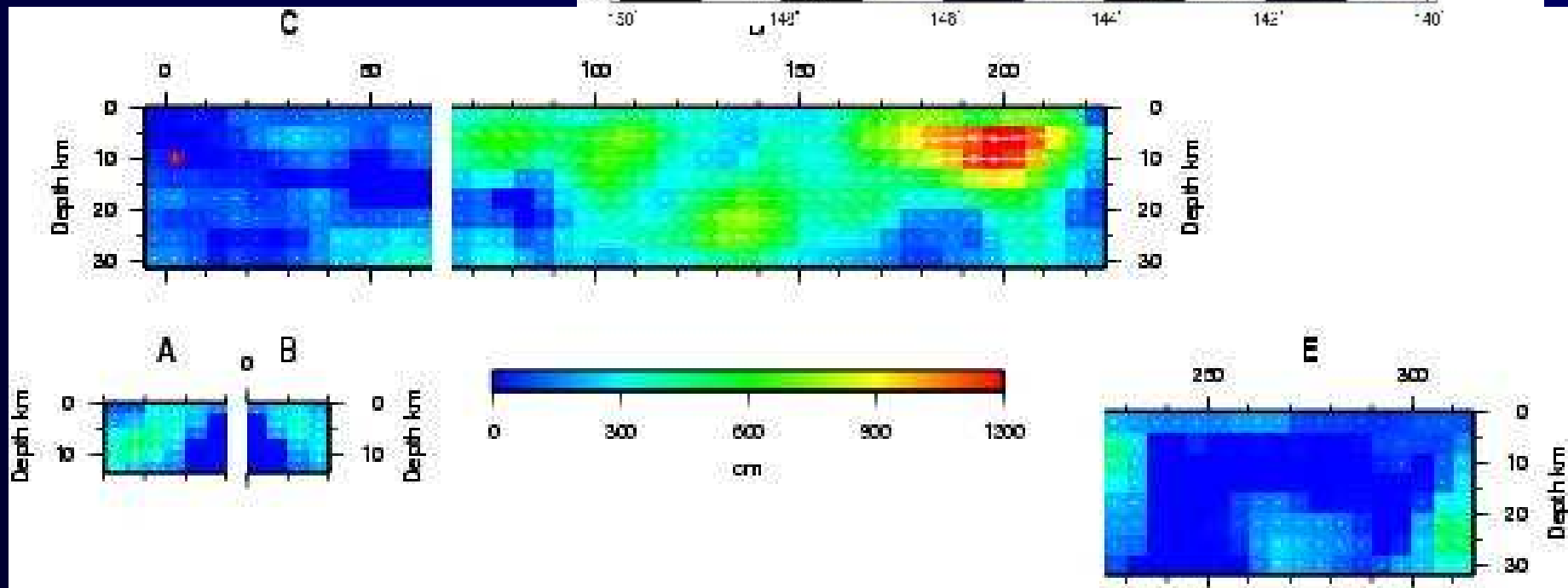
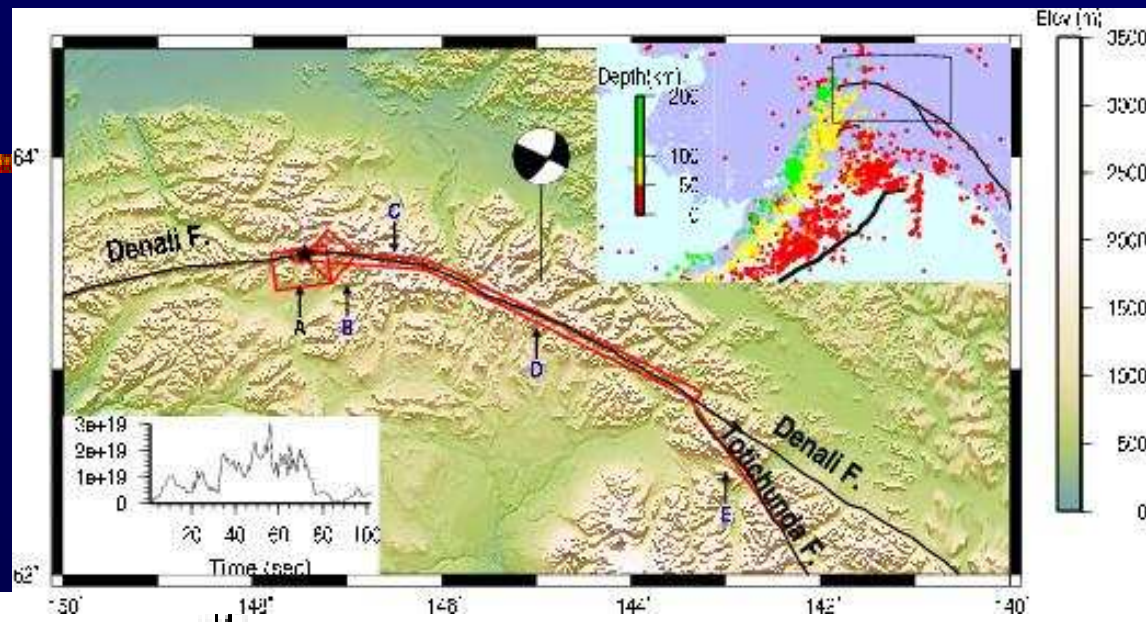
Denali

Alaska

Mw 7.9

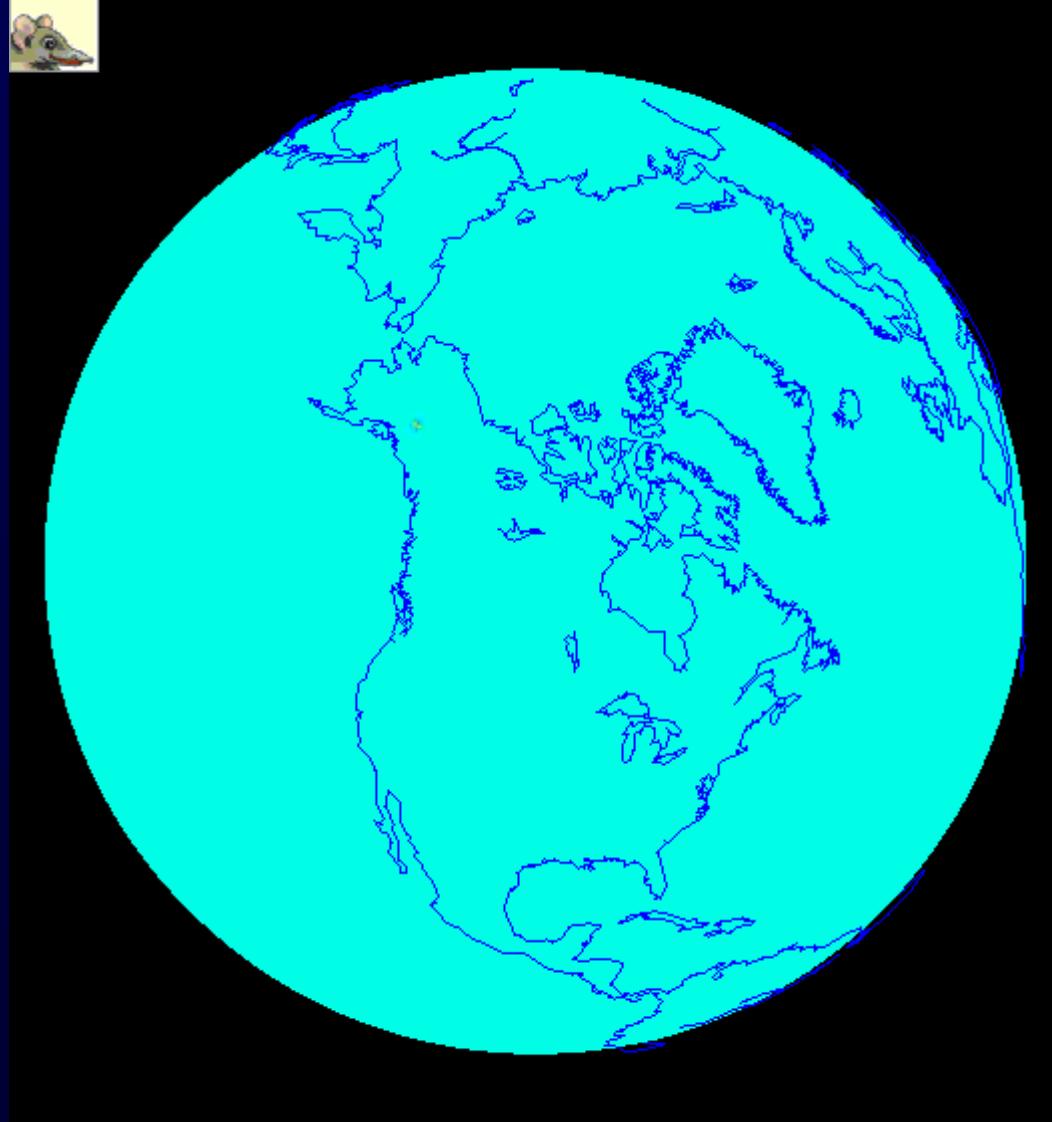
3 novembre 2002

220 km strike-slip

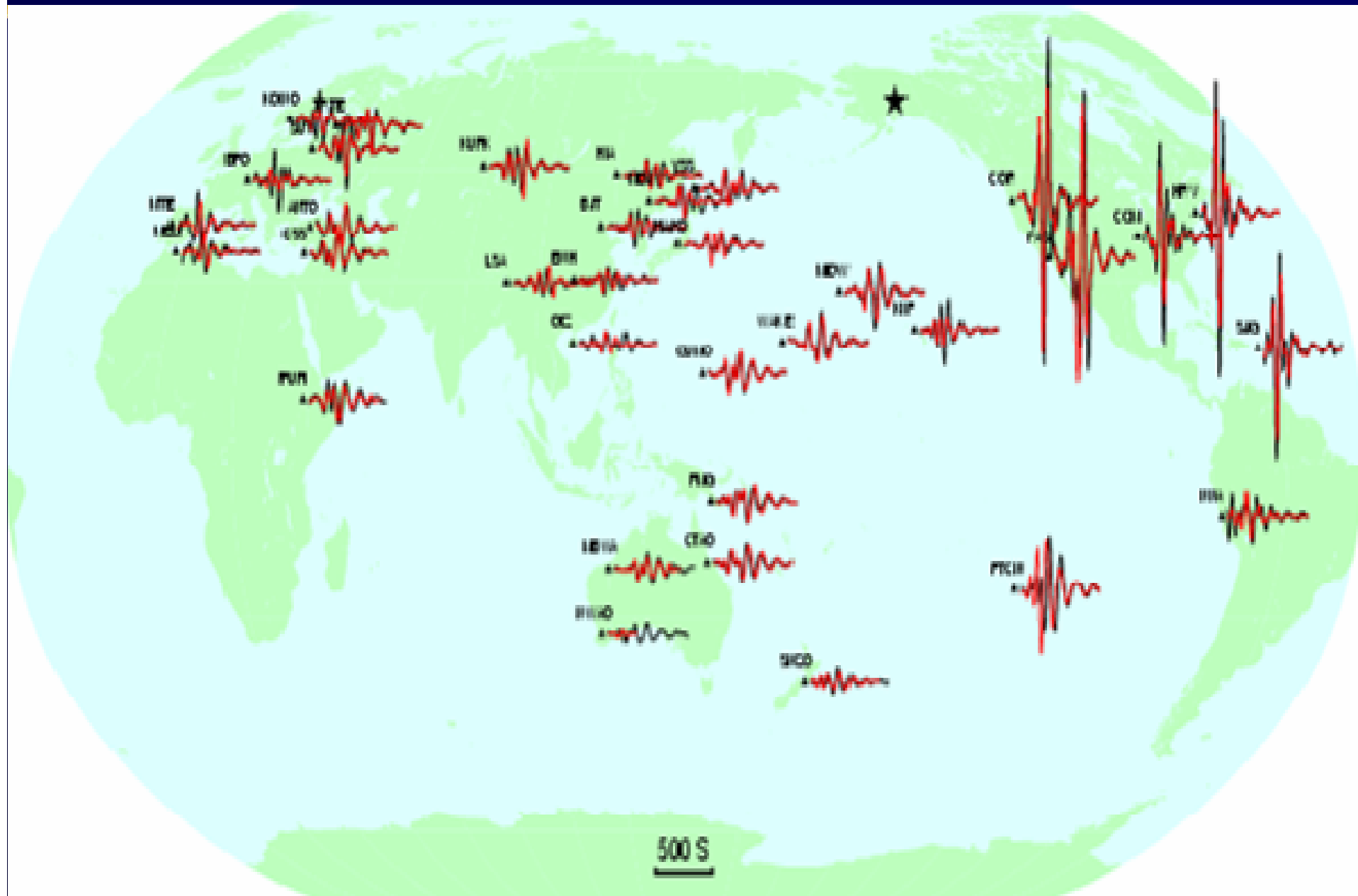


Inversion source (ondes de volume télésismiques + déplacements en surface) par Ji Chen et al.

Denali, Alaska – Rayleigh wave

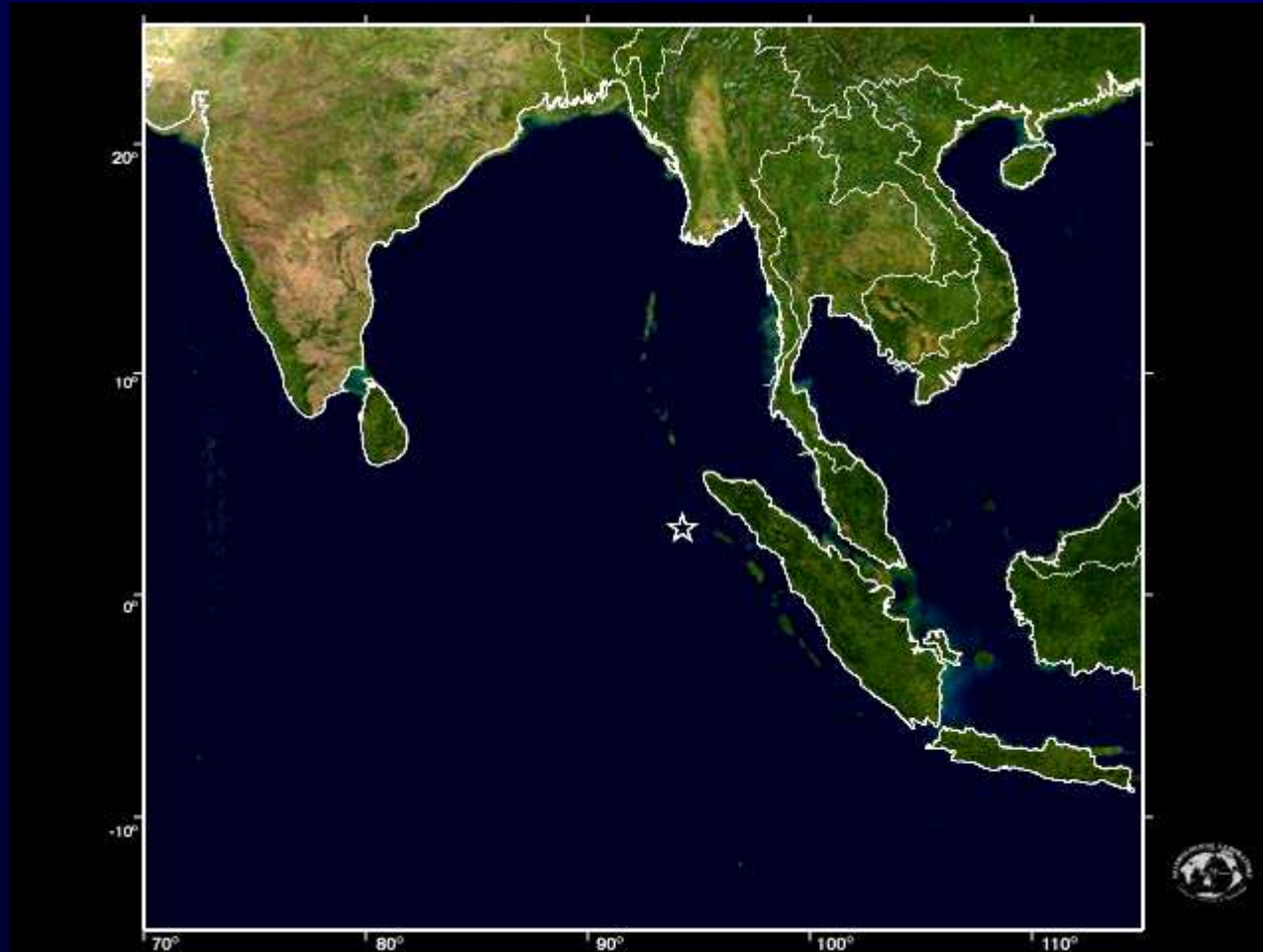


Rayleigh wave



Sumatra
earthquake
(but no tsunami)

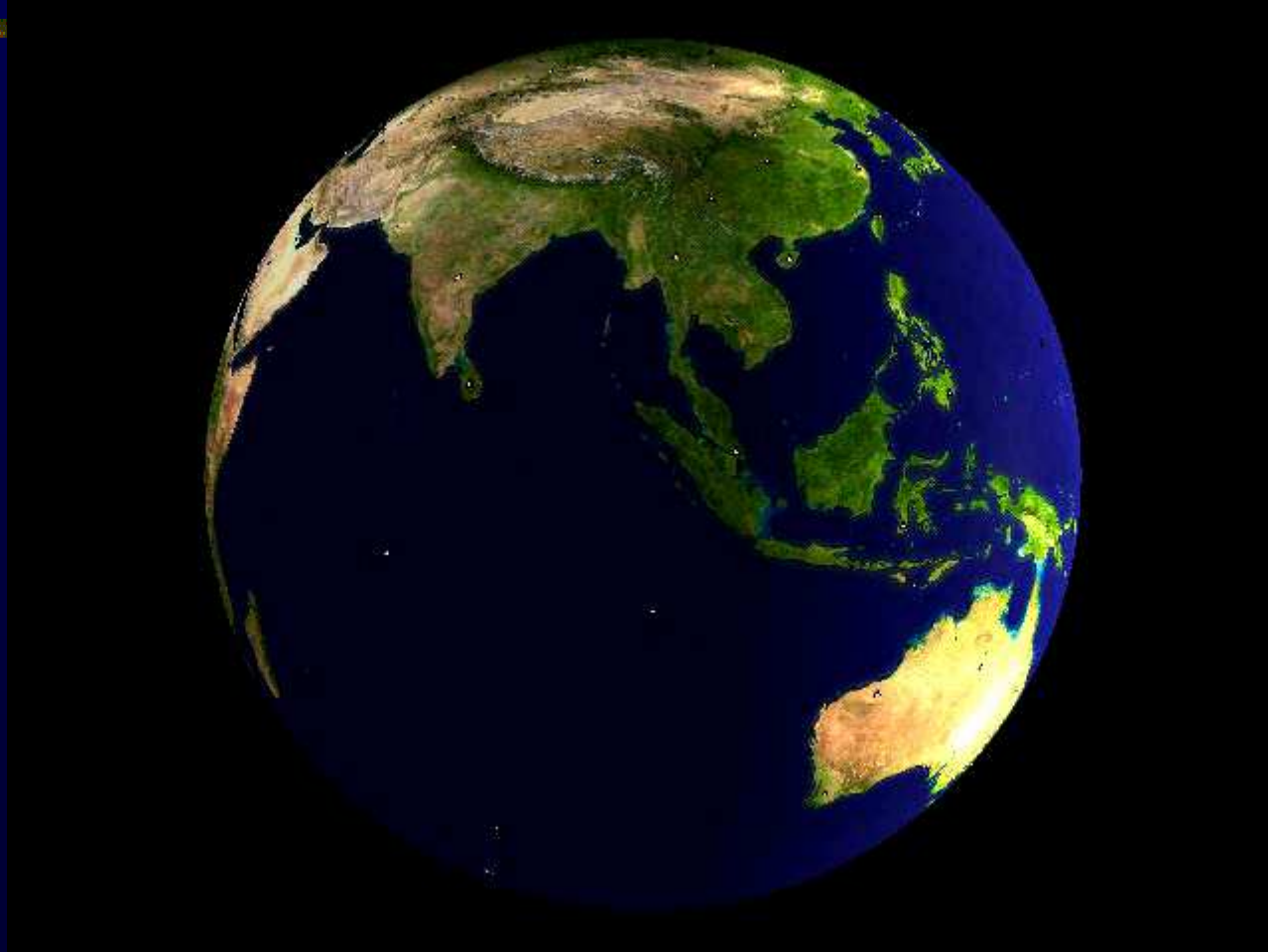
Dec 26, 2004 Sumatra event



vertical component
of velocity at
periods of
10 s and longer on a
regional scale

From Tromp et al., 2005

Dec 26, 2004 Sumatra event



From Tromp et al.,
2005

the two dispersive Rayleigh waves R1 and R2 at the scale of the globe (vertical component of velocity, periods of 18 s and longer), including the caustics and refocusing at the antipode and pole (3 hours worth of data)